Activity in the ventral hippocampal-medial prefrontal cortical pathway during anxiety in mice

Avishek Adhikari

Submitted in partial fulfillment of the

requirements for the degree of

Doctor of Philosophy

in the

Graduate School of Arts and Sciences

COLUMBIA UNIVERSITY
2011

ABSTRACT

Activity in the ventral hippocampal-medial prefrontal cortical pathway during anxiety in mice

Avishek Adhikari

Anxiety-related disorders are highly prevalent and can cause great disability. However, a thorough understanding of the neurobiological underpinnings of anxiety is missing. In an effort to study innate anxiety-related behaviors several rodent anxiety paradigms have been developed. Two commonly used anxiety paradigms are the elevated plus maze (EPM) and the open field. Both of these paradigms have well defined aversive areas (the open arms and center, for the EPM and open field, respectively) and safe areas (the closed arms and periphery, for the EPM and open field, respectively). The most commonly used measure to estimate anxiety in these paradigms is the amount of time spent exploring the aversive compartment of these environments. In order to identify which brain areas may have a role in this behavior, several lesion studies have been conducted. Such studies have found that the ventral hippocampus (vHPC) and the medial prefrontal cortex (mPFC) are required for normal levels of avoidance of the aversive areas in these paradigms. Intriguingly, the vHPC projects to the mPFC, suggesting that the vHPC may influence mPFC activity during anxiety. Previous reports suggest that such influence may occur through modulation of synchrony of activity in the theta range (4-12 Hz) between the hippocampus and the mPFC, as such modulation has been found between the hippocampus and downstream target areas during other behaviors, such as working memory. We hypothesize that electrophysiological correlates of anxiety exist in the vHPC and the mPFC and that theta range synchrony between these areas is modulated by anxiety. To test these hypotheses, we recorded neural activity simultaneously from the mPFC and vHPC from mice exploring control and anxiogenic environments. Recordings were also obtained from the dorsal hippocampus (dHPC), an area not required for anxiety and not directly connected to the mPFC, to serve as a negative control. Spikes and local field potentials (LFPs), which are thought to be a

measure of synchronized synaptic activity) were obtained from the mPFC, while only LFPs were recorded from the hippocampal sites.

We initially sought to investigate whether we could detect evidence that the vHPC influences the mPFC awake-behaving mouse. To this end, we developed a method to detect the directionality of functional connectivity across brain areas using only LFP recordings. It is noteworthy that estimating the directionality of information flow in a circuit with LFP recordings is a problem of general interest among system neuroscientists. Current methods used to address this problem such as Granger causality and partial directed coherence are mathematically complex, which in turn creates difficulty for both implementing and interpreting such methods. Thus, we created a mathematically simple method to address this issue. Our method consists of crosscorrelating the amplitude envelopes of two signals filtered in a frequency band of interest. The position of the peak of the crosscorrelation provides an estimate of the lag between the two signals in the chosen frequency range. Applying this method to the vHPC-mPFC dataset revealed that theta range activity in the vHPC leads the mPFC with a lag comparable to the conduction delay of this pathway. Furthermore, a consistent lag between these two structures was found only in the theta range. Lastly, this method was found to be more robust than Granger causality and partial directed coherence to artifacts induced by noise. Importantly, these data are consistent with the hypothesis that theta range activity propagates from the vHPC to the mPFC.

We next used this approach to characterize synchrony in the theta range in this circuit and study its modulation during anxiety. Recordings from hippocampal and mPFC sites were obtained in the EPM, the open field and a control familiar environment that is not anxiogenic. Interestingly, theta-frequency activity in the mPFC and ventral, but not dorsal hippocampus was highly correlated at baseline, and this correlation increased in both anxiogenic environments. Increases in mPFC theta power predicted avoidance of the aversive compartments of each arena, and were larger in serotonin 1A-receptor knockout mice, a genetic model of increased anxiety-like behavior. These results suggest a role for theta-frequency synchronization between the ventral hippocampus and the mPFC in anxiety. They are in line with the notion that such

synchronization is a general mechanism by which the hippocampus communicates with downstream structures of behavioral relevance.

Lastly, we sought to characterize single unit activity in the mPFC while mice explored the EPM. As task-related firing modulated by behavioral demands has been found in the mPFC in other tasks, we hypothesized that task-related firing would also be present in anxiety paradigms that require the mPFC such as the EPM. Intriguingly, firing rates in arms of the same type were positively correlated, independently of the position of the arms relative to each other. Strikingly, cells with task-related firing were more robustly phase-locked to ventral hippocampal (vHPC) and mPFC, but not dHPC, theta (4-12 Hz) oscillations. Lastly, mPFC cells that were led by vHPC theta had more prominent task-related firing. These data show that mPFC unit activity is consistent with a role in anxiety, and suggest that neurons with anxiety task-related firing are preferentially integrated into a vHPC-mPFC circuit.

In summary, these data show that neural correlates of anxiety were found in mPFC single and multiunit activity, as well as in mPFC and vHPC LFPs. Intriguingly, higher coupling of mPFC activity to vHPC theta oscillations during anxiety was observed both in mPFC spike and LFP activity. Furthermore, measures of directionality show that vHPC activity in the theta range lead mPFC spikes and LFPs. These results are consistent with a model in which contextual information is propagated from the vHPC to the mPFC in the theta range. The mPFC may in turn evaluate the aversiveness of the environment and guide behavior appropriately. Further studies are needed to obtain a more comprehensive characterization of the neural activity in structures thought to be involved in anxiety and to make perturbations in the relevant circuits in order to gain understanding of the causal relationship between specific patterns of neural activity and anxiety-related behavior.

Table of Contents

Chapter 1: Introduction…….....1-17

1.1 Background……..…..…….....2

Overview…….....…….…….....2

Innate anxiety and learned fear.....3

Learned fear in rodents…….....….…....4

Innate anxiety paradigms in rodents…….....5

The effects of anxiolytic and anxiogenic drugs on anxiety tests in rodents..….....7

Neural circuitry of innate anxiety…….....8

vHPC-dHPC differentiation…….....…10

The hippocampus-mPFC circuit…….....….....14

Theta oscillations and anxiety…….....16

1.2 Approach…….....16

Chapter 2: Cross-correlation of instantaneous amplitudes of field potential oscillations: a straightforward method to estimate the directionality and lag between brain areas……..……..…….....……18-49

2.1 Introduction…….....……....19

2.2 Results……...…….....…….21

2.3 Discussion…..……..…….....…….……...27

2.4 Methods…….…….…….....……...31

Chapter 3: Synchronized activity between the ventral hippocampus and the medial prefrontal cortex during anxiety……..…….…..……50-91

3.1 Introduction…….…….....…….……..51

3.2 Results……...…….....…….……...51

3.3 Discussion…..…….…….....…….……...60

3.4 Methods…….…….…….…..…….....…….…….…..66

Chapter 4: Single units in the medial prefrontal cortex with anxiety paradigm-related firing patterns are preferentially influenced by ventral hippocampal activity…….....….92-125

4.1 Introduction…….....…….……..…..93

4.2 Results……...…….....…….……...95

4.3 Discussion…..…….…….....…….……..……101

4.4 Methods…….…….…….…..…….....……..……...106

Chapter 5: Discussion……..…….....…….…..…126-146

5.1 Summary of principal findings…….....…….…..127

5.2 Role of the mPFC in defensive behaviors…….…….....…….129

5.3 vHPC and dHPC functional differentiation in anxiety……..…134

5.4 vHPC input to the mPFC…….…….…….…….....……...136

5.5 The vHPC-mPFC circuit during anxiety……...…….....…….…..…139

5.6 Electrophysiology during anxiety……..…….…..…….....…….……143

References……...…….....……147-160

List of Figures

Chapter 2: Cross-correlation of instantaneous amplitudes of field potential oscillations: a straightforward method to estimate the directionality and lag between brain areas……18-49

Figure 2.1 Calculating lags using the amplitude cross-correlation method. ….....39

Figure 2.2 Estimation of lags between the vHPC and the mPFC using the amplitude cross-correlation and phase locking methods…….....…..40

Figure 2.3 Estimation of lags between dHPC and mPFC using the amplitude cross-correlation and phase locking methods …….....41

Figure 2.4 Application of the amplitude cross-correlation method to bidirectionally-connected areas ……..….....…42

Figure 2.5 Partial directed coherence indicates that vHPC is leading the mPFC in the theta range. ……..…….....….....…..43

Figure 2.6 Partial directed coherence is more sensitive to noise than the amplitude cross-correlation method …….....44

Figure 2.7 Partial directed coherence, but not the cross-correlation method, is biased if one of the signals has different noise levels than the other signal.....….....45

Figure 2.8 Granger causality is more susceptible to noise than the amplitude crosscorrelation method……..……46

Figure 2.9 Cross-correlation of filtered LFPs cannot be used to estimate the lag between two areas……..……47

Figure 2.10 Identification of the frequency band at which directionality of functional connectivity occurs……..……48

Figure 2.11 vHPC-mPFC lags calculated with the Gabor transform and the Hilbert transform are in good agreement…….....49

Chapter 3: Synchronized activity between the ventral hippocampus and the medial prefrontal cortex during anxiety…….....……..…50-91

Figure 3.1 Location of electrodes.....74

Figure 3.2 Characterization of LFPs from the mPFC, vHPC and dHPC in the familiar arena. …….....75

Figure 3.3- mPFC-HPC synchrony and HPC changes in theta power in the EPM and open field do not vary substantially across HPC layers**…….....…76**

Figure 3.4 Power correlations and phase coherence across areas 77

Figure 3.5 Effects of anxiety on additional measures of synchrony……..…78

Figure 3.6 Modulation of mPFC gamma power by hippocampal theta phase……79

Figure 3.7 Theta power correlation between mPFC and vHPC increases in the EPM and open field ….....80

Figure 3.8 Multiunit phase locking to mPFC and vHPC theta increases in the open field. …….....81

Figure 3.9 Theta power in the mPFC and dHPC increases during exposure to the EPM and open field. ….....82

Figure 3.10 Locomotor behavior does not account for mPFC theta power increases in the open field and EPM……..83

Figure 3.11 mPFC theta power is increased specifically in the safe zones of the anxiogenic arenas…….....84

Figure 3.12 mPFC theta power and mPFC-vHPC coherence increase prior to leaving the closed arms ……....,.....85

Figure 3.13 mPFC theta power increases in the EPM and the open field correlate with behavioral measures of anxiety.....86

Figure 3.14 5-HT1A knockouts (5-HT1A KO) have a higher increase in mPFC theta power in the EPM and the open field relative to wildtype (WT) mice.....….....87

Figure 3.15 Coherence with the mPFC and changes in theta power in the middle hippocampus (mHPC) are intermediate between vHPC than dHPC…….……..……88

Figure 3.16 Temporal dynamics of coherence between vHPC, dHPC and mPFC……89

Figure 3.17 vHPC local field potential has local relevance……90

Figure 3.18 Main results are not reference-specific……91

Chapter 4: Single units in the medial prefrontal cortex with anxiety-related firing patterns are preferentially influenced by ventral hippocampal activity…….....92-125

Figure 4.1 mPFC single units appear to have anxiety-related firing in the EPM.....113

Figure 4.2 mPFC single units have similar firing rates in arms of the same type in the EPM …….....115

Figure 4.3 Anxiety-related firing patterns in the EPM are not related to novelty…….....116

Figure 4.4 Locomotor behavior does not vary across arms of the EPM…….....117

Figure 4.5 Anxiety-related firing patterns do not depend on the geometric arrangement of the arms …….....118

Figure 4.6 mPFC single units respond similarly to different anxiogenic stimuli.....120

Figure 4.7 mPFC units with anxiety-related firing patterns are over-represented in the population. …….....121

Figure 4.8 mPFC units with more prominent anxiety-related firing patterns are more robustly phase-locked to vHPC and mPFC theta oscillations…….....122

Figure 4.9 mPFC units that follow vHPC theta oscillations have more robust task-related firing patterns…….....123

Figure 4.10 mPFC theta power is higher in the safe compartment of all EPM configurations…124

Figure 4.11 Isolation of single unit clusters…….....125

Acknowledgements

First and foremost, I would like to thank my advisor Joshua Gordon, for training me in neuroscience and for taking me into his then empty lab at a time in which I had very limited knowledge of neuroscience, as I majored in biochemistry. I greatly appreciated the effort with which he helped me learn not only how to plan and perform the experiments described here, but also how to discuss and present them clearly. Being in his lab was a terrific experience because of the great team assembled there. I am immensely grateful to our lab technician Mihir Topiwala, for teaching me how to perform several experiments, for serving as an invaluable collaborator for all the work described here and for being a great friend. Torfi Sigurdsson was also very helpful for the many discussions we had both about neuroscience and other topics, such as 18th century humor derived from wearing monocles. I would also like to thank Pia O'Neill and Tim Spellman for making the lab a fun place to be, for the many interesting conversations we had and for all the 2$ Sapporo beers we bought each other. In addition, extra thanks to Pia for taking care of my avocado tree and answering the many women-people and scientist-people questions I posed over the years. Special thanks also to Malcolm Nason and Ekaterina Likhtik for their luminous presence and insightful input.

I was also fortunate for having as my co-adviser Rene Hen, who is truly an inspiring scientist for me. He not only introduced me to Josh, but also allowed me to present my data in his lab meetings. I am grateful to all the Hen lab members, especially Amar Sahay, for his constant encouragement, Navieta Ramasami for helping me navigate Columbia bureaucracy, Jesse Richardson-Jones and Clay for graciously sending me their theses to help me in writing mine. Many thanks for Clay Lacefield, for his creative scientific input and for all the parties (and one APARty) he hosted.

One of the advantages of being at Columbia is the possibility to learn from great scientists such as Steven Siegelbaum, Holly Moore and Stuart Firestein, all of whom I thank for being in my committee and advising me along the way.

I also benefited from the advice of the Buzsaki lab in the early stages of this work, so I thank them as well.

I am greatly thankful to all the friends I made while at Columbia. Thanks Adam, Joan, Johannes, Amit, Esther and Hugo for all the Sunday dinners. I would also like to thank Armen, Michael Bales and Elana Ernstoff for all the fun things we did, and I am sincerely thankful to Saroja and Ukraine for their unfaltering support and friendship. I am equally in debt to my friends in Brazil, Jun, Felipe, Alexandre, Andrea, Nilson, Carlos and Haroldo, whose friendship does not diminish even though I only see them once a year.

I would not be in Neuroscience today if it were not for my undergraduate adviser Etelvino Bechara and Carlos Penatti, who always encouraged me to be a scientist, so I would like to thank them also.

I also thank my family, Dadu, Dida, Kaka, Kakima, Sunny and Rai for their constant encouragement. Lastly, I would like to thank my parents, who from an early age instilled in me the curiosity and love of knowledge without which science cannot exist.

Chapter 1

Introduction

Introduction

1.1. Background

Overview

Anxiety disorders are highly prevalent, as according to recent estimates 20% of the population will suffer from an anxiety-related disorder in their lifetime (Lecrubier, 2007). This results in considerable financial costs, on the order of tens of billions of dollars annually in the US (Mendlowicz and Stein, 2000). Furthermore, mood disorders also increase the burden of symptoms from other conditions, as the presence of a mood disorder greatly worsens the prognosis for several health diseases, such as diabetes mellitus and heart disease (Roy-Byrne et al., 2008). Existing treatments for anxiety disorders are ineffective in a large fraction of patients, as half of the patients are not responsive to the first drug treatment (Rush et al., 2006). Unfortunately, the pathophysiology of anxiety is not well understood, creating difficulty in the generation of more effective treatments. In order to better study anxiety-related behaviors animal models of anxiety have been created, such as the elevated plus maze (EPM) and the open field. To identify brain regions that have a role in influencing anxiety in these paradigms, numerous lesion studies have been conducted. These studies have identified several brain regions that are required for normal anxiety-like behavior in rodents, such as the ventral hippocampus (vHPC) (Bannerman et al., 2004), and the medial prefrontal (mPFC) (Shah and Treit, 2003). Although many brain areas are now known to be involved in anxiety, the activity of the neural circuitry underlying anxiety has not been studied. To this end, we have characterized the activity in the vHPC-mPFC pathway during anxiety in rodents. In order to describe these results in the context of previously published reports, an overview of the related literature is provided in this chapter. First, innate anxiety-like behaviors in rodents will be discussed and contrasted to learned fear. Second, the behavioral paradigms used to study such innate defensive behaviors and the pharmacological validity of these paradigms will be evaluated. Third, the neural circuitry thought to be involved in anxiety will be discussed, with an emphasis in the vHPC-mPFC pathway. We

will then review the literature on the functional differentiation between the ventral and dorsal poles of the hippocampus. Lastly, previous reports of recordings in the HPC-mPFC pathway during other behavioral conditions will also be discussed. Emphasis will be given to activity in the theta range (4-12 Hz), as it has been suggested to be propagated from the hippocampus to the mPFC (Siapas et al., 2005; Sigurdsson et al., 2010; Taxidis et al., 2010) and to have a role in anxiety (Gordon et al., 2005; McNaughton and Gray, 2000).

Innate anxiety and learned fear

Anxiety disorders arise from exaggerations or maladaptive use of defensive behavioral patterns that under normal circumstances help an organism respond appropriately to threats in its environment. Unfortunately, the pathophysiology of anxiety is poorly understood. A common approach of understanding a disease state and testing potential treatments is to develop an accurate animal model. The principal issue to resolve is how to develop animal models of relevance to human disorders. This is especially problematic with symptoms of psychiatric disorders such as anxiety disorders, as it is not trivial to estimate how anxious an animal is.

In mice, while it is not possible to measure anxiety directly, measuring avoidance from aversive stimuli is straightforward. Given a choice between two rooms in a given apparatus, for example, a mouse will avoid a room in which it has previously received a shock; it has learned to be afraid of that room. Similarly, given a choice between a bright room and a dark room, a mouse will avoid the bright room; mice are innately afraid of bright lights, presumably because light makes them more visible to potential predators.

The repertoire of defensive behaviors in animals extends beyond simple avoidance. Animals engage in a progression of defensive behaviors. When faced with an environment suggestive of a potential threat, rodents engage in approach/avoidance behavior. An actual threat (such as the presence of a predator) evokes an escape response; an immediate threat (such as a predator about to strike) evokes freezing behaviors. The animal literature tends to classify approach/avoidance and other responses to *potential* threats as “anxiety,” and freezing and other responses to *immediate* threats as “fear.”

Defensive fear and anxiety behaviors have been extensively studied in rodents, using behavioral paradigms that test such behaviors in response to both learned and innately threatening stimuli. Fear responses to immediate threats have typically been studied in the context of learning – animals are taught that particular stimuli signal threats. These learned fear stimuli then evoke a pattern of behavior consistent with the immediate presence of danger. In contrast, anxiety-like responses to potential threats have typically been studied in the context of innate responses to non-learned stimuli. Behavioral paradigms to study both learned (fear) and innate (anxiety-like) defensive behaviors have been developed for rodents. The rationale and validity of these models will be discussed below.

Learned fear in rodents

A principal advantage of learned fear is that it can be easily modeled in rodents, an approach which has been exploited by numerous groups to identify the neural circuits responsible for the learning, expression and regulation of fear responses (Davis, 1997; LeDoux, 2003; Quirk and Beer, 2006). All learned fear paradigms involve the same basic elements: a standardized, neutral stimulus (for example, a particular tone); a directly threatening stimulus (such as a mild shock); and a behavioral or physiological measure of the fear response (such as freezing behavior or increase in heart rate). In the often-studied paradigm of conditioned freezing to tone, a rat or mouse is presented simultaneously with both a neutral tone and a mild electrical shock. The animal rapidly learns that the tone predicts a shock through a process known as classical conditioning. Subsequent playback of the same tone evokes a freezing response, in which the animal stops exploring its cage and remains motionless while the sound is being played.

Indeed, playback of the fear-conditioned tone induces a host of behavioral and physiological fear behaviors that can be measured in rodents, revealing a network of activated brain regions responsible for each (Davis, 1997). Increased heart and respiratory rate, dilated pupils, decreased responses to pain, facial expressions of fear, increased startle responses, defecation and urination, and stimulation of the corticosteroid release have been documented in rodents exposed to fear-conditioned stimuli. Specific brain regions, such as the hypothalamus

and various brainstem nuclei, are involved in the expression of specific fear responses. The activation of the lateral hypothalamus leads to increased activity in the sympathetic nervous system and tachycardia and pupillary dilation. Activation of the midbrain central gray leads to freezing behavior. The roles of each of these regions were established through a combination of lesion and electrical stimulation studies: Lesioning a specific region abolishes and stimulating that region mimics the fear response for which that region is responsible.

Neurons in the amygdala send their axons to each and every one of the brain regions responsible for the various fear reactions. Lesions of the central nucleus prevent all of the various fear reactions to conditioned stimuli; stimulating the central nucleus mimics a variety of these responses (Davis, 1997). The central nucleus serves to trigger the myriad fear-related behavioral and physiological responses to conditioned stimuli by activating specific brain areas in the hypothalamus and brainstem. The central nucleus is activated by the basolateral nucleus of the amygdala, which in turn is activated by thalamic auditory nuclei. However, the basolateral nucleus is only activated by the conditioned tone due to NMDA receptor–mediated plasticity of thalamic input. Thus, learned fear is a process dependent on facilitation of the thalamic input to the amygdala, which in turn leads to expression of a set of defensive behaviors by activating downstream areas such as the periaqueductal grey.

Innate anxiety paradigms in rodents

Learned fear allows an animal to adapt flexibly its behavior according to relevant environmental demands. However, not all defensive behavior is learned, as animals also display innate aversiveness to certain stimuli. Rodents are innately fearful of bright lights, as given a choice of a bright or dark room a rodent will spend most of its time exploring the dark room. Rodents avoid bright and open spaces presumably because these animals are more vulnerable to potential predators in such environments. Several behavioral paradigms have been developed over the years to measure anxiety related behaviors in rodents. These anxiety tests explore the conflict between approach and avoidance behaviors displayed by rodents placed in a novel environment. When exposed to a new place, rodents have a drive to explore the environment, an adaptive trait

considering that, in their natural habitat; rodents depend on foraging to find food. However, a novel environment is also potentially threatening for a rodent, for rodents may be more exposed to predators in such locations. Rodents therefore take a cautious approach to exploring novel settings, exhibiting approach/avoidance behaviors and physiological signs of arousal. Moreover, rodents tend to spend more time in the safer (e.g., less exposed) areas of the new environment, an easily measured trait that has been exploited in several laboratory-based tests of innate anxiety (Whishaw et al., 2006). In the open field test, for example, a large, well-illuminated circular arena is surrounded by high walls; mice and rats tend to avoid the brightly lit center and spend most of their time near the walls (Belzung and Griebel, 2001; Crawley, 1985; Prut and Belzung, 2003). The fraction of time spent in the periphery vs. the center of the field is used as behavioral measure of anxiety. A similar preference for closed spaces is seen in the elevated plus maze test, in which rodents prefer either of two enclosed arms to two open ones, and the light-dark test, in which they spend most of their time in the dark half of a two-chambered environment (Belzung and Griebel, 2001; Montgomery, 1955; Pellow et al., 1985; Rodgers, 1997). Findings such as elevated plasma levels of the stress-related hormone corticosterone support the notion that these tests are indeed anxiogenic (Cruz et al., 1994; Pellow et al., 1985).

Not all tests of anxiety rely on physical aspects of the environment to induce defensive behaviors. In the social interaction test, a paradigm used as a model of social anxiety, a similar approach/avoidance conflict occurs (File and Seth, 2003). In this test the dependent variable is the time two rats spend in social interaction (sniffing, grooming, etc). The conflict in this test is between the drive to interact socially and the risk of being harmed by the other animal. Rodents that are more anxious spend less time interacting with others. Although the nature of the stimuli in this test is different from that in the EPM and in the open field, all these tests fundamentally exploit approach/avoidance conflicts to measure anxiety-related behavior. Interestingly, there are suggestions of both similarities and differences in the neurobiology underlying these different tests of innate anxiety. In general, animals that perform on the anxious end of the scale on one test often tend to perform on the anxious end of the scale on other tests. However, factor analysis suggests that there are several independent factors contributing to anxiety in the tests (Aguilar et

al., 2002; Griebel et al., 1996; Ramos et al., 1997). Thus, any given animal might avoid the open arms of the plus maze, for example, and subsequently fail to avoid a novel animal in the social interaction test. Such findings raise the possibility that there are different kinds of innate anxiety.

The principal advantage of these tests is that they explore innate behaviors. They are thus thought to examine ethologically relevant sources of anxiety, and may reflect a different neural circuitry compared to learned behaviors. Given that many human anxiety disorders are not fully explained by learned responses to fearful stimuli, understanding the neural circuitry of innate anxiety in animals may be of use in understanding anxiety disorders. Moreover, these tests of anxiety have been exploited both to screen for novel pharmacological compounds, as described below, and to screen genetically altered mice for anxiety-related phenotypes.

The effects of anxiolytic and anxiogenic drugs on anxiety tests in rodents

Although these innate tests appear to accurately model aspects of normal and pathological anxiety in humans, such tests would not be very useful if they lacked pharmacological validity: Drugs that reduce or increase anxiety in humans, ought to have similar effects in these laboratory-based tests of rodent behavior. As the most commonly used anxiolytic drugs in humans are benzodiazepines (such as diazepam) and serotonin reuptake inhibitors (SSRIs; such as fluoxetine), these two classes of drugs have been used extensively to validate rodent conflict anxiety tasks. Benzodiazepines reduce anxiety in virtually all tests of innate anxiety. In the open field these drugs increase time spent in the aversive center (Britton and Britton, 1981; Crawley, 1985; Pellow and File, 1986; Schmitt and Hiemke, 1998; Siemiatkowski et al., 2000). In the social interaction test, they increase interaction time (de Angelis and File, 1979; File and Hyde, 1979). In the elevated plus maze, they increase time spent on the exposed arms (Cruz et al., 1994; Pellow and File, 1986), and in the light-dark test these drugs increase time spent exploring the bright compartment (Bourin and Hascoet, 2003).

The effects of SSRIs are much more complex (Gordon and Hen, 2004). It is noteworthy that SSRIs are anxiogenic in humans when given acutely (Grillon et al., 2007) and anxiolytic during chronic treatments (Gorman et al., 2002).The effects of both acute and chronic SSRI

treatment have been tested in animal models of anxiety. Similarly to the data in humans, in the open field, chronic but not acute fluoxetine was found to be anxiolytic, increasing center time (Dulawa et al., 2004) although others have failed to see such effects (Durand et al., 1999). In the social interaction test, acute treatment with the SSRIs appears to be anxiogenic, decreasing interaction time (Bagdy et al., 2001; Dekeyne et al., 2000; To and Bagdy, 1999). The effects of chronic treatment with the SSRI fluoxetine in the social interaction test are unclear, as it has been reported to be both anxiogenic (Kantor et al., 2001) or to have no effect (To and Bagdy, 1999). The effects of SSRI treatments in the elevated plus maze are similarly inconclusive. Generally, acute treatments with SSRIs are anxiogenic, increasing avoidance of the open arms (Drapier et al., 2007; Griebel et al., 1994), in agreement with human studies. The effect of chronic SSRIs in elevated plus maze, however, are unclear, as some studies show increased anxiety (Griebel et al., 1999; Silva and Brandao, 2000) while other reports show decreased anxiety (Durand et al., 1999; Griebel et al., 1994; Kurt et al., 2000). The one consistent finding from these studies is that acute SSRI administration is anxiogenic, as it seems to be in anxiety disorder patients.

The inconsistent effects of chronic SSRIs in tests of innate anxiety are troubling, given that these drugs are typically effective in many patients with anxiety disorders. However, not all patients (and not all disorders) benefit from even chronic SSRI administration. Furthermore, the inconsistency in the animal literature may be the result of methodological differences between laboratories in what is a relatively young field of research. While the SSRI data at present do not firmly support the validity of these tests as models of human anxiety disorders, it is perhaps too early to make a conclusion on this issue.

Neural circuitry of innate anxiety

The validity of learned fear models has been confirmed in part by neuroanatomical approaches in animals. Contrary to learned fear, which is centered in the amygdala, the neuroanatomical basis of innate anxiety tests suggest a network of sites, closely aligned with but somewhat separate from the learned fear network. Unlike the clear effects of amygdala lesions and manipulations on fear conditioning, most lesion studies suggest that the amygdala is not required for innate anxiety

(Kjelstrup et al., 2002; Kondo and Sakuma, 2005; Moller et al., 1997). Instead, lesions of a related network of sites disrupt anxiety-like behavior in these tests, including the ventral hippocampus (vHPC), the medial prefrontal cortex (mPFC), and the bed nucleus of the stria terminalis. Lesions of these regions result in effects that are similar to those of benzodiazepines in several of these tests, reducing open arm and bright chamber avoidance and increasing social interaction, among other effects (Bannerman et al., 2004; Duvarci et al., 2009; Gonzalez et al., 2000; Kjelstrup et al., 2002; Lacroix et al., 2000; Shah and Treit, 2003; Treit et al., 1998; Walker et al., 2009). The vHPC, mPFC and bed nucleus are components of the limbic system, a circuit involved in the generation of emotional behaviors; each also is tightly connected with the amygdala. Intriguingly, lesions in all of these areas decrease anxiety in the same anxiety paradigms, and these three areas are interconnected, suggesting that they may be part of a putative anxiety-related circuit. Moreover, these areas also send efferent output to many of the same downstream regions as the central nucleus of the amygdala, such as the hypothalamus and brainstem. They are therefore well situated to generate and/or modulate anxiety-related behaviors either independent from or in concert with the amygdala.

While the aforementioned lesion studies have shown that the amygdala is not required for normal anxiety-like behavior in innate anxiety tests, there is considerable evidence that it nonetheless plays an accessory role. Infusing drugs (typically inhibitory agents such as GABA receptor agonists and benzodiazepines) into an otherwise intact amygdala has profound effects in several of these tasks, including the elevated plus maze, open field and social anxiety tests (Green and Vale, 1992; McNamara and Skeleton, 1993; Pesold and Treit, 1995; Sanders and Shekhar, 1995; Zangrossi Junior and Graeff, 1994).

Neuroanatomical data supports the notion that the various structures implicated in innate forms of anxiety are part of the same circuit as the amygdala. For example, both the vHPC and the mPFC project to many of the same brainstem structures involved in producing defensive behaviors, such as the periaqueductal grey (Burwell et al., 1995; Vertes, 2004), as does the central nucleus of the amygdala (Veening et al., 1984). Moreover, the BNST, mPFC and vHPC each project directly to the amygdala itself (Burwell et al., 1995; Vertes, 2004), suggesting that

the separable innate anxiety and learned fear pathways nonetheless are capable of interacting. Importantly, both the mPFC and the vHPC receive highly processed contextual information from association cortices and rhinal cortices (Hoover and Vertes, 2007). This suggests that the mPFC and the vHPC are in an ideal position to evaluate threats in the environment and activate downstream structures (such as the brainstem) to induce defensive responses.

Studies of neural activity also confirm that notion that the hippocampus, mPFC and amygdala work together in both innate anxiety and learned fear. For example, although the hippocampus is not required for normal freezing responses to fear conditioned tones, neural activity in the hippocampus nonetheless synchronizes with activity in the amygdala during presentation of the tone (Seidenbecher et al., 2003).

These findings suggest that the mPFC, vHPC, amygdala and BNST are indeed part of a functional circuit involved in the generation and modulation of defensive behaviors. While certain elements of the circuit play particularly important roles in certain forms of anxiety (BNST for light-enhanced startle, an innate response; amygdala for fear conditioning to tone, a learned response), it is likely that under normal circumstances the circuit operates together to compare and evaluate threats in the environment and generate the appropriate specific defensive responses.

vHPC-dHPC differentiation

Intriguingly, several lines of evidence indicate that the hippocampus is not functionally homogenous. Rather, the dorsal and ventral (or septal and temporal, respectively) poles of this structure appear to have differences in anatomy, physiology and gene expression (Fanselow and Dong), indicating that the dHPC and vHPC have different functions. Furthermore, lesion studies have found that the vHPC and the dHPC are required for different behaviors.

Lesion studies have shown that the vHPC is required for normal anxiety-related behaviors in rodents (Kjelstrup et al., 2002). Intriguingly, while the vHPC has been implicated in anxiety, its dorsal counterpart has not. For instance, lesions of the vHPC, but not of the dHPC increase exploration of the aversive open arms of the EPM (Bannerman et al., 2004; Kjelstrup et

al., 2002). Similar results, indicating a dissociation of function along the long axis of the hippocampus, were also obtained in several other innate anxiety tests. For example, animals with vHPC, but not dHPC, lesions displayed reduced hyponeophagia (i.e., displayed a shorter latency to eat food in a novel environment), had higher social interaction and were quicker to cross from the black (safer) to the white (more anxiogenic) compartment in the two-compartment test (Bannerman et al., 2002). Furthermore, a decrease in the display of defensive behaviors in vHPC, but not dHPC, lesioned rats was also found in a test of learned fear, as vHPC lesioned rats freeze less during contextual fear conditioning (Maren, 1999; Maren et al., 1997). Thus, in diverse behavioral paradigms vHPC, but not dHPC, lesioned rodents display a decrease in defensive behaviors, similarly to rats treated with anxiolytic drugs such as benzodiazepines (Bourin and Hascoet, 2003; Britton and Britton, 1981; de Angelis and File, 1979).

The dHPC, in contrast to the vHPC, does not seem to be required for normal behavior in anxiety tests, but instead appears to play a role in spatial working memory and navigation tests, as performance in the Morris water maze has been shown to require the dHPC, but not the vHPC (Kjelstrup et al., 2002). Furthermore, lesions of the dHPC, but not the vHPC, were also reported to impair performance in other spatial memory tests, such as the alternation T-maze (Bannerman et al., 2002) and the radial arm maze (Pothuizen et al., 2004).

Results from lesion studies generally suggest that the vHPC is preferentially involved in tasks related to mood and defensive behaviors, whereas the dHPC has a role in learning, memory and spatial navigation. Interestingly, the anatomy of these areas also supports a similar distinction, as the dHPC is mainly connected to areas involved with spatial representation and cognition while the vHPC is strongly connected to limbic structures, supporting a role for the vHPC in defensive behaviors (Swanson and Cowan, 1977).

The most prominent projection of the dHPC is to the entorhinal cortex (Swanson and Cowan, 1977), an area in which a high density of grid cells is found (Moser et al., 2008), indicating a role in spatial representation. Interestingly, the dorsal, but not ventral, entorhinal cortex is required for normal spatial memory (Steffenach et al., 2005), suggesting that the hippocampal dorso-ventral differentiation may be inherited from its major input area, the rhinal

cortices. Moreover, dHPC CA1 cells project strongly to the dorsal subiculum (Amaral et al., 1991), which is the region of the subiculum with the highest density of head direction cells (Taube, 2007). The dorsal, but not ventral pole of the hippocampus, also projects robustly to retrosplenial and anterior cingulate cortices (Cenquizca and Swanson, 2007), which are areas thought to be involved in processing of visuospatial information (Frankland et al., 2004; Lavenex et al., 2007). Furthermore, the dHPC, but not the vHPC, also projects to the mammilllary nucleus (Ishizuka, 2001; Kishi et al., 2006), an area with a high density of cells encoding navigation-related information (Taube, 2007). Thus, the dHPC projects primarily to areas involved with spatial navigation and exploration, suggesting that the dHPC also has a prominent role in these processes.

The vHPC, on the other hand, appears to be connected primarily to areas involved in defensive behaviors and mood regulation. The vHPC is bidirectionally connected to the posteromedialcortical and posterior basomedial amygdalar nuclei (Cenquizca and Swanson, 2007), which are structures that influence freezing (LeDoux, 2000). Furthermore, the lateral and basolateral nuclei of the amygdala project to the vHPC and the ventral subiculum (Petrovich et al., 2001; Pitkanen et al., 2000).These nuclei are required for ffear conditioning, supporting a role for the vHPC in defensive behaviors. The vHPC also projects to the BNST (Canteras et al., 1992), an area known to be involved in innate anxiety (Duvarci et al., 2009; Walker et al., 2009). In summary, the connectivity of the vHPC suggests that this structure is involved in anxiety and defensive behaviors, contrary to the dHPC, which is more involved in spatial navigation.

As expected from the differential connectivity displayed by the vHPC and the dHPC, the physiology of these structures is also remarkably distinct. Pyramidal cells from the dHPC ("place cells") have been extensively studied due to their spatially selective-firing properties (Harris et al., 2003; Moser et al., 2008). Reports of recordings from vHPC cells show that only a small fraction of ventral pyramidal cells have place fields (Kjelstrup et al., 2008). Furthermore, the place fields of vHPC cells are much larger and have less-well defined boundaries compared to dHPC place fields (Jung et al., 1994; Kjelstrup et al., 2008; Royer et al., 2010). Intriguingly, vHPC cell firing seems to be related to behavioral demands of the task being performed, as a disproportionately

large fraction of the observed place fields occur near the reward locations of the task (Kjelstrup et al., 2008; Royer et al., 2010). Furthermore, in rats exploring an eight arm radial maze in which six arms were enclosed by high walls and two arms were open platforms, several cells in the vHPC, but not in the dHPC, fired selectively in both open arms (Royer et al., 2010), even though the arms were far from each other. These results indicate that whereas dHPC cells represent context at a fine spatial scale, vHPC cell firing seems to be modulated by task-demand and might be involved in large-scale contextual representation.

Remarkably, functional differentiation across the long axis of the hippocampus was found in large-scale gene expression studies as well, in agreement with anatomy and physiology results suggesting that the vHPC and dHPC have distinct functions. Previous reports have identified dozens of genes that have expression patterns that vary across the septo-temporal axis of the hippocampus (Dong et al., 2009; Leonardo et al., 2006; Thompson et al., 2008). These genes encode proteins with diverse functions, such as intracellular signaling molecules, cell adhesion proteins and ion channels (Dong et al., 2009; Leonardo et al., 2006), indicating that the molecular heterogeneity between the dHPC and the vHPC is likely to have important and wide-ranging functional consequences.

Thus, results from gene expression, physiology and anatomy studies suggest, with remarkable consistency, that the dHPC and the vHPC have different functions. Intriguingly, all of these studies indicate that no sharp boundary exists between the dHPC and the vHPC. Rather, both anatomical projections and molecular markers change gradually across the long axis of the hippocampus. Furthermore, place fields of cells in the intermediate hippocampus are larger than those of the dHPC (Jung et al., 1994), but smaller than the ones displayed by vHPC cells (Kjelstrup et al., 2008). This pattern of results demonstrates that while dramatic differences between the vHPC and the dHPC exist, there is no clear anatomical boundary between these structures.

The hippocampus-mPFC circuit

As discussed above, anatomy and lesion studies suggest that the BNST, the vHPC and the mPFC may form a functional circuit involved in anxiety. As a first step to characterize the activity of this circuit, we recorded activity in the mPFC-vHPC pathway. Several reports of simultaneous recordings form the hippocampus and the mPFC from awake-behaving rodents (Jones and Wilson, 2005; Siapas et al., 2005; Sigurdsson et al., 2010) suggest that input from the hippocampus affects mPFC neural activity. To this end it has been shown that mPFC cells are more likely to fire after hippocampal cells fire (Siapas et al., 2005), suggesting that firing of mPFC cells may be induced by hippocampal activity. Furthermore, mPFC cells are more synchronized, as measured by phase-locking, to hippocampal theta oscillations (4-12 Hz) if the spike train is shifted into the past by a short temporal offset (Siapas et al., 2005; Sigurdsson et al., 2010), which presumably reflects the conduction and synaptic delay of the pathway. Lastly, it has been shown that in urethane-anesthetized rats the directionality of functional connectivity in the theta range, as measured by partial directed coherence, is from the hippocampus to the mPFC (Taxidis et al., 2010).

The finding that hippocampal theta activity leads mPFC activity is interesting, as theta is the most prominent oscillation of the hippocampus in an ambulating rodent, and hippocampal pyramidal cells phase-lock robustly to the ongoing theta oscillation, both in the dHPC (Buzsaki, 2002; Harris et al., 2003) and the vHPC (Royer et al., 2010). These results suggest that contextual information from the hippocampus is propagated to the mPFC through theta range activity. In line with this idea, hippocampal-mPFC theta synchrony increased during epochs of working memory (Jones and Wilson, 2005; Sigurdsson et al., 2010). Modulation of theta synchrony due to changes in behavioral demands of the task being performed has also been reported between the hippocampus and other downstream target areas. For example, theta-range correlations increased between the hippocampus and the amygdala during fear conditioning (Seidenbecher et al., 2003), and between the hippocampus and the striatum during learning of a working-memory task (DeCoteau et al., 2007).

Thus, modulation of theta range synchrony between the hippocampus and downstream target areas according to behavioral demands may be a general feature of circuits involving the hippocampus. However, it is noteworthy that all the simultaneous hippocampal-cortical recordings were performed in the dHPC, which contrary to the vHPC, does not have a direct robust projection to the mPFC. Thus, it is not known whether synchrony between the vHPC and the mPFC is modulated by behavioral demands in the same way as dHPC-mPFC synchrony. Nevertheless, considering that the hippocampus and the mPFC are both required for the same anxiety paradigms, such modulation of theta synchrony might also occur during anxiety. Intriguingly, previous authors have argued for a link between theta oscillations and anxiety.

Theta oscillations and anxiety

An association between theta oscillations and anxiety was proposed by Gray and McNaughton (McNaughton and Gray, 2000). The proposed link is based on four suppositions: First, the actions of anxiolytic drugs in animal models can provide important insights for anxiety in humans. Second, all anxiolytic drugs act by decreasing the activity of the behavioral inhibition system, in which the septum and the hippocampus have prominent roles. Third, all anxiolytic drugs impair theta-range activity in the septo-hippocampal pathway. Fourth, changes in the function of the septo-hippocampal system, by modulating theta activity, may influence normal and pathological anxiety states (McNaughton and Gray, 2000).

While this theory has not gained wide acceptance, most of its basic tenets are supported by experimental evidence. For instance, both in rodents (Bourin and Hascoet, 2003) and in humans (Rao and Zisook, 2009) benzodiazepines decrease anxiety, suggesting that the neurobiological underpinnings in both share some similarities. Furthermore, hippocampal lesions have been shown to decrease behavioral inhibition and to increase exploration of aversive environments (Bannerman et al., 2002; Bannerman et al., 2004; Kjelstrup et al., 2002). Lastly, several anxiolytic drugs have been shown to decrease theta-range activity in the septo-hippocampal system (Quintero et al., 1985; Zhu and McNaughton, 1994) and it is known that theta range activity is a very prominent feature of these structures (Buzsaki, 2002; Buzsaki et al.,

2003). However, currently, the association between theta oscillations and anxiety is only weakly supported by experimental evidence. To this end, it has been shown that rats treated with anxiolytics have a lower propensity to display hippocampal theta oscillations (Quintero et al., 1985; Zhu and McNaughton, 1994). Furthermore, it has also been reported that 5-HT1A receptor knockout mice, a genetic model of increased anxiety, have larger hippocampal theta oscillations during exploration of the EPM compared to wild type mice (Gordon et al., 2005). It is important to note that these results are correlational, and do not establish whether there is a causal link between hippocampal theta activity and anxiety. Unfortunately, this hypothesis is difficult to test, as it is unclear how to disrupt theta activity without impairing hippocampal function in general. Emerging approaches such as optogenetics may prove valuable in investigating the role of theta oscillations in anxiety.

1.2 Approach

As explained above, although anxiety disorders are highly prevalent, the mechanisms underlying pathological and normal anxiety-related responses are not well understood. Lesion studies have demonstrated that normal anxiety-related behaviors in rodents are disrupted following lesions of several brain areas, such as the mPFC and the vHPC. However, there are no recordings in these areas obtained from animals experiencing heightened anxiety. In order to understand the neural underpinnings of anxiety-related circuits it is necessary to study the activity in areas required for anxiety, such as the vHPC and the mPFC, during exploration of anxiogenic environments. Intriguingly, there is a unidirectional direct projection from the vHPC to the mPFC, suggesting that flow of vHPC information to the mPFC may have a role in guiding behavior during anxiety. However, it is not known if the vHPC and mPFC are part of a circuit relevant for anxiety. Although it is not known if these areas synchronize with each other during anxiety, it has been shown that theta range synchrony between the hippocampus and the mPFC varies according to behavioral demands in working memory tasks, suggesting that propagation of hippocampal theta activity to the mPFC may play an important role in this circuit. Considering these previous

findings, we hypothesize that the mPFC follows the vHPC, that vHPC-mPFC theta-range synchrony is modulated by anxiety and that neural correlates of anxiety exist in these structures. Before analyzing the relationship between these areas during anxiety, we sought to find evidence suggesting that activity from the vHPC may be propagated to the mPFC. To this end, we developed a straightforward method to estimate the lag between two brain areas, enabling us to study the directionality of functional connectivity between the vHPC and the mPFC (chapter 2). This method indicated that the vHPC leads mPFC activity in the theta range, suggesting that activity in this frequency range is transmitted along the vHPC-mPFC pathway. Next, in chapter 3, we studied the vHPC-mPFC circuit during anxiety. In order to identify changes in activity in these brain areas related to anxiety, we compared recordings obtained in a control environment with those from two anxiogenic arenas, the EPM and the open field. These analyses showed that theta-range synchrony between the vHPC and the mPFC increased during anxiety. Lastly, in chapter 4, we studied the activity of mPFC single units and their synchrony to vHPC LFPs during exploration of the elevated plus maze (EPM). Data from chapter 4 suggest that a large fraction of mPFC units have firing patterns that are related to anxiogenic features of the EPM and that units with anxiety-associated firing patterns are more robustly synchronized to vHPC input in the theta range.

Chapter 2

Cross-correlation of instantaneous amplitudes of field potential oscillations: a straightforward method to estimate the directionality and lag between brain areas

Cross-correlation of instantaneous amplitudes of field potential oscillations: a straightforward method to estimate the directionality and lag between brain areas

2.1 Introduction

Anatomy studies show that there is a unidirectional monosynaptic projection from the vHPC to the mPFC, suggesting that vHPC activity may be propagated to and influence the mPFC. In agreement with this notion, previous studies have shown that mPFC units phase lock more robustly to hippocampal theta of the past (Siapas et al., 2005). The lag between mPFC spikes and hippocampal fields presumably reflect the conduction and synaptic delay of the pathway. However, it is unclear if a lag between the mPFC and the hippocampus can be estimated using only local field potentials (LFPs), which are more easily obtainable than spikes. To address this issue we developed a method to estimate the lag between brain areas using only LFP recordings.

It is noteworthy that estimating the directionality of functional connectivity using LFPs is of general interest, as recent advances in multi-site recording technology have enabled researchers to sample LFPs simultaneously from multiple brain regions (DeCoteau et al., 2007). A common interest in such studies is to determine whether one brain region is leading or lagging relative to another, and to estimate the time lag between putatively connected areas. Several groups have estimated the lag across brain areas using recordings of spike trains. Most of these studies estimate directionality by calculating the cross-correlation of spike trains of two areas (Alonso and Martinez, 1998; Holdefer et al., 2000; Lindsey et al., 1992; Snider et al., 1998). Other studies have used related approaches, such as calculating the cross-covariance of spike trains (Siapas et al., 2005), or different methods, such as the computation of spike-triggered joint histograms(Paz et al., 2009) or the change in phase-locking after shifting the spikes relative to the LFP (Siapas et

al., 2005). Although such methods are effective, they are not applicable to studies that record only LFPs. This situation is common, as often spike trains cannot be sampled from multiple areas, or firing rates are too low to determine the directionality of functional connectivity across regions. Recording LFPs in areas with low firing rates can be advantageous, as LFPs can be sampled continuously, while spikes can occur infrequently and irregularly. LFP-based methods may therefore yield higher temporal resolution and greater statistical power than spike-based methods.

Existing methods such as Granger causality (Cadotte et al., 2010; Gregoriou et al., 2009; Popa et al., 2010) and partial directed coherence (PDC) (Astolfi et al., 2006; Baccala and Sameshima, 2001; Taxidis et al., 2010; Winterhalder et al., 2005) are able to estimate the directionality of functional connectivity using only LFPs. However, these methods are mathematically complex (Gourevitch et al., 2006), relying on multivariate models with a large number of free parameters, obscuring the intuitive understanding of what these methods are actually computing. They can also be sensitive to noise (Taxidis et al., 2010; Winterhalder et al., 2005). Furthermore, such methods generally do not provide estimates of the time lag between brain areas.

Here we report a novel and mathematically straightforward method to estimate the lag between two brain areas that does not require spikes and that can be applied to datasets in which only LFPs have been acquired. The method requires that functional connectivity between the examined structures be accompanied by reasonably coherent activity within a specific frequency range. The method consists of determining the position (or “lag”) of the peak of the cross-correlation of the amplitude envelopes of the LFPs after filtering for the frequency range of interest. Lastly, a non-parametric signed rank test is performed to verify if the distribution of lags obtained from multiple experiments differs from zero.

To investigate its validity, this method was applied to a dataset in which both spikes and LFPs were recorded from the medial prefrontal cortex (mPFC), while only LFPs were sampled from the ventral hippocampus (vHPC). These areas were chosen because there is

a unidirectional projection from the vHPC to the mPFC (Parent et al., 2009; Verwer et al., 1997), suggesting that activity in the vHPC should lead that in the mPFC. Moreover, we have shown theta-frequency (4-12 Hz) coherence between these structures during behavior (Adhikari et al.), suggesting that directionality analysis can be performed in this frequency range with the amplitude cross-correlation measure.

Using the amplitude cross-correlation method, we demonstrate that the vHPC leads the mPFC in the theta-frequency range, with a lag consistent with estimates of the conduction delay of this pathway. Furthermore, there is good agreement between vHPC-mPFC lags calculated with this method and those calculated from phase locking of mPFC spikes to vHPC theta oscillations. Finally, a consistent lag between the vHPC and the mPFC was only found in the theta, but not in the delta and gamma frequency ranges, in line with studies suggesting that theta-frequency oscillations drive functional connectivity between the hippocampus and the mPFC (Adhikari et al.; Jones and Wilson, 2005; Siapas et al., 2005). The current method was also compared to partial directed coherence (PDC), an existing method to calculate the directionality of functional connectivity with LFPs. This method, similarly to the amplitude cross-correlation method, also demonstrated that the vHPC leads the mPFC in the theta range. To further compare the two methods, both were applied to simulations in which pink noise was added to biological signals. Strikingly, PDC was more susceptible to errors induced by noise than the amplitude cross-correlation method. These results show that the cross-correlation of the amplitude of filtered field potentials may provide a valid, relatively robust estimation of the lag and the directionality of information flow across brain areas.

2.2 Results

Computation of the lag between two LFPs by amplitude cross-correlation

Each step of the method used to estimate the lag between two brain regions from LFPs is illustrated in Figure 2.1. Examples of simultaneously recorded traces from the vHPC and mPFC are shown in Figure 2.1A and 1B. The middle panels (Figure 2.1C and 3.1D) show the same

traces after filtering the signals in the theta range (7-12 Hz). This frequency range was chosen because it is the predominant hippocampal oscillation in the awake moving rodent (Buzsaki, 2002), and previous reports have suggested that hippocampal activity in the theta range may be propagated to the mPFC (Siapas et al., 2005). Note that the amplitude of the theta-filtered traces varies considerably across time. In order to obtain a reliable measure of the signal's amplitude with high temporal resolution, the Hilbert transform of the LFPs were calculated. The absolute magnitude of the Hilbert transform provides the amplitude of the signal for each time point at which the LFP was recorded. The amplitude traces (Figure 2.1C and D, grey traces) reveal the existence of a temporal microstructure that reflects increasing and decreasing theta oscillation power and is not readily apparent in the raw LFPs. Careful visual inspection of Figure 2.1E suggests that the peaks in vHPC theta amplitude precede those of the mPFC. Accordingly, the cross-correlation of the two amplitude traces (Figure 2.1F, grey trace) has a peak at a negative lag, indicating that theta activity in the vHPC leads that in the mPFC.

Cross-correlations of the amplitudes of the theta-filtered LFPs from 17 mice are shown in Figure 2.2. Note that most of the curves peak at a negative lag (dark red bands in Figure 2.2A). The mean of the distribution was negative (mean lag= -28.1 +- 16.7 ms, median= -9.5 ms) and significantly different from zero ($p<0.01$, Wilcoxon's rank sum test). The narrow peak of the vHPC-mPFC lag distribution (Figure 2.2A, lower panel) suggests that the estimate of the lag calculated through this method is consistent across animals. Although the distribution of lags appears to be bimodal, it is still significantly negative if the points with large negative lags (< 50) ms) are excluded. Finally, there was no correlation of the computed lag with the layer from which vHPC signals were recorded (data not shown).

Test of the amplitude cross-correlation method

To further test the validity of this method, the lag estimated with the amplitude cross-correlation method was compared with the lag computed through a previously published method (Siapas et al., 2005; Sigurdsson et al., 2010) that uses spikes and LFPs. In this method, the strength of phase locking of mPFC spikes to vHPC theta oscillations is

calculated after shifting the spike train both forwards and backwards in time. If neural activity in the vHPC leads that in the mPFC, phase locking of mPFC spikes to vHPC field potentials would be maximal when the spike train is shifted slightly to the past. Indeed, in line with previous reports (Siapas et al., 2005; Sigurdsson et al., 2010), mPFC spikes phase locked to hippocampal theta oscillations more robustly when shifted to the past (n=30 multiunit recordings from 12 mice, mean shift= -24.5±15.7 ms, $p<0.05$, Wilcoxon's rank sum test). Furthermore, the vHPC-mPFC lag calculated with the phase locking and the cross-correlation methods are not significantly different from each other or from the conduction delay (-16 ms) of the vHPC-mPFC pathway (Thierry et al., 2000) ($p>0.05$, Wilcoxon's signed rank test) indicating that both methods may provide valid estimates of the lag between the vHPC and the mPFC.

The amplitude cross-correlation method is frequency-specific

The above results indicate that the amplitude cross-correlation method can estimate lags that are in good agreement with the phase locking method and with the conduction delay of the vHPC-mPFC pathway. To further evaluate the amplitude cross-correlation method, vHPC-mPFC lags were calculated across multiple frequency ranges. We applied the amplitude cross-correlation method after band-pass filtering the LFPs in the delta (1-4 Hz), theta (7-12 Hz), low gamma (30-50 Hz) and high gamma (50-100 Hz) frequency bands (Figure 2.2C). Strikingly, a consistent and significant lag between the vHPC and the mPFC was only found at the theta range.

Applying the amplitude cross-correlation to areas that are bidirectionally connected

The above results suggest that the amplitude cross-correlation method can be applied to areas that have a unidirectional monosynaptic connection. However, often researchers wish to study the directionality of functional connectivity in areas that have indirect or bidirectional connections. To explore whether the method can be generalized to these situations, we applied it to simultaneous recordings from the dHPC and mPFC, which are

indirectly connected, and from the vHPC and dHPC, which are directly and bidirectionally connected.

The dHPC and mPFC are bidirectionally and indirectly connected, through the rhinal cortices, the vHPC and the *nucleus reuniens* of the thalamus (Burwell R.D. and Witter, 2002; Hoover and Vertes, 2007). In the dHCP-mPFC dataset, LFPs were sampled from the dHPC and single units and LFPs were recorded through stereotrodes from the mPFC. An example dHPC-mPFC theta amplitude cross-correlation (Figure 2.3A) shows that the peak occurs at a negative lag, suggesting that dHPC activity in the theta range leads the mPFC. Similar profiles were found in each of five animals (Figure 2.3B), and the population of lags obtained by this method (Figure 2.3C) has a significantly negative mean ($p<0.05$, Wilcoxon's test, mean lag=-15.4 ± 7.9 ms). As in the vHPC-mPFC dataset, we also calculated lags calculated using the spike-shift method in the same mice. A representative example of the effect of shifting the spike train relative to the dHPC LFP on the phase-locking strength (Figure 2.3B) shows that this unit phase locks more robustly to dHPC theta of the past (optimal lag=-17 ms). The distribution of optimal lags of for all the single units recorded (Figures 3.3 D and F) reveals that the mean of this distribution is significantly negative ($p<0.01$, Wilcoxon's test, mean lag=-20.2 ± 5.8 ms), in rough agreement with the lag calculated by the amplitude cross-correlation method and with previous reports (Siapas et al., 2005; Sigurdsson et al., 2010). These data suggest that the amplitude cross-correlation method can be used to estimate the directionality of functional connectivity and the lag across brain areas that have indirect, bidirectional connections.

In an awake-behaving rodent, the predominant direction of information flow is thought to be from the hippocampus to the cortex (Sigurdsson et al., 2010). Accordingly, we found that in both vHPC-mPFC and in the dHPC-mPFC datasets, hippocampal activity leads the mPFC. However, in many cases the predominant direction of information flow between the brain areas recorded may change across time (Gregoriou et al., 2009). To study the results of applying the method in such cases, we recorded LFPs simultaneously from the vHPC, dHPC and mPFC, and calculated lags from successive windows across

time. In line with the findings described above for the vHPC-mPFC recordings, a negative lag in the theta-filtered amplitude cross-correlation was present across time (Figure 2.4A), with peaks occurring consistently at negative lags (mean lag -12.5 ms, $p<0.001$, Wilcoxon's test; Figure 2.4A and 3.4C). Conversely, the lag between vHPC and dHPC varied across time, between positive and negative lags (Figure 2.4B). The mean lag between these areas connected monosynaptically and bidirectionally did not differ from zero across time (Figure 2.4D, mean lag – 3.3 ms in this example animal; histogram has one count per time window) and across animals (Figure 2.4E, mean lag –8.8±10.2 ms, histogram has one count per animal). This result suggests that when applied to bidirectionally-connected areas, the amplitude crosscorrelation method can reveal the temporal dynamics of the directionality of the circuit, by indicating which area is leading in a given time window.

In summary, these results demonstrate the utility of the amplitude cross-correlation method in examining bidirectionally and indirectly connected brain regions, and further demonstrate its utility in examining how directionality may change across time.

Comparison of amplitude cross-correlation method with Partial Directed Coherence

In order to compare the results of the amplitude cross-correlation with an existing method that calculates directionality with LFPs, we applied partial directed coherence (PDC) to the raw signals of the vHPC-mPFC dataset. Consistent with the results obtained using amplitude cross-correlation and phase-locking methods, PDC values averaged across animals had peaks in the theta-frequency range, and these peaks were significantly greater for the vHPC to mPFC (Figure 2.5B) direction than vice-versa. This result is also in line with a previous analysis of hippocampal-cortical connectivity with PDC in anesthetized rats (Taxidis et al., 2010).

To compare the two methods, we used simulations to analyze how sensitive each method is to noise. We first studied the amount of noise that must be added to a signal to prevent each method from identifying the directionality between two signals where the underlying directionality is known. To this end, a 2-second segment of a randomly chosen

vHPC recording was filtered in the theta-frequency range. A second signal was then created by shifting the original signal by 28 ms, resulting in two identical signals separated by a defined lag (Figure 2.6A). A 28 ms shift was chosen because it is the average lag calculated for the vHPC-mPFC pathway with the cross-correlation method. Varying levels of pink noise were then generated (10 levels of noise) and added to both signals in 500 independently generated simulations for each noise level (Figure 2.6B). For each simulation, the directionality was then calculated using both PDC and the amplitude cross-correlation methods. Figure 2.6C and D show the results of three example simulations at each of the 10 noise levels (the same three simulations are shown in both panels). In these examples, the amplitude cross-correlation method correctly quantified directionality and lag at noise levels at which the PDC failed to identify directionality. In general, across the population of simulations, PDC failed to identify the correct directionality at lower levels of noise than did the amplitude cross-correlation method ($p<0.05$, Fisher's exact test; Figure 2.6E and F).

Previous reports have demonstrated that PDC can incorrectly find directionality between signals when the two signals have different variances (Taxidis et al., 2010; Winterhalder et al., 2005). We therefore asked whether the cross-correlation method is similarly sensitive to the presence of different levels of noise across two signals. To do so, we first selected a one-minute sample of simultaneously recorded vHPC and mPFC signals. Both signals were filtered for the theta range. Short segments of the samples are shown in Figure 2.7A (Black traces). Note that the vHPC clearly leads the mPFC. Next, we added a constant and modest amount of pink noise to the mPFC signal, while adding varying amounts of noise to the vHPC signal (grey traces). The directionality between the two signals was then calculated using both PDC and amplitude cross-correlation methods. Noise was independently generated 500 times for each of the six levels of noise shown. Regardless of the ratio of noise added to the two signals, the amplitude cross-correlation method consistently indicated that the mPFC follows the vHPC. While increasing vHPC noise increased the variability in the detected lags, there was no effect of increasing vHPC

noise on the mean estimated lag (Figure 2.7B, $p<0.72$, one-way ANOVA). In dramatic contrast to the amplitude cross-correlation method, the directionality indicated by PDC was dependent on the amount of noise added to the vHPC signal (Figure 2.7C). When the ratio of noise added to the vHPC signal was smaller or equal to that added to the mPFC, PDC correctly identified the directionality. However, when the noise added to the vHPC signal was larger than that added to the mPFC, PDC incorrectly calculated the reverse directionality. These results indicate that PDC, but not the amplitude cross-correlation, is greatly biased if different signals have different amounts of noise in them. In such cases, PDC results suggest that the cleaner signal leads the noisier signal, independently of the underlying directionality, in line with previous reports (Taxidis et al., 2010; Winterhalder et al., 2005). The amplitude cross-correlation is less precise but equally accurate with the addition of differential amounts of noise.

While the PDC and amplitude cross-correlation methods both show appropriate directionality in our dataset, these simulations suggest that PDC may be less robust to noise that the amplitude cross-correlation. Interestingly, a similar susceptibility to noise was found with Granger causality, another multivariate autoregressive model-dependent measure of directionality, in both types of simulations (Figure 2.8).

2.3 Discussion

We report a novel, mathematically straightforward method to calculate the lag in neural activity between two brain areas utilizing multi-site LFP recordings. The method does not require sampling of spikes. The present data indicate that the amplitude cross-correlation method can estimate the principal direction of functional connectivity between two brain regions and provide a reliable and consistent estimate of the lag between them. We further demonstrate that in the hippocampal-prefrontal circuit, the lag calculated with the amplitude cross-correlation method is consistent with lags calculated through the phase locking (Siapas et al., 2005), and with the experimentally determined conduction delay between the two areas (Thierry et al., 2000). Each method indicates that the direction of functional connectivity is from the vHPC to the mPFC. We

further demonstrate that the amplitude crosscorrelation method can detect frequency-specific connectivity, and can identify indirect and bidirectional connectivity as well as monosynaptic, unidirectional connectivity. Finally, we demonstrate that the amplitude cross-correlation method is relatively robust to added noise, when compared to existing methods of determining directionality from LFPs.

The principal advantage of the method lies in its practicality and theoretical simplicity. Estimating directionality and lag using exclusively LFPs is of great value as LFP recordings are much more straightforward to obtain than single unit spike data, especially simultaneously from multiple areas. While widely used and straightforward methods for calculating directionality with LFPs exist, they are limited. Direct cross-correlation of filtered or raw signals, for example, can fail to produce reliable lag estimates even in the presence of large, synchronous oscillations. This failure results from the potential for variable phase offsets in the rhythms between the two LFPs (Figure 2.9), which does not contaminate the amplitude cross-correlation. Instantaneous phase difference is another method that has been used to calculate directionality (Gregoriou et al., 2009), even though it is unclear how to convert a phase difference in degrees into a lag in milliseconds, as each area may oscillate in a different peak frequency. For example, in the current data set, the mean phase difference between mPFC and vHPC is 0.22 radians. However, as mPFC and vHPC have different mean theta frequencies, converting this phase difference to a time lag will produce different results depending on whether mPFC or vHPC mean theta frequency is used to calculate the lag, and there is no justification for choosing one of the peak frequencies over the other. Furthermore, as phase is a circular measure, phase difference calculations cannot determine if a difference of 60 degrees indicates that signal 1 is leading signal 2 by 60 degrees or if it is lagging signal 2 by 300 degrees.

Mathematically more sophisticated methods to calculate the directionality of functional connectivity across brain areas with LFPs such as Granger causality and PDC also exist. These methods, while useful, are conceptually complex and not yet widely accepted in the literature. Moreover, Granger causality and PDC are not typically used to obtain lag estimates. As PDC and Granger are based on fitting multivariate regression models to a dataset, the data must conform

to several constraints, such as having stationarity and a Gaussian distribution. Furthermore, the residuals of the model must describe a white noise process (Cadotte et al., 2010; Gregoriou et al., 2009). In contrast, the data does not need to fulfill these conditions for the cross-correlation method to be applicable. In fact, the non-stationarity in power over time is precisely what is used to estimate directionality in the cross-correlation method. There are, however, three main advantages of PDC and Granger causality relative to our method. First, these methods can be applied to the entire frequency range at once, while the amplitude cross-correlation needs to be separately calculated for each frequency range and is therefore somewhat dependent on the choice of filter boundaries and filter type. Second, PDC and Granger causality provide a measure of the degree of functional connectivity in both directions, whereas the amplitude cross-correlation method only provides the overall directionality for a pair of areas. Third, if PDC and Granger causality are applied to datasets in which three or more areas were recorded, they will provide measures of functional connectivity for all possible brain area pairs in a single step. The cross-correlation method would have to be applied in separate steps for each pair of brain areas.

In order to compare PDC and the cross-correlation method we applied both to our dataset. Importantly, both methods were in good agreement with each other and with the spike-shift phase-locking method, indicating that on average, across animals, the vHPC leads the mPFC. However, simulations with noise indicate that the amplitude cross-correlation method may be more robust to certain types of noise, compared to PDC. First, the cross-correlation method is less sensitive when pink noise of equal amplitude is added to both signals. This result suggests that PDC is more likely to not find directionality if the frequency band of interest has low power in one of the signals, as is often the case. Second, if one of the signals has higher levels of noise than the other, PDC, but not the cross-correlation method, tends to indicate that the less noisy signal leads the noisier signal, as reported elsewhere (Taxidis et al., 2010; Winterhalder et al., 2005). This is a relevant point to consider, as the ratio of power in the frequency band of interest to total power can be widely different across brain areas. Although these simulations suggest the amplitude crosscorrelation method is more resilient to digitally added pink noise, further studies are needed to verify if this is the case in biological signals recorded in noisy conditions.

Although the amplitude cross-correlation method may be applicable to many datasets, it does have limitations that will potentially restrict its utility. One such limitation is that it will only produce positive results in the presence of coherent oscillations at a given frequency band. Moreover, it may not always be clear on which frequency band the method should be applied. In these cases, several steps can be taken to find the relevant frequency band at which directionality is present and is detectable. The most straightforward one is to use bands defined by prominent peaks in the coherence or power spectra in the brain areas of interest. Knowledge of previous literature may also be of help. For instance, the observations reported here rely on theta-frequency synchrony, which is known to be prominent between the hippocampus and its targets. However, gamma-frequency synchrony can occur across functionally connected cortical regions (Hermer-Vazquez et al., 2007), raising the possibility that the method reported here may be of use in evaluating cortico-cortical functional connectivity if applied to this frequency range. Lastly, in the absence of candidate frequency bands it is possible to apply the amplitude cross-correlation method in successive frequency windows over a broad range, for example, from 1 to 100 Hz. Indeed, we have used such an unbiased approach to show that the theta range is the only frequency band with a consistent and significant lag between the vHPC and the mPFC across animals in our dataset (Figure 2.10).

It is important to note that like any method to estimate lag or functional connectivity between areas, the amplitude cross-correlation method does not conclusively demonstrate a causal relationship. These analyses indicate only that mPFC activity follows vHPC activity, and does not prove that mPFC activity is driven by vHPC activity. Neither the current method nor the others mentioned here rule out the possibility that a third area drives both the vHPC and mPFC with different lags. Nonetheless, evidence of monosynaptic, unidirectional connectivity between the vHPC and mPFC has been demonstrated both anatomically (Parent et al., 2009; Verwer et al., 1997) and physiologically, (Thierry et al., 2000), consistent with the notion, suggested by the amplitude cross-correlation method, that the vHPC drives mPFC activity.

2.4 Materials and Methods

Animals

Three to six month old male wildtype 129Sv/Ev mice were obtained from Taconic (Germantown, NY, USA). Seventeen mice were used for the simultaneous mPFC and vHPC recordings. Sixteen mice were used for the simultaneous vHPC and dorsal hippocampus (dHPC) recordings. An additional cohort of five C57/Bl6 mice bred at Columbia University was used for the simultaneous dHPC and mPFC recordings, from which mPFC single units were isolated. The procedures described here were conducted in accordance with National Institutes of Health regulations and approved by the Columbia University and New York State Psychiatric Institute Institutional Animal Care and Use Committees.

Surgery and Microdrive Construction

Custom microdrives were constructed using interface boards (EIB-16, Neuralynx, Bozeman MT) fastened to a Teflon platform, as described previously (Adhikari et al.). Briefly, animals were anesthetized with ketamine and xylazine (165 and 5.5 mg/kg, in saline) and secured in a stereotactic apparatus (Kopf Instruments, Tujunga, CA). Screws were implanted on the posterior and anterior portions of the skull to serve as ground and reference, respectively. mPFC electrodes were implanted in the deep layers (V/VI) of the prelimbic cortex, at +1.65 mm anterior, 0.5 mm lateral and 1.5 mm depth, relative to bregma. vHPC electrodes were implanted in the CA1 region at 3.16 mm posterior, 3.0 mm lateral and 4.2 mm depth, and dHPC electrodes were targeted to 1.94 posterior, 1.5 lateral and 1.3 mm depth. Depth was measured relative to brain surface.

Behavioral Protocol

Animals were permitted to recover for at least one week or until regaining pre-surgery body weight. Mice were then exposed to a small rectangular box in the dark, in which they

foraged for pellets for 10 minutes for the mPFC-vHPC and vHPC-dHPC datasets. Mice performed an alternation task in a T- shaped maze for the dHPC-mPFC dataset as described in (Sigurdsson et al., 2010).

Data Acquisition

Recordings were obtained via a unitary gain head-stage preamplifier (HS-16; Neuralynx) attached to a fine wire cable suspended on a pulley so as not to add any weight to the animal's head. LFPs were recorded against a reference screw located at the anterior portion of the skull. Field potential signals were amplified, bandpass filtered (1-1000 Hz) and acquired at 1893 Hz. Multiunit activity from the mPFC was recorded simultaneously from the same electrodes used to obtain LFPs; multiunit signals were bandpass filtered (600-6000 Hz) and recorded at 32 kHz. Events exceeding a threshold of 40 μV were selected for analysis of phase locking to theta (see below). Both LFP and multiunit data were acquired by a Lynx 8 programmable amplifier (Neuralynx) on a personal computer running Cheetah data acquisition software (Neuralynx). The animal's position was obtained by overhead video tracking (30 Hz) of two light-emitting diodes affixed to the head stage.

Cross-correlation analysis.

Band-pass filtering

Data was imported into Matlab for analysis using custom-written software. To calculate the lag between the vHPC and the mPFC, signals were initially band-pass filtered between 7-12 Hz. A finite impulse response filter of order n, where n is the sampling frequency, was implemented with a Hamming window, utilizing the MATLAB function *fir1*.

Instantaneous amplitude using the Hilbert transform

The Hilbert transform of each signal was computed with the MATLAB function *hilbert*. The output of the Hilbert transform is a vector containing complex numbers that has the same number of elements as the input signal. The real portion of the complex number is the input

itself, while the imaginary part is the input LFP shifted by 90 degrees (π/2 radians). The absolute magnitude of the complex number at a given time point is the amplitude of the filtered signal at that sample. The magnitude of a complex number is the length of the vector in the complex plane.

All the results shown in the main text (Figures 3.1-3.4) were obtained by using the Hilbert transform to calculate the instantaneous amplitudes of the LFPs. Importantly, these results are not dependent on the specific method used to calculate instantaneous amplitudes, as they were reproduced using the Gabor Transform (Figure 2.11) (Le Van Quyen et al., 2001).

Cross-correlation of the instantaneous amplitudes

After the instantaneous amplitude for all the points in the vHPC and mPFC signals was calculated, the cross-correlation between the amplitudes of the two signals was computed with the MATLAB function *xcorr*, over lags ranging from +0.1 to -0.1 seconds. The mean amplitude was first subtracted from each vector prior to crosscorrelating them, as the DC component of a signal has no relevance for a cross-correlation. The lag at which the cross-correlation peaked was then determined. The significance of each vHPC-mPFC theta amplitude crosscorrelation was verified before inclusion in additional analyses using a bootstrap procedure. mPFC and vHPC theta-amplitude envelopes were randomly shifted 5-10 seconds relative to each other 1000 times. The shifted amplitude envelopes were then cross-correlated, yielding a distribution of cross-correlation peaks expected by chance. The original crosscorrelation was considered significant if its peak value was greater than 95% of these randomly generated cross-correlation peaks. The peaks of the mPFC-vHPC theta-filtered amplitude envelope crosscorrelations of all 17 animals were significant by this criterion.

Distribution of cross-correlation lags.

After cross-correlations of the filtered amplitude vectors were computed, the distribution of the lags at which the cross-correlation peaks occur was obtained. Wilcoxon's non-

parametric rank sum test was performed on the sample of lags to verify whether the mean of the distribution was significantly different from zero.

In the convention used in the current work, a negative lag indicates that the vHPC leads the other brain area.

Phase-locking analysis

In order to verify if the above method produces reliable estimates of the lag between two brain areas, the results were compared with an alternative method. In this method, the strength of phase locking of mPFC spikes to vHPC theta oscillations was computed after shifting the spike train by positive or negative shifts. Multiunit spikes represent all the spikes that exceeded 40 μV, whereas spikes for single unit measurements were clustered offline using spike sort 3-D (Neuralynx). Phase locking of spikes to oscillations was assessed by calculating the mean resultant length vector (MRL), a measure from which Rayleigh's z statistic of circular uniformity is derived (Sigurdsson et al., 2010).

To determine whether spikes were significantly phase-locked to theta, theta phases of LFPs were determined through the Hilbert transform, and a phase was assigned to each spike based on the time of the spike's occurrence. The phase is obtained by calculating the angle of the absolute magnitude of the Hilbert transform output. A phase of zero refers to the trough of the theta cycle. To determine the lag between multiunit activity and theta oscillations in each area, phase locking was calculated for 40 different temporal offsets for each multiunit recording, ranging from -100 to +100 ms. Recordings with significant Bonferroni-corrected phase locking in at least one of the shifts were used for the analysis in Figure 2.2.

Partial Directed Coherence

To compare the current method to an existing method of calculating directionality between LFPs, we analyzed our dataset using partial directed coherence (PDC) . PDC is a frequency-domain representation of Granger Causality. Given two time series $X_1(t)$ and $X_2(t)$, $X_2(t)$ is said to

Granger-cause $X_1(t)$ if knowledge of the past of $X_2(t)$ improves the prediction of $X_1(t)$ beyond how much the past of X_2 can predict itself in the present. $X_2(t)$ may Granger-cause $X_1(t)$ without $X_1(t)$ Granger-causing $X_2(t)$, in which case the predominant directionality would be from X_2 to X_1 ($X_1 \leftarrow X_2$). It is important to note that Granger-causation is directly related only to an increase in predictability and not to causality *per se* or to precedence in time of one signal relative to the other.

In order to compute Granger Causality of an m-variate time-series, a vector autoregressive model was fit to the process, as shown below and reported previously in more detail (Taxidis et al., 2010):

$$\begin{bmatrix} x_1(t) \\ \vdots \\ x_m(t) \end{bmatrix} = \sum_{r=1}^{p} A_r \begin{bmatrix} x_1(t-r) \\ \vdots \\ x_m(t-r) \end{bmatrix} + \begin{bmatrix} u_1(t) \\ \vdots \\ u_m(t) \end{bmatrix}$$

Here, the model was fit with MATLAB's ARFIT toolbox, with m=2, as only two time-series were considered (vHPC and mPFC raw LFPs).

In the above equation, $u_1(t) \ldots u_m(t)$ are the residuals of the model. The residuals were analyzed to verify if they described a white noise process. As expected, the residuals were normally distributed and had the same power at all frequencies. The order of the process, p, determines how many past lags are considered in the model, and was selected using Schwarz's Bayesian Criterion. In most animals the order chosen was around 90 samples, corresponding to approximately 47 ms. This model order is appropriate to detect directionality in the vHPC-mPFC circuit, as it represents a period of time larger than the conduction delay of the pathway (approximately 16 ms). To obtain a frequency-domain representation of the data, the Fourier transform of the coefficients of the vector auto-regressive model was taken, which for a given frequency f, was computed as shown:

$$A(f) = \sum_{r=1}^{p} A_r e^{-2\pi i f r}$$

PDC is an estimate of the strength of the directionality between the signals for each frequency. PDC for time series j to time series i at frequency f (represented as $|\pi i \leftarrow j(f)|$), was calculated as shown below, using custom MATLAB routines provided by B. Lau and A. Saez (Columbia University).

$$|\pi i \leftarrow j(f)| = \frac{|\overline{A}_{ij}(f)|}{\sqrt{\sum_k |\overline{A}_{kj}(f)|^2}},$$

where k varies from 1 to m (the number of time-series being modeled), $\overline{A}(f) = I - A(f)$, and I is the identity matrix. The denominator normalizes PDC for each frequency, such that PDC values fall between 0 and 1. PDC values at a given frequency attempt to estimate the strength of the directionality (or improvement in prediction) between the time-series j(t) and i(t) at that frequency.

Simulations with pink noise

Generation of pink noise

In order to verify if the amplitude crosscorrelation method is more robust than PDC to artifacts induced by noise in the signal, simulations were used to test both methods by adding noise to the signals. Pink noise (power falls with 1/f, where f is the frequency) was used instead of white noise (same power for all f), because noise in LFPs generally has a 1/f spectrum. Pink noise was generated by passing Gaussian zero-mean white noise through a 1/f filter. As expected, the power spectra P(f) of the resulting process was very well-fit by the formula $P(f)=P(f_0)*(1/f)$, where $P(f_0)$ is the power at the lowest frequency. To compare the resilience of the current method with PDC to pink noise, two types of simulations were performed:

Addition of pink noise of the same amplitude to both LFPs

In the first simulation, two copies of the same theta-filtered trace were shifted relative to each other by 28 ms to induce a well-defined lag. 28 ms was chosen because it is the mean vHPC-mPFC lag calculated by the amplitude crosscorrelation method. Pink noise was then generated independently and added to each signal In 500 simulations at each of ten different noise levels, corresponding to signal-to-noise power ratios of 1 to 0.2. The amplitude crosscorrelation method and PDC were then used to calculate directionality between the signals for each simulation.

Addition of pink noise of different amplitudes to the leading LFP

For the second simulation experiment, two theta-filtered segments of simultaneously recorded vHPC and mPFC signals were used. As indicated by the arrows in Figure 2.7A, in these traces, the vHPC clearly leads the mPFC. In each simulation, pink noise of small but fixed amplitude was added to the mPFC signal, while noise traces of varying amplitudes were added to the vHPC. The power of the noise added to the vHPC was varied from 0.1 to 4-fold the power of the noise added to the mPFC. For each of the six noise levels added to the vHPC, 500 simulations were run, in which both vHPC and mPFC noise was newly generated. After adding noise to the signals, the directionality between the two signals was calculated using the amplitude crosscorrelation method and PDC.

Statistics

Wilcoxon's two-tailed signed-rank non-parametric test was used throughout. $p<0.05$ was considered statistically significant.

Histology

Upon the completion of recording, animals were deeply anesthetized and electrolytic lesions were made to determine the position of the electrode tips. Lastly, animals were perfused with formalin. Brain sections were mounted on slides to visualize and photograph lesions.

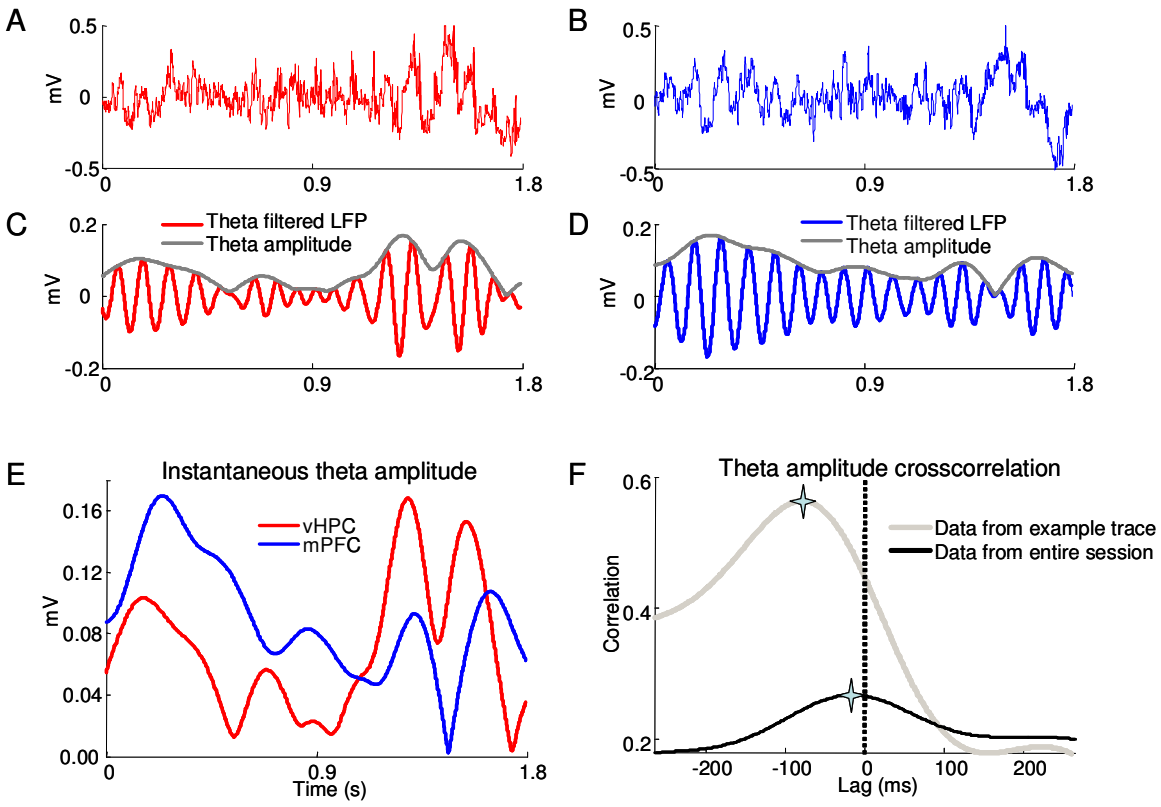

Figure 2.1- **Calculating lags using the amplitude cross-correlation method.** (A,B) Simultaneous local field potential recordings obtained from the vHPC (A) and mPFC (B) of a behaving mouse (C,D) Traces in (A) and (B), filtered for theta-frequency activity (7-12 Hz) (red), overlaid with the instantaneous amplitude obtained from the Hilbert transform (grey). (E) The instantaneous amplitudes of the theta-filtered vHPC (red) and mPFC (blue) signals shown in (C) and (D) overlaid for comparison. (F) Cross-correlation of the example amplitude traces shown in (E) (grey). The amplitude cross-correlation from the entire recording session is overlaid (black). The peaks are indicated by stars.

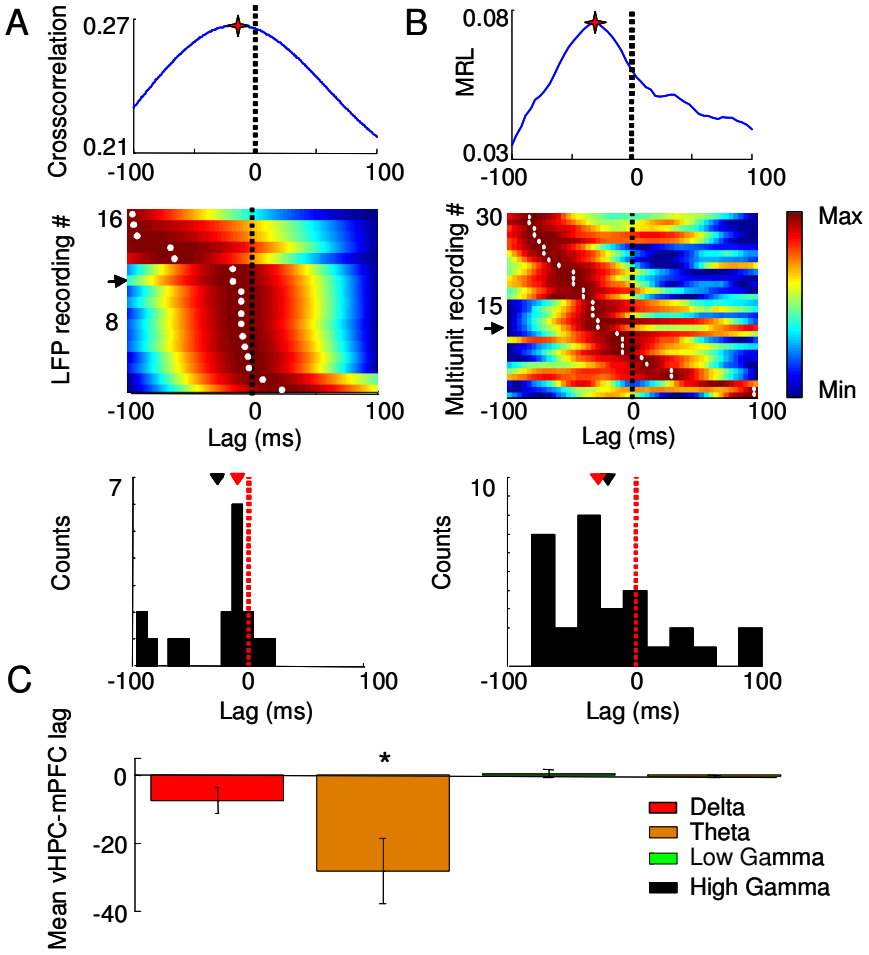

Figure 2.2- Estimation of lags between the vHPC and the mPFC using the amplitude cross-correlation (A) and phase locking (B) methods. Upper Panels: vHPC-mPFC lag estimate from single recording sessions using the amplitude cross-correlation (A), and the effect of shifting the mPFC spike train on the strength of phase-locking (MRL) to vHPC theta oscillations (B). Stars mark the peaks. Middle panels: Normalized color plots of amplitude cross-correlations from 17 recordings (A) and phase-locking shifts from 30 recordings (B). Warmer colors indicate higher cross-correlation peaks or greater phase-locking strength. Each row corresponds to a single LFP (A) or multiunit (B) recording. Rows are arranged according to the peak lag. Arrows mark the rows representing the data shown in the upper panels. The lags at which the cross-correlation (A, middle panel) and phase-locking (B, middle panel) peaks occur are marked with white dots. Lower panels: histograms showing the distribution of peak lags calculated with each method. The distribution of lags is significantly negative for both the amplitude cross-correlation ($p<0.05$, Wilcoxon rank-sum test, mean lag -28±16.7 ms, median=-9.5 ms, n=17 recordings) and phase-locking ($p<0.05$ for a paired Wilcoxon's rank sum test, mean lag -24.5±15.7 ms, median=-32 ms. n=30 recordings). Means and medians of the lag distributions are indicated, respectively, by black and red arrowheads. (C) Lag estimates are frequency-specific. Lags were calculated by cross-correlating the amplitudes after filtering for delta (1-4Hz), theta (7-12 Hz), low gamma (30-50 Hz) and high gamma (50-100 Hz) frequency ranges. Data are presented as means ± 95% confidence intervals. *$p<0.01$ for a paired Wilcoxon's rank sum test. In all panels, negative lags indicate that the vHPC leads the mPFC.

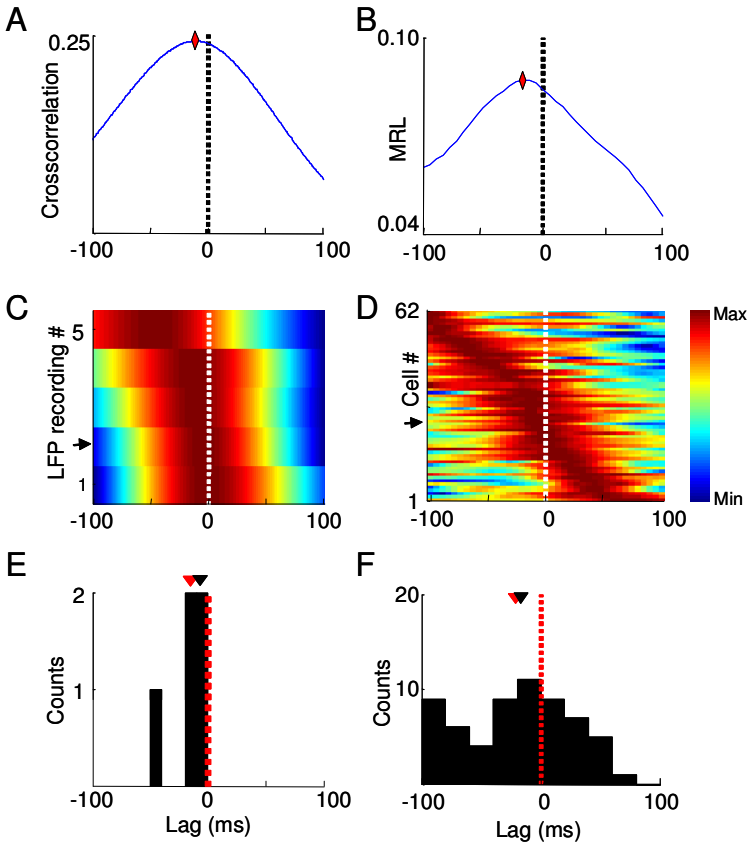

Figure 2.3- Estimation of lags between dHPC and mPFC using the amplitude cross-correlation and phase locking methods. (A) dHPC-mPFC lag estimated from a single recording session by crosscorrelating the amplitudes of theta-filtered traces. Note that the peak occurs at a negative lag, indicating that the dHPC leads the mPFC in the theta range. (B) Effect of shifting an mPFC spike train from a single unit on the strength of phase-locking (MRL). The plot shows that this mPFC single unit phase locks best to dHPC theta of the past, in agreement with the directionality shown in (A). Diamonds denote the peaks in both (A) and (B). (C) Normalized color plots of amplitude cross-correlations from 5 recordings and phase-locking shifts from 62 mPFC single units (D). Warmer colors indicate higher cross-correlation peaks or greater phase-locking strength. Each row corresponds to a single LFP (C) or single unit (D) recording. Rows are arranged according to the peak lag. Arrows mark the rows representing the data shown in the upper panels. (E, F) Histograms showing the distribution of peak lags calculated with each method. The distribution of lags is significantly negative for both the amplitude cross-correlation (E) ($p<0.05$, Wilcoxon rank-sum test, mean lag -15.4 ± 7.9 ms, n=5 recordings) and phase-locking method (F) ($p<0.003$ for a paired Wilcoxon's rank sum test, mean lag -20.2 ± 5.8 ms, n=30 recordings). Means and medians of the lag distributions are indicated, respectively, by black and red arrowheads.

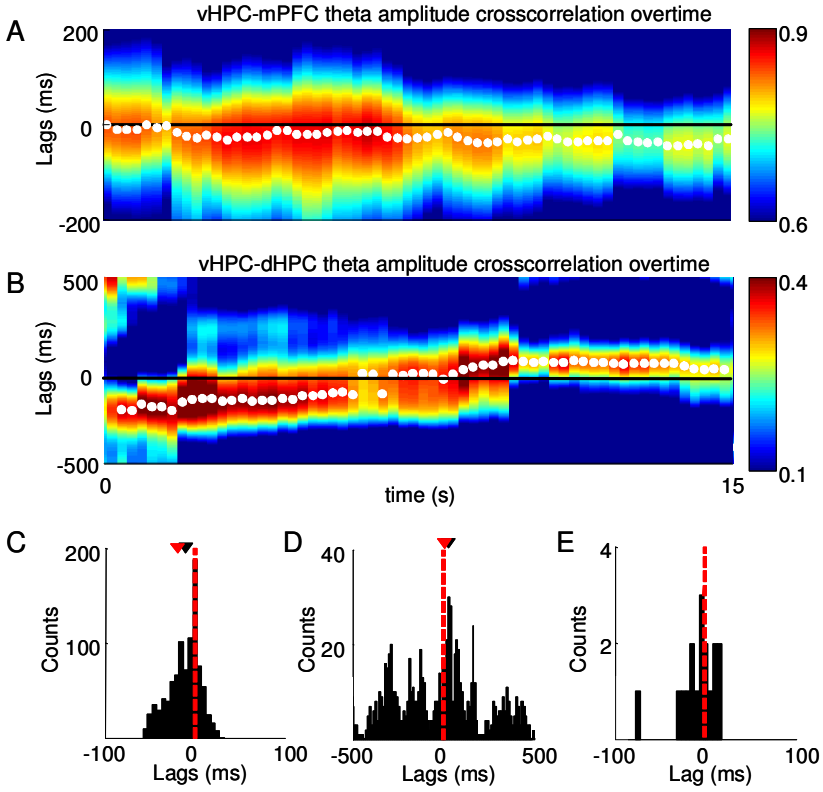

Figure 2.4- Application of the amplitude cross-correlation method to bidirectionally-connected areas. (A) A representative 15-second theta amplitude cross-correlation over time for the vHPC-mPFC is shown. Warmer colors correspond to higher cross-correlation values and white points mark the peak of the cross-correlation for each time window. Note that consistent with the existence of a unidirectional monosynaptic projection from the vHPC to the mPFC, the peaks of the cross-correlation fall primarily on negative lags for the vHPC-mPFC cross-correlation, indicating that the vHPC leads the mPFC. (B) same as (A), but for simultaneously recorded vHPC and dHPC traces. In agreement with the existence of bidirectional monosynaptic projections between the vHPC and dHPC, at different time points the cross-correlation peaks at positive or negative lags, presumably reflecting periods in which the vHPC is leading or lagging relative to the dHPC, respectively. (A-B) Cross-correlations were calculated in 8 sec windows with 97% overlap between successive windows. (C) Histogram of the lags at which the cross-correlation peaks occur for the entire 10 minute recording from which the data plotted in (A) was obtained show that the distribution of vHPC-mPFC lags has a negative mean ($p<0.005$, Wilcoxon's test), while the distribution of vHPC-dHPC lags (D) is not significantly different from zero ($p<0.72$, Wilcoxon's test). (C-D) Each count of the histogram refers to one 8 sec window in which the cross-correlation was computed. The distribution of the mean vHPC-dHPC lag for each animal is shown in (E), and it is not significantly different from zero. Each count in the histogram corresponds to the mean lag of one animal. In (C-E), red and black arrowheads indicate the means and medians of the distribution, respectively.

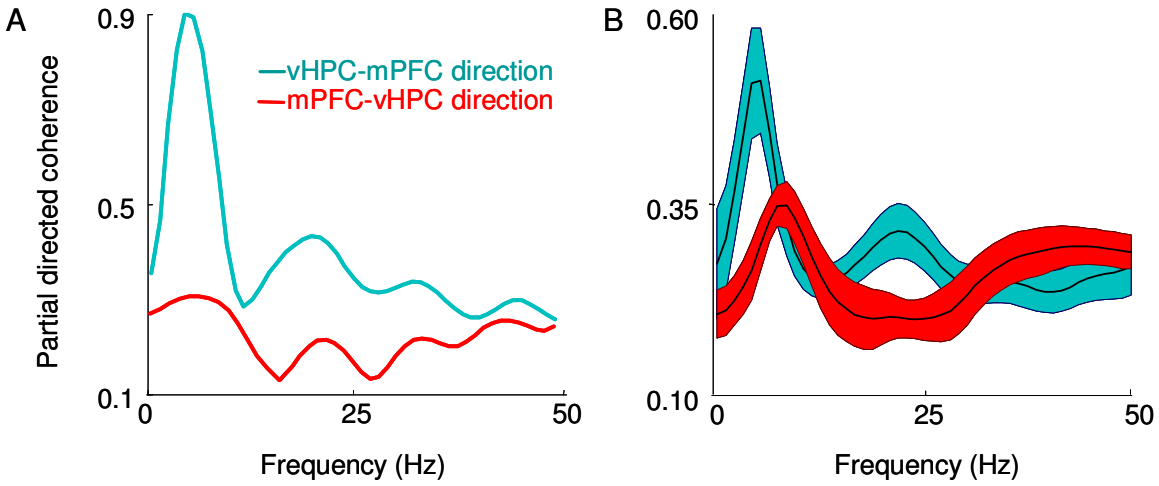

Figure 2.5- **Partial directed coherence indicates that vHPC is leading the mPFC in the theta range**. (A) Representative example of PDC on simultaneously recorded vHPC and mPFC LFPs from a single session. Note the prominent peak in the theta range of the PDC in the vHPC to mPFC direction. (B) Average PDC across animals is plotted. Note that in the theta range the predominant direction of flow, as indicated by higher PDC values, is in the vHPC to mPFC direction. Shaded areas indicate S.E.Ms.

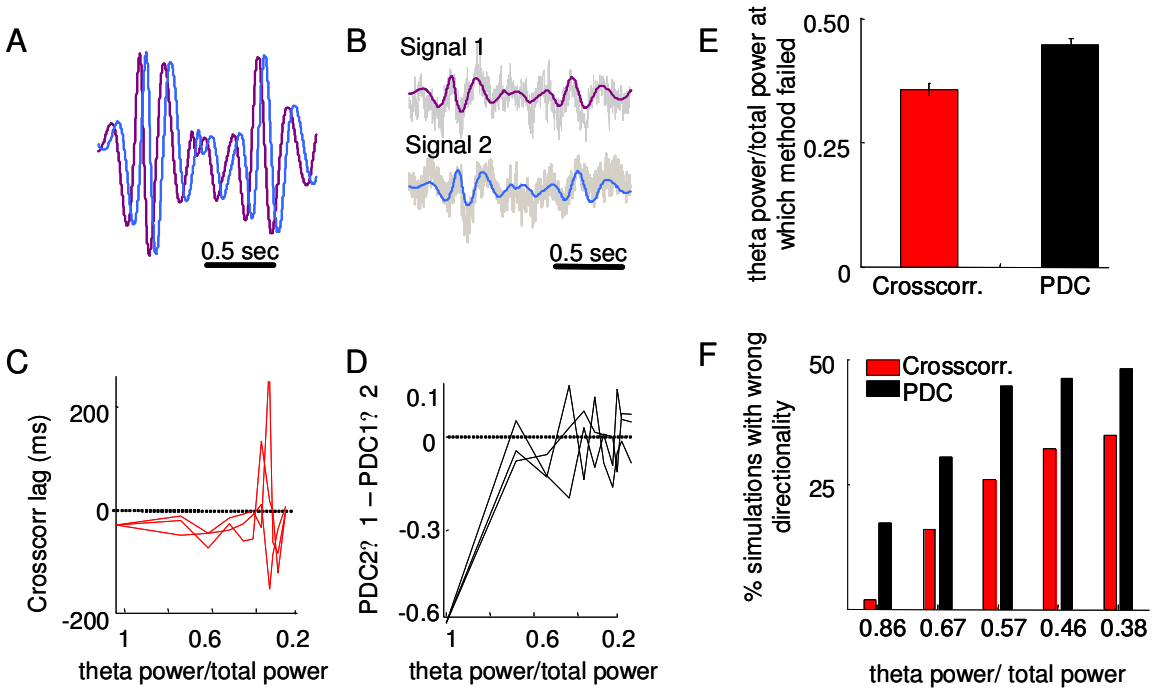

Figure 2.6- **Partial directed coherence is more sensitive to noise than the amplitude cross-correlation method.** (A) Two signals were created from the same two-second segment of vHPC theta-filtered trace. One signal was shifted relative to the other by 28 ms (this is the mean delay between the vHPC and the mPFC calculated by the amplitude cross-correlation method). Thus, the purple trace leads the blue trace with a lag of 28 ms. (B) Pink noise was generated randomly and added to both signals. Ten different levels of noise were added, such the fraction of theta power relative to total power in the signals after adding noise was varied from 1 to 0.2. In the example shown, theta power/total power=0.67. (C)The amplitude cross-correlation method was applied to verify the directionality after adding pink noise to both signals, in 500 simulations in which noise was newly generated, at 10 different amplitudes. Calculation of the lag by the cross-correlation method for three representative simulations is shown. Points with negative lags have the expected directionality. The cross-correlation method fails only when high levels of noise are added, as shown by the points with positive lags with low theta power to total power ratios. Note that the x axis is reversed, such that higher values (high signal to noise ratios) are on the left. (D) Same as in (C), but for PDC calculated from the identical simulations. Correct directionality is reflected as negative values on the y axis. PDC1→2 indicates PDC in the purple trace in A causing the blue trace. Note that this method does not consistently indicate that the purple trace leads the blue trace even after adding only moderate amounts of noise to the signal. (E) Mean noise level at which each method first failed, averaged across 500 simulations. The PDC method on average fails at lower noise levels than the amplitude cross-correlation method ($p<0.0001$, ranksum test). (F) For five noise levels, the percentage of simulations in which the wrong directionality was calculated is shown. At every noise level PDC had a significantly higher failure rate than the amplitude cross-correlation method ($p<0.05$, Fisher's exact test). All PDC values shown are averages across the theta-range.

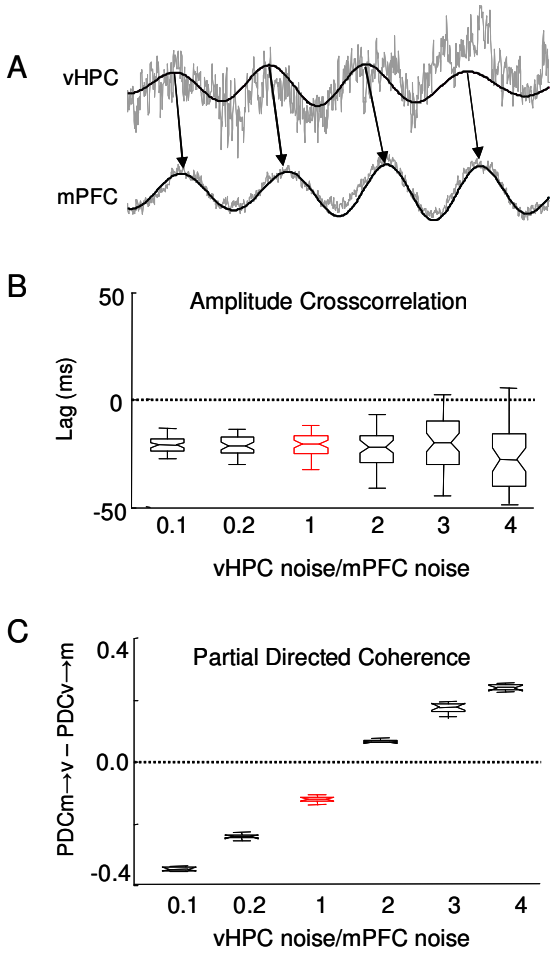

Figure 2.7- Partial directed coherence, but not the cross-correlation method, is biased if one of the signals has different noise levels than the other signal. (A) Half-second segments of one-minute long signals are shown. Black traces are theta-filtered traces from the vHPC and mPFC. Note that the vHPC leads the mPFC in these traces, as indicated by the black arrows. Grey traces were obtained after adding different levels of pink noise to each of the filtered signals. In this example, the noise added to the vHPC is four-fold greater than the mPFC noise. Across the simulations, the noise added to the mPFC remained constant, while the noise added to the vHPC was varied from 0.1 to 4-fold of the noise added to the mPFC. Noise was generated in six increasing amplitudes in 500 simulations and added to the vHPC. The signals were then analyzed by the amplitude cross-correlation method (B) and PDC (C). (B) Boxplot shows the median lags calculated by the amplitude cross-correlation method after different amounts of noise were added to the vHPC signal while keeping constant the amplitude of the noise added to the mPFC signal. The lag calculated by the amplitude cross-correlation method remains negative, indicating that mPFC follows the vHPC, even when the amount of noise added to the vHPC is greater than the mPFC noise. Boxplots show the mean lag and the 25th and 75th percentiles of the distributions. Whiskers indicate the range. (C) PDC was calculated for the same simulations used in (B) . Correct directionality (vHPC leading) is represented as negative values on the y axis (PDC v→m greater than PDC m→v, where v and m stand for vHPC and mPFC, respectively). PDC indicates that the vHPC leads the vHPC only when the vHPC is equally or less noisy than then the mPFC. Note that PDC consistently indicates that the less noisy signal leads the noisier signal, regardless of the underlying directionality. In (B) and (C), the condition of equivalent noise levels in the two signals (VHPC noise/mPFC noise=1) is shown in red. All PDC values shown are averages across the theta-range.

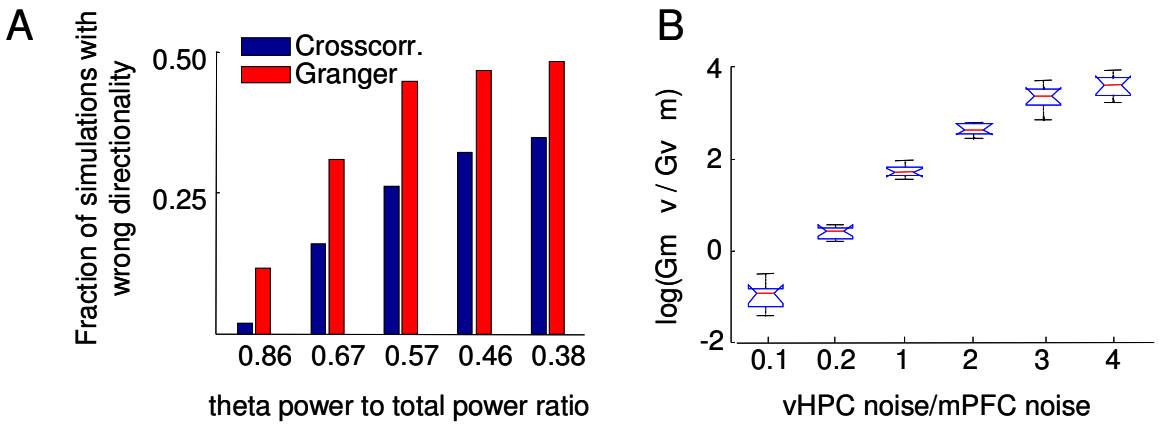

Figure 2.8-- Granger causality is more susceptible to noise than the amplitude crosscorrelation method. (A) As described in the text and Figure 2.6, we added equal amounts of pink noise to two identical signals shifted by 28 ms and calculated the predominant directionality using Granger Causality (REF). The percentage of simulations in which the wrong directionality was calculated is shown separately for each noise level. At every noise level Granger causality had a significantly higher failure rate than the amplitude crosscorrelation method ($p<0.05$, Fisher's exact test). All Granger causality values shown are averages across the theta-range. (B) As described in the text and in Figure 2.7, we tested the ability of unequal amounts of noise to artifactually induce directionality. A small and constant-level amount of pink noise was added to the mPFC, while different levels of noise was added to the vHPC signal. The directionality of the traces after adding noise was computed through Granger causality in 500 simulations at each noise level, Note that Granger Causality tends to find directionality from the signal with lower variance to the signal with higher variance, independently of the underlying directionality. Gm→v indicates Granger causality values for the mPFC to vHPC direction.

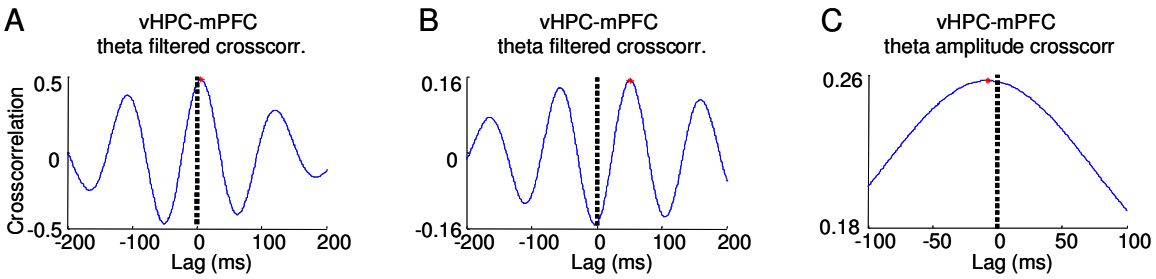

Figure 2.9- Cross-correlation of filtered LFPs cannot be used to estimate the lag between two areas. (A) Example of a cross-correlation between 7-12 Hz filtered vHPC and mPFC LFPs. As the position of the peak is strongly influenced by the phase offset between the two areas, the position of the peak (marked with a star) does not reflect the lag between these signals. (B) Another example cross-correlation of filtered LFP showing multiple peaks. Frequently, due to the phase offset, multiple peaks may be visible near the 0 ms lag. In such cases, it is unclear which peak represents the true lag between the signals. Amplitude crosscorrelation of the same signals in (A) are shown in (C). Amplitude crosscorrelations do not have this problem, as they always have only one peak. Note that the crosscorrelation peaks at a negative lag, indicating that the vHPC is leading the mPFC.

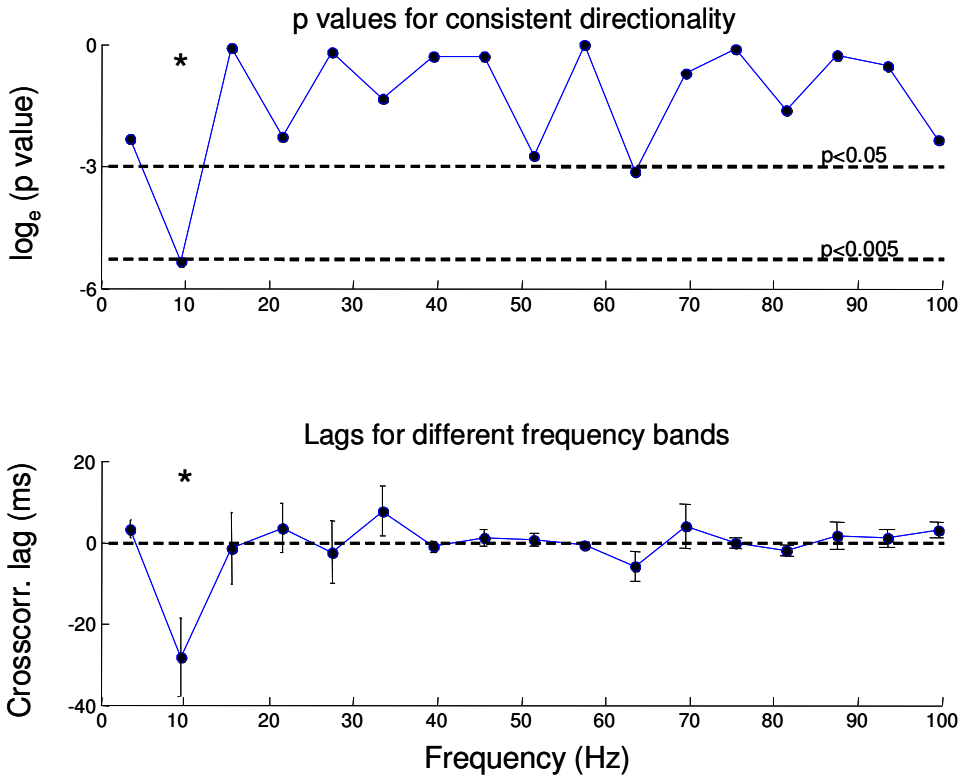

Figure 2.10- Identification of the frequency band at which directionality of functional connectivity occurs. Crosscorrelations of the amplitude envelopes of vHPC and mPFC LFPs were computed after filtering the signals for different 5 Hz ranges. The p values (upper panel) and lags (lower panel) are shown for a broad range of frequency ranges, from 1 to 100 Hz, in non-overlapping 5 Hz windows. Note that a lag significantly different from zero across animals ($p<0.0048$, Wilcoxon's test, $n=17$) occurs only for the theta (7-12 Hz) range. Applying the amplitude crosscorrelation method in this unbiased way allows for the identification of the frequency range at which directionality occurs.

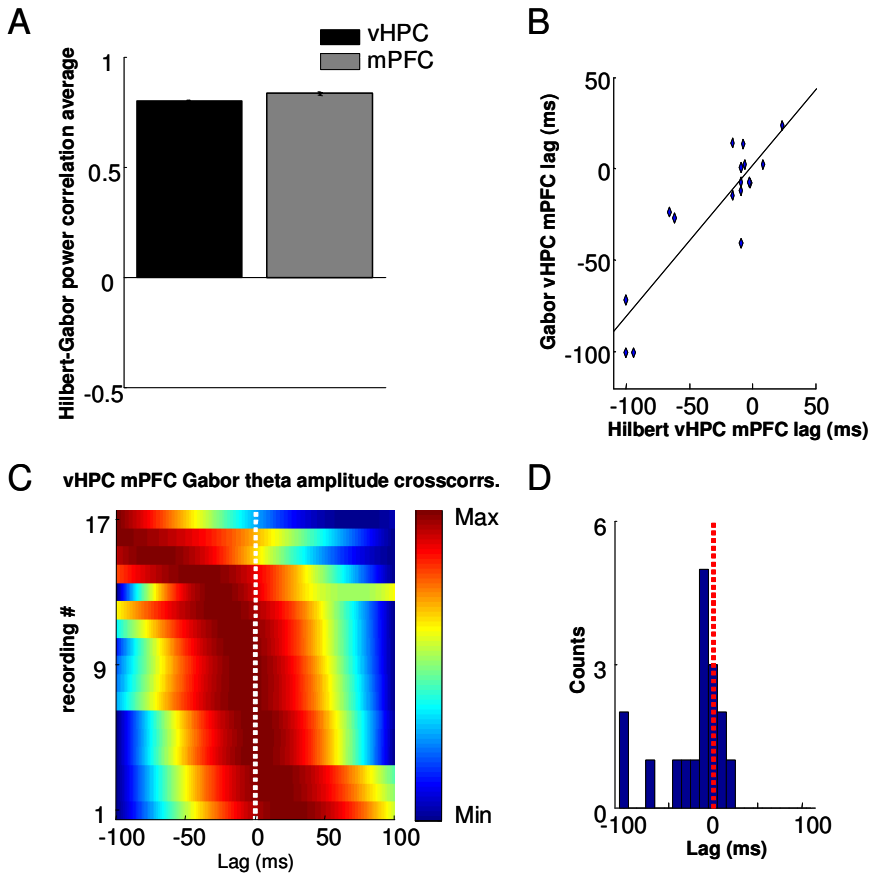

Figure 2.11- vHPC-mPFC lags calculated with the Gabor transform and the Hilbert transform are in good agreement. To calculate the Gabor transform instantaneous amplitudes are calculated by convolving the signal at each frequency with a complex sinusoidal wavelet with a Gaussian envelope that has a standard deviation proportional to 1/frequency. The squared absolute magnitude of the result of the convolution at a given frequency provides the estimate of power. (A) The average correlation of instantaneous theta amplitude, calculated via the Hilbert Transform, and power, calculated using the Gabor Transform, in recordings made in the vHPC (black bar) and mPFC (grey bar). Note that both methods produce very similar estimates of instantaneous power. (B) Correlation (r=0.88) of vHPC-mPFC lags calculated by Gabor and the Hilbert transforms. (C) Normalized color plots of amplitude cross-correlations from 17 recordings. Warmer colors indicate higher cross-correlation. Each row corresponds to a single LFP recording. Rows are arranged according to the peak lag. (D) histogram showing the distribution of lags calculated through the Gabor transform. This distribution is significantly negative ($p<0.05$, Wilcoxon's test, mean lag=-21±9.1 ms).

Chapter 3

Synchronized activity between the ventral hippocampus and the medial prefrontal cortex during anxiety

Synchronized activity between the ventral hippocampus and the medial prefrontal cortex during anxiety

3.1 Introduction

Anxiety in rodents is commonly modeled through paradigms such as the elevated plus maze (EPM) and the open field. Multiple lines of evidence, including lesion and local drug infusion studies, have shown that the hippocampus is necessary for normal anxiety-like behavior in these environments (Deacon et al., 2002; File et al., 1996). Recently, more selective lesions have demonstrated that the ventral (vHPC), but not the dorsal hippocampus (dHPC), is required for normal anxiety-related behavior (Bannerman et al., 2004; Kjelstrup et al., 2002). Although these reports implicate the vHPC, the mechanisms by which this structure exerts its role in anxiety are unknown. One possibility is that the vHPC influences the activity of downstream targets involved in anxiety modulation.

One such target region shown to be involved in anxiety is the medial prefrontal cortex (mPFC). The mPFC receives direct projections from the vHPC in both rats (Verwer et al., 1997) and mice (Parent et al., 2009), whereas its inputs from the dHPC are indirect, (Burwell R.D. and Witter, 2002; Hoover and Vertes, 2007). Numerous studies have demonstrated an important role for the mPFC in the modulation of anxiety, likely through its reciprocal connections with the amygdala and other limbic structures (Vertes, 2004). In addition to its well-characterized role in extinction of learned fear (Burgos-Robles et al., 2007), the mPFC may play a role in anxiety tests that require the hippocampus (Gonzalez et al., 2000; Lacroix et al., 2000; Shah et al., 2004; Shah and Treit, 2003) although there is some disagreement on this point in the literature (Corcoran and Quirk, 2007; Lacroix et al., 1998).

These findings suggest that the vHPC and mPFC might cooperate during anxiety. Previous reports have measured theta-frequency (4-12 Hz) synchronization between the hippocampus and downstream targets to demonstrate such cooperation during a variety of behaviors. Theta-

frequency synchrony has been shown between the dHPC and the mPFC during working memory (Jones and Wilson, 2005), the striatum during learning (DeCoteau et al., 2007), and the amygdala during fear conditioning (Seidenbecher et al., 2003). Whether the vHPC might use a similar mechanism to synchronize with its targets is unclear. Consistent with this possibility, various lines of evidence have suggested that theta oscillations may play a role in anxiety. For example, anxiolytic agents decrease the propensity of the hippocampus to oscillate in the theta range (Zhu and McNaughton, 1994). Moreover, dorsal hippocampal theta power has been correlated with anxiety-related behavior in 5-HT1A receptor knockout mice (Gordon et al., 2005), a genetic model of enhanced anxiety (Heisler et al., 1998; Parks et al., 1998; Ramboz et al., 1998).

Taking into account these reports implicating theta oscillations, the vHPC and the mPFC, we hypothesized that synchronization in the theta range between the mPFC and the vHPC might underlie anxiety-like behavior. The present study tests this hypothesis by recording neural activity simultaneously from the mPFC, vHPC and dHPC in freely behaving mice during exploration of a familiar environment, a novel open field, and an elevated plus maze. In all environments, mPFC field potentials were more coherent with field potentials recorded from the vHPC than the dHPC. Exposure to either anxiogenic environment specifically increased theta-frequency synchrony between the mPFC and vHPC, as well as theta power in both regions. Notably, mPFC theta power was higher specifically in the “safe” compartments of each arena, decreased immediately prior to entry into the aversive compartments, and correlated with behavioral measures of anxiety. Finally, 5-HT1A KO mice, a genetic model of increased anxiety, had larger mPFC theta power increases than wild type mice. These results further implicate hippocampal theta oscillations in anxiety and suggest that these oscillations may mediate communication between the vHPC and mPFC during exposure to anxiogenic environments.

3.2 Results

Neural activity in the medial prefrontal cortex is highly coherent with the ventral but not dorsal hippocampus

To examine the relationship between medial prefrontal cortical and hippocampal activity across the septo-temporal axis of the hippocampus, tungsten microwire electrodes were implanted into the mPFC and the CA1 region of the dHPC and vHPC (Figure 3.1). For the vHPC electrode, care was taken to ensure placement within the ventral-most third of the hippocampus, as this region in particular has been demonstrated to be crucial for normal anxiety behaviors in lesion studies (Kjelstrup et al., 2002). The mPFC electrode was aimed at the deep layers of the ventral portion of the prelimbic cortex. Following an appropriate recovery period, mice were food deprived and allowed to forage for pellets in a small rectangular familiar arena. Local field potentials (LFPs) were recorded from each site during daily 10 minute foraging sessions.

As previously described (Buzsaki, 2002), LFPs obtained from the dHPC revealed prominent movement-dependent theta-frequency oscillations (Figure 3.2). These oscillations were evident both in raw traces (Figure 3.2A) and in power spectra computed from these traces (Figure 3.2B). Theta oscillations in the mPFC and vHPC were smaller than in the dHPC (Figure 3.2B), regardless of hippocampal layer (Figure 3.3). Nonetheless, activity in the theta range could be measured in vHPC and mPFC power spectra, particularly when the animals were moving at higher speeds.

The similarity of the raw LFP traces from the vHPC and the mPFC (Figure 3.2A) suggested that the LFPs from these areas might be highly coherent. Indeed, in all animals mPFC-vHPC coherence was high at all frequencies, with peaks in both theta (4-12 Hz) and gamma (30-100 Hz) frequency ranges (Figure 3.2C). Coherence between dHPC and mPFC was only high for frequencies below 4 Hz, consistent with previous reports that show high synchrony of slow oscillations across the forebrain (Sirota and Buzsaki, 2005). Contamination by motor artifacts may also partially contribute for high coherence at very low frequencies (<1 Hz). Intriguingly, mPFC-vHPC coherence was even higher than coherence between the two hippocampal sites at most frequencies. Notably, dHPC-vHPC coherence was high only in the theta range, and low at gamma frequencies, consistent with similar findings from *in vitro* studies (Gloveli et al., 2005).

High coherence between two LFPs suggests synchronization but does not disambiguate whether the synchrony is due to correlated fluctuations in power (oscillation amplitude) or due to

a consistent phase relationship between the two signals (oscillation timing). To further study coherence between the hippocampus and the mPFC we separately calculated power correlation and phase coherence for theta and gamma frequency ranges. Power correlation was computed by measuring theta and gamma power in each brain area over time throughout the first 10 minutes of each behavioral session. Phase coherence was estimated by computing a histogram of the difference in instantaneous phase across each signal and measuring the width at half height of the histogram peak; narrower peaks indicate a more consistent phase relationship.

For the theta frequency range, both measures revealed stronger synchronization between the mPFC and vHPC than dHPC (Figure 3.4). The power correlation between mPFC and vHPC was statistically significant for all animals ($n=13$, $p<0.05$), and the mean r^2 value (0.24) suggests that a considerable portion of the variance in mPFC theta is accounted for by fluctuations in vHPC (or vice-versa). Notably, theta correlations were strongest when the mPFC trace was shifted backwards in time relative to the vHPC (median lag -8 ms, $p<0.05$, signrank test; Figure 3.8F and G), suggesting the directionality of the relationship is vHPC to mPFC. In contrast to the strong relationship between vHPC and mPFC theta power, weaker correlations were seen between mPFC-dHPC and vHPC- dHPC pairs ($n=13$, $p<0.05$ for paired t-tests; Figure 3.4B).

Similarly, theta phase coherence was higher between the mPFC and vHPC than dHPC, as demonstrated by the narrower peak in the phase difference histogram (Figure 3.4 C & D). Surprisingly, vHPC and dHPC showed high theta phase coherence, but low theta power correlation, suggesting that the timing and amplitude of theta oscillations may be influenced by different mechanisms across the dorso-ventral axis of the hippocampus. As expected from the low coherence in the theta range, mPFC and dHPC had low theta power correlations and reasonably independent variation of theta phases, as shown by the wider theta phase difference histogram (Figure 3.4 C&D).

In addition to high theta range coherence, LFPs from the mPFC and vHPC also had high gamma coherence. We therefore also examined power correlations and phase coherence of gamma-frequency oscillations. Even though gamma oscillations are thought to be generated

locally, power correlations in the gamma range were higher for mPFC-vHPC than for mPFC-dHPC or dHPC-vHPC ($n=13$, $p<0.01$ for each paired t-test; Figure 3.4B). Similar to theta phase coherence, gamma phase coherence was moderately high between mPFC-vHPC and dHPC-vHPC electrode pairs (Figure 3.5 panel B).

To further study hippocampal-mPFC interactions we also investigated whether hippocampal theta phase influences mPFC gamma power. In the dHPC, gamma power is modulated by local theta phase, (Buzsaki et al., 2003; Csicsvari et al., 2003) presumably because the activity of interneurons that give rise to dHPC gamma is modulated by the theta oscillation. If the vHPC projections to the mPFC oscillate at theta and influence the activity of mPFC interneurons that generate gamma (Szabadics et al., 2001; Tierney et al., 2004), vHPC theta phase may be expected to modulate mPFC gamma power, as shown previously for the dHPC (Sirota et al., 2008). Indeed, mPFC gamma power was more strongly modulated by vHPC theta than dHPC theta (Figure 3.6).

Theta power correlations between the mPFC and vHPC increase in the EPM and the open field

Since the mPFC and vHPC are likely involved in the regulation of anxiety-like behavior, we examined whether the synchronization between these areas was modulated during exposure to anxiogenic environments. Following testing in the familiar arena, mice were exposed to a novel open field and an EPM, in counterbalanced order with two intervening rest days. Results from each anxiety paradigm were compared to the recordings obtained from the familiar environment on the same day. Percent time spent, and path length in the center of the open field, as well as percent time spent and entries into the open arms of the EPM, were used as pharmacologically validated measures of anxiety-like behavior (Choleris et al., 2001; Lister, 1987). Mice demonstrated a variable anxiety-like response to the two environments, ranging from complete avoidance to robust exploration of the aversive parts of each arena (Figure 3.13). Measures of anxiety-like behavior correlated well across the two tests, suggesting that both measured similar anxiety-like traits (see Methods).

During these exposures to the EPM and open field, raw LFP traces from the mPFC displayed more robust and regular theta oscillations compared to the familiar arena (Figure 3.9A). The higher prominence of theta in the raw traces suggested that theta-range synchrony between the vHPC and mPFC might be increased. Indeed, we found increases in theta-frequency power correlations between the vHPC and the mPFC in the open field compared to the familiar arena ($n=11$, $p<0.04$ for a paired t-test) (Figure 3.7C). Similar results were found in the EPM ($n=11$, $p<0.01$ for a paired t-test), supporting the idea that theta synchrony between the mPFC and vHPC increases during exposure to these environments (Figure 3.7D). Moreover, the increase in power correlation was specific to the theta range and to the mPFC-vHPC pair (Figure 3.7C and D and 3.5). Power correlations with the dHPC did not change in any of the anxiety paradigms. Peak mPFC theta frequency increased to nearly 8 Hz in the EPM and the open field, becoming closer to vHPC theta frequency (Figure 3.5 panel D), consistent with increased synchrony between these two regions. This pattern of results was observed in all HPC layers (Figure 3.3) and was present in all compartments of both the EPM and the open field (Figure 3.5, panels E and F). Other measures of synchrony did not change significantly in either test (Figure 3.5).

Phase-locking of mPFC neurons to local and vHPC theta oscillations increases in the open field

The above data obtained from LFPs suggest that theta synchrony between the mPFC and vHPC increases in the open field and the EPM. However, the anatomical origins of LFPs may be unclear due to possible contamination by volume-conducted signals from more distant sites, or signals in the reference wire. By contrast, spiking activity is not subject to either artifact. To confirm the observed increases in mPFC-vHPC theta synchrony, we measured the phase-locking of mPFC multiunit spiking activity to local and hippocampal theta during exposure to the familiar environment and the open field. The magnitude of phase-locking was measured using the mean resultant length (MRL), a measure of circular concentration derived from Rayleigh's test of circular uniformity (see Experimental Procedures). By this measure, the open field led to

increases in phase-locking to both mPFC and vHPC, but not dHPC theta oscillations (Figure 3.8B).

Analysis of phase locking of mPFC spikes to hippocampal theta also permits confirmation of the directionality of the functional connectivity between the vHPC and mPFC. To address this issue, phase locking of multiunit activity was calculated after shifting the spikes forward and backward in time relative to the LFP. If mPFC cells are influenced by the hippocampal field, phase locking should be maximal when spikes are shifted backwards (i.e., negative temporal offsets in Figure 3.8 C-E). Interestingly, this analysis shows that on average mPFC spikes were maximally phase locked to hippocampal theta of the past (Figure 3.8D and E), both for vHPC (mean shift=-32 ms, n=30 recordings, $p<0.01$, Wilcoxon's signed rank test) and dHPC theta oscillations (mean shift=-36 ms, n=30 recordings, $p<0.03$, Wilcoxon's signed rank test). Reports of a similar analysis performed in rats for dHPC theta and mPFC spikes found a mean shift of -45 ms, in broad agreement with the present results (Siapas et al., 2005). These shifts are also generally consistent with delays of antidromic spikes (16 ms) between the ventral hippocampus and mPFC taking into account polysynaptic connectivity (Thierry et al., 2000), and confirm the directionality suggested by the analysis of theta power correlation in the LFPs (Figure 3.8G). Furthermore, as expected, mPFC spikes are maximally phase locked to local theta oscillations at a temporal offset close to zero (mean shift=1.7 ms, n=28 recordings), suggesting that theta recorded in the mPFC has immediate local relevance. These results are consistent with the notion that theta-frequency input to the mPFC from the ventral hippocampus modulates mPFC unit activity, and the strength of this modulation is increased during exploration of anxiety-provoking environments.

Theta power in the mPFC and vHPC increases in the open field and the EPM

Consistent with our observations from the raw LFP traces, we found that theta power increased in the vHPC and the mPFC in both anxiety tests (Figure 3.9). To reliably measure low values of theta power, we fit all spectra with the sum of an exponential and a Gaussian curve, the latter centered at theta frequency (see Experimental Procedures). The area under the Gaussian was

used as a measure of total theta power. The finding that theta power increases with higher speeds (Figure 3.2) shows that theta power can be modulated by behavioral variables other than anxiety. Thus, comparisons of power across environments were done during epochs of similar movement (7-15 cm/s, unless otherwise stated). In the vHPC, but not the dHPC, theta power was higher in both the open field and the elevated plus maze relative to the familiar arena (Figure 3.9C, n=11, $p<0.05$ in a paired Wilcoxon's signed rank test). In the mPFC, theta power also increased in the open field (Figure 3.9C, n=18, $p<0.05$ for a paired Wilcoxon's signed rank test), although the increase did not reach statistical significance in the EPM (Figure 3.9C, n = 12, p = 0.3). Importantly, these results cannot be explained by novelty, because theta power in the mPFC and vHPC in the anxiogenic environments was also increased relative to the first day of exposure to the then-novel “familiar” arena (Figure 3.9C, right panel). These results were consistent across all hippocampal layers (Figure 3.3) and could not be explained by differences in speed or acceleration (Figure 3.10).

To better define the behavioral relevance of these increases in theta power, we separately compared theta power in each compartment of the open field and EPM to that in the familiar arena (Figure 3.11A & B). The observed increases in vHPC theta power were present in both the center and periphery of the open field, and in all three compartments of the EPM (open arms, closed arms and center). Intriguingly, theta power in the mPFC was significantly modulated by location within each environment; mPFC theta power was increased only in the relatively protected periphery of the open field and closed arms of the EPM.

These results suggest the possibility that theta-frequency activity in the mPFC reflects a role for the structure in inhibiting the active exploration of the aversive areas within each environment. To further explore this possibility, we examined the temporal dynamics of mPFC theta power in the EPM, where transitions between compartments could be precisely identified based on the animal’s location. Spectrograms of mPFC field potentials were calculated centered on the transition point when the animal passed from the closed arm into the center of the EPM. The averaged spectrogram of all such transitions (Figure 3.12A) shows a dramatic decline in mPFC theta power 2-3 seconds *before* the animal leaves the closed arm. mPFC theta power also

increased before the reverse, center-to-closed arm transitions (Figure 3.12 B). Notably, mPFC-vHPC coherence showed a similar pattern, decreasing before the animal leaves the closed arms (Figure 3.12 C and D). The timing of these changes suggests the possibility that theta-frequency activity in the mPFC is involved in actively inhibiting exploratory behavior, rather than simply reflecting the position of the animal with the maze. Importantly, there are no overt changes in locomotor behavior during transitions that could account for these results (Figure 3.12 E-G).

To further characterize the behavioral role of mPFC theta activity, we directly examined the relationship between the increase in mPFC theta power and anxiety-related behavior in each test across animals. In both the open field (Figure 3.13 A) and the EPM (Figure 3.13 B) there was a significant correlation between the magnitude of the increase in mPFC theta power and anxiety-related behavioral measures. Animals with the largest increases in theta power spent the least time in the center of the open field, or in the open arms of the EPM. The relationship between theta and behavior held even when considering only the magnitude of the increase only in the periphery of the open field (Figure 3.13 C) or the closed arms of the EPM (Figure 3.13 D). These data further support the hypothesis that that increases in mPFC theta power are associated directly with anxiety-like behavior.

Serotonin 1A receptor knockout mice have higher increases in mPFC theta power with anxiety

Serotonin 1A receptor (5-HT1AR) knockout mice display increased anxiety-like behavior relative to wild-type animals in hippocampal-dependent anxiety tests, including the EPM and the open field (Ramboz et al., 1998). 5-HT1AR knockout mice also were shown to have increased theta power in the pyramidal layer of the dHPC in the EPM relative to a control environment (Gordon et al., 2005). Considering that our data show increased theta power in the EPM and in the open field in the vHPC and the mPFC in wildtype mice, we hypothesized that the more anxious 5-HT1A knockout mice would have a larger increase in theta power during exploration of the EPM and open field. 5-HT1AR knockouts and wildtype littermates underwent electrode implantation and were tested in familiar, EPM and open field environments. In knockouts, as in wildtypes, the mPFC was more tightly coupled to the vHPC than the dHPC in the familiar environment (data not

shown). In both the EPM and open field, however, knockouts had a larger increase in mPFC theta power than their wildtype littermates (Figure 3.14 A and B, n= 7 WT and 7 5-HT1A KO mice, $p<0.04$). The fold increase in mPFC theta power in 5-HT1A knockouts was also significantly greater than that of the pooled group of all wildtype mice. The theta power increase in the vHPC was not statistically different from that of the wildtypes in our small sample. We also did not find significant theta power increases in the dHPC of 5-HT1A knockouts, contrary to that found in the pyramidal layer of the dHPC in our previous report (Gordon et al., 2005),perhaps due to the smaller sample size or decreased anxiogenicity of the EPM in the current study. It should be noted that the 95% confidence interval for the dHPC increase seen in the current study (1.03 fold ± 0.33) overlaps with the fold increase reported in the previous study (1.2).

3.3 Discussion

While a role for the vHPC in anxiety has been clearly established (Bannerman et al., 2004; Kjelstrup et al., 2002), the mechanism by which the vHPC exerts its anxiogenic effect has not been previously explored. Here, for the first time, we demonstrate theta-frequency synchronization between the vHPC and a principal downstream target, the mPFC. At baseline, this synchronization is significantly larger than that between the dHPC and mPFC. Anxiety further enhances the strength of vHPC-mPFC synchrony without affecting mPFC-dHPC synchrony, as found with both multiunit and LFP data. Accompanying this increase in synchrony is an increase in theta-frequency activity in the mPFC that appears to be involved in inhibition of exploratory behavior. These results are consistent with the known anatomical relationship between the hippocampus and the mPFC, and indicate that the vHPC and mPFC may act together to generate behavioral inhibition during anxiety tests.

Functional connectivity between the hippocampus and the mPFC

Previous studies have demonstrated that neural activity in the mPFC synchronizes with theta-frequency oscillations in the dHPC (Hyman et al., 2005; Jones and Wilson, 2005) despite the fact that these two regions are indirectly connected (Burwell R.D. and Witter, 2002); (Hoover and

Vertes, 2007). In contrast, the vHPC and the mPFC are directly connected (Hoover and Vertes, 2007; Parent et al., 2009; Thierry et al., 2000; Verwer et al., 1997). However, no previous attempts have been made to measure functional coupling between these two structures. Here we find that the mPFC is more highly coherent with the vHPC than the dHPC, over a broad range of frequencies, though only theta-range synchrony was modulated by anxiety. Further studies are needed to investigate if mPFC-vHPC synchrony in other frequency ranges is modulated by different tasks. It is noteworthy that previous HPC-mPFC anatomy work shows that mid HPC, (mHPC), also projects to mPFC, although less robustly than the vHPC (Hoover and Vertes, 2007). In agreement with these reports, recordings performed in mHPC displayed theta-range coherence and anxiety-induced changes in theta power that are in between those of dHPC and vHPC (Figure 3.15). A higher degree of coupling between the mPFC and vHPC was also reflected in other measures, such as gamma-frequency coherence, and modulation of mPFC gamma power by hippocampal theta phase. Finally, theta-frequency synchronization between the vHPC and mPFC increased in anxiogenic environments. Taken together, these data strongly argue that the vHPC-mPFC functional connection is an important one.

An interesting finding with functional implications is that the vHPC has high theta-frequency coherence with both the dHPC and mPFC, despite low dHPC-mPFC coherence. This seemingly paradoxical result is possible because vHPC-mPFC and vHPC-dHPC theta coherence may occur at different times or in different theta sub-frequencies (see example in Figure 3.16, panel A). Furthermore, measurements of vHPC-dHPC and vHPC-mPFC theta coherence over time seem to be negatively correlated (Figure 3.16, panel B). These findings argue that while theta generators in the dHPC and vHPC are synchronized, they are nonetheless somewhat independent, possibly subserving different behavioral functions. Perhaps the vHPC might synchronize with the dHPC to process spatial information, while it synchronizes with the mPFC to modulate anxiety-related behaviors.

Such interpretations must, however, be tempered by the caveats inherent in experiments relying on LFPs. Although LFPs reflect the activity of large groups of synapses, allowing analysis of synchronous activity within and across areas, the anatomical origins of LFPs can sometimes

be questionable. Recorded voltage fluctuations can arise from volume conduction of distant signals. Several of our findings suggest that it is unlikely that volume conduction accounts for a substantial fraction of the theta-frequency coherence seen in our recordings. First, we found mPFC-vHPC coherence to be higher than mPFC-dHPC coherence, despite the fact that the mPFC is much further from vHPC (5.9 mm) than dHPC (3.7 mm). Since volume-conducted signals reflect distance rather than anatomical connectivity, coherence between more distant areas would be smaller, rather than larger, if accounted for by volume conduction. Second, we found that multiunit activity in the mPFC, which is not subject to volume conduction artifacts, phase-locks more robustly to local and vHPC theta, but not dHPC theta, during exploration of the open field. Third, in the familiar environment theta oscillations in the mPFC and in the hippocampus occur at different frequencies (Figure 3.5, panel D). Cortical and hippocampal oscillations would have the same frequency if they were volume conducted from the hippocampus. These results argue strongly that the synchrony described is not due to volume conduction of signals into the mPFC from elsewhere. Finally, to show that our vHPC field potential recordings have local relevance, we show that multiunit activity recorded in the vHPC is phase locked both to local theta and gamma oscillations (Figure 3.17).

Another possible source of artifacts in field potential analysis is contamination of the LFP by oscillations recorded not in the brain area of interest, but in the reference electrode. In order to rule out this possibility we demonstrate that the vHPC LFP traces are similar when recorded against the frontal reference or the posterior ground screw (Figure 3.18), and that each of the main findings can be reproduced using the ground screw as an alternate reference (Figure 3.18). Furthermore, spikes in the mPFC were found to be maximally phase-locked to the simultaneously occurring mPFC theta, while phase locking to vHPC and dHPC theta was strongest after a lag of tens of milliseconds, consistent with previously reported delays for this pathway (Thierry et al., 2000). If a substantial amount of vHPC and mPFC theta oscillations were due to contamination from the reference this result would not be possible, as spikes would be expected to phase lock maximally to both vHPC and mPFC theta with a similar temporal offset. These analyses strongly

support the notion that increases in vHPC-mPFC synchrony reflect hippocampal influences on local neuronal activity within the mPFC.

mPFC and vHPC in anxiety

Previous work has shown that lesions of the vHPC (Bannerman et al., 2004; Kjelstrup et al., 2002) or mPFC (Gonzalez et al., 2000; Lacroix et al., 2000; Shah and Treit, 2003) decrease anxiety-related behaviors in anxiety tests. The current study is the first to record neural activity from these areas in anxiogenic environments. Our data demonstrate that mPFC-vHPC theta-frequency synchrony is increased in anxiety tests, as shown by both LFP and multiunit data, suggesting that these areas cooperate to modulate anxiety. Furthermore, mPFC spikes were found to be optimally phase locked to HPC theta oscillations of the past, and crosscorrelations of mPFC and vHPC theta power peaked at a negative lag, consistent with the hypothesis that theta range activity is propagated from the vHPC to the mPFC.

Recent experiments showing a role for the vHPC in spatial representation (Kjelstrup et al., 2008) suggest how the vHPC might act in anxiety. The role of the hippocampus in contextual representation has been studied extensively in the dHPC, where place-selective cells provide fine-scale spatial information. A recent report has shown that the vHPC also has place cells, but with much larger place fields than dHPC cells (Kjelstrup et al., 2008). Larger place fields may be well suited to guide emotional behavior, because generally the stimuli involved in anxiety tests are less spatially discrete. Thus it may be that the vHPC provides contextual (or other larger-scale spatiotemporal) information to downstream structures such as the mPFC, where the decision to engage in defensive vs. exploratory behaviors may be made, perhaps by modulating activity in downstream structures such as the amygdala.

The known anatomical and functional characteristics of the mPFC are consistent with the notion that it interprets contextual information to influence the expression of anxiety-like behaviors. The mPFC receives projections not only from the vHPC but also from multi modal association cortices and the rhinal cortices (Hoover and Vertes, 2007), giving it access to highly processed information about the environment. The mPFC then projects directly to structures such

as the amygdala and the periaqueductal grey (Vertes, 2004), which can act to produce appropriate defensive behaviors. Stimulation of the prelimbic cortex decreases recall of fear extinction, consistent with the idea that this subregion of the mPFC acts to increase anxiety-like behaviors (Vidal-Gonzalez et al., 2006). The mPFC recordings reported here were from the deep layers of the prelimbic cortex, suggesting that the physiological differences found in the mPFC in the EPM and open field may have an anxiogenic role.

The specificity of the increase in theta power in the mPFC is intriguing from a mechanistic and functional standpoint. The high theta coherence throughout the anxiety-provoking environment suggests that coordination of vHPC-mPFC activity is uniformly expressed. The selective increase in theta power in the "safe" aspects of each environment raises the possibility that a change intrinsic to the mPFC increases the gain of this functional connection. Functionally, the spatial distribution and dynamics of the theta power increase are consistent with a role for mPFC theta in inhibition of exploratory behavior during anxiety. A role for the mPFC in behavioral inhibition is in line with prior work, such as reports of higher aggressiveness in rats with lower levels of mPFC GABA (Sustkova-Fiserova et al., 2009). Involvement of the mPFC in behavioral inhibition has also been found in attention tasks, such as the 5-choice serial reaction time task, where higher levels of the serotonin metabolite 5-hydrohyindoleacetic acid in the mPFC were found to correlate with impulsive and premature choices (Puumala and Sirvio, 1998). Furthermore, cytotoxic lesions of the mPFC have been shown to decrease prepulse inhibition and induce hyperlocomotion (Yee, 2000). Lastly, various studies have showed that mPFC lesions decrease fear and anxiety -related responses, both in tasks that depend on the vHPC, such as the EPM (Shah and Treit, 2003, 2004), and paradigms that do not require the vHPC, such as extinction of conditioned fear (Burgos-Robles et al., 2007) and the Vogel conflict test (Resstel et al., 2008). Thus, diverse studies using different behavioral paradigms support a role for the mPFC in behavioral inhibition, consistent with the present work.

The data obtained from the 5-HT1AR knockouts are consistent with the hypothesis that both the vHPC and mPFC have a role in the generation of anxiety. A role for the hippocampus in their anxiety phenotype has already been hypothesized based on several factors: hippocampal 5-

HT1A receptors have been shown to modulate anxiety (File et al., 1996); 5HT1AR knockout mice are specifically more anxious only in paradigms which require the hippocampus (Buzsaki et al., 2003; Gordon et al., 2005; Klemenhagen et al., 2006); restoring forebrain expression of the receptor rescues the anxiety phenotype (Gross et al., 2002); and the elevated plus maze induces an increase in theta power in the knockouts (Gordon et al., 2005). Here we report a larger anxiety-induced increase in mPFC theta power in the knockouts. While these results do not resolve whether the primary alteration in 5-HT1AR knockouts resides in hippocampal hyperactivity or in the ability of the vHPC and mPFC to synchronize, they lend further credence to the hypothesis that the increases in mPFC theta power seen in the wild-types are indeed due to anxiety rather than unrelated behavioral effects of the open field and EPM.

While theta-frequency oscillations are prominently featured in the data supporting the current model, their importance is debatable. On one hand, we present data from two different anxiety tests linking the strength of theta oscillations in the mPFC with behavioral measures of anxiety. These data are consistent with existing hypotheses suggesting a specific role for hippocampal theta oscillations in behavioral inhibition and hippocampal-dependent anxiety (McNaughton and Gray, 2000). On the other hand, we cannot rule out the possibility that anxiety may require only that the vHPC communicates with the mPFC, and not that it uses theta oscillations to do so. Experiments aimed at perturbing theta generation by pharmacological or genetic manipulations are necessary to elucidate this question. In any case, our data suggests that the vHPC-mPFC connection is important for the modulation of anxiety-related behavior.

The present results show that theta range synchrony between the vHPC and the mPFC is modulated by anxiety. This finding suggests a model in which the vHPC sends the mPFC large-scale information about the emotional salience of the environment, which allows the mPFC to recognize the environment as threatening. The mPFC may in turn modulate the amygdala to produce appropriate defensive and anxiety-related behaviors. Importantly, behavioral modulation of theta synchrony has been shown previously between the dHPC and other structures such as the amygdala in fear conditioning (Seidenbecher et al., 2003), the striatum in learning (DeCoteau et al., 2007), and the mPFC in working memory (Jones and Wilson, 2005). Together these

studies are consistent with the emerging notion that theta range synchronization between the hippocampus and other areas is a general mechanism by which information is transmitted between the hippocampus and downstream structures relevant to ongoing behavior.

3.4 Materials and Methods

Animals

Three to six month old male wildtype 129Sv/Ev mice were obtained from Taconic (Germantown, NY, USA). 5-HT1AR knock-out mice and littermate controls were generated from heterozygote breeding pairs on a 129SvEv background as described previously (Ramboz et al., 1998). Eighteen wild type and seven 5-HT1AR knockout mice were used for the simultaneous mPFC, dHPC and vHPC recordings. An additional two wild-type mice were used for the ventral hippocampus multiunit recordings. Experiments comparing knockouts and wild-types were conducted blind to genotype. The procedures described here were conducted in accordance with National Institutes of Health regulations and approved by the Columbia University and New York State Psychiatric Institute Institutional Animal Care and Use Committees.

Microdrive Construction

Custom microdrives were constructed using interface boards (EIB-16, Neuralynx, Bozeman MT) fastened to a Teflon platform. This platform was fastened to Teflon cuffs via fine machine screws (SHCX-080-6, Small Parts, Inc, Miramar, FL), permitting the platform to advance by turning the screws into the cuffs. Electrodes were made from Formvar-coated tungsten microwire (California Fine Wire, Grover Beach, CA). The mPFC electrodes were fastened to a cannula attached to the platform to permit them to be lowered precisely after implantation; hippocampal electrodes were stereotactically placed and cemented directly to the skull during surgery.

Surgery

Animals were deeply anesthetized with ketamine and xylazine (165 and 5.5 mg/kg, in saline) and supplemented with inhaled isoflurane (0.5-1%) in oxygen. Mice rested on a heating pad regulated by a feedback controller; temperature was monitored with a rectal probe. Mice were secured in a stereotactic apparatus (Kopf Instruments, Tujunga, CA) and the skull was leveled using bregma and lambda landmarks. Screws were implanted on the posterior and anterior portions of the skull to serve as ground and reference, respectively. Anterior-posterior and medial-lateral coordinates were measured from bregma, while depth was calculated relative to brain surface. Tungsten wire electrodes were implanted through burr holes targeting the following locations: dHPC CA1 (1.94 mm posterior, 1.5 mm lateral and 1.4 mm depth), vHPC CA1 (3.16 mm posterior, 3.0 mm lateral and 4.2 mm depth) and mPFC (+1.65 mm anterior, 0.5 mm lateral and 1.5 mm depth). These coordinates resulted in electrode tips located near the fissure or in the stratum lacunosum-moleculare for the hippocampal electrodes, and in the deep layers of the ventral portion of the prelimbic cortex for the mPFC electrodes. Electrodes were implanted at the vHPC and dHPC sites and cemented directly to the skull with Grip Dental Cement (Dentsply, Milford, DE). The microdrive was then placed carefully over the skull with a micromanipulator, and the attached mPFC electrode was lowered to the appropriate depth. The Teflon cuffs were then cemented to the skull, and the ground and reference screws as well as the hippocampal electrodes were connected to the interface board. Lastly, walls of dental cement were built between adjacent cuffs to protect the electrodes from external debris. Animals were monitored postoperatively and given analgesics (Carprofen, 5 mg/kg S.C.) as necessary. Following surgery, animals were housed individually with bedding squares provided for enrichment.

Behavioral Protocol

Animals were permitted to recover for at least one week or until regaining pre-surgery body weight. Mice were then food restricted to 85% body weight. During food restriction animals were familiarized to the recording setup and handling by being tethered to the head stage preamplifier in their home cages for 5-7 daily sessions of 20 minutes each. Upon reaching their target weight, mice were exposed to a small rectangular box ("familiar arena", 30X20 cm) in the dark in which

they foraged for pellets for 4 or more daily sessions of 10 minutes. Twelve wild type and seven 5HT1AR knockout mice were exposed to either the open field or the EPM for 10 minutes following a one hour resting period after the exposure to this familiar arena. After 2 days of rest the procedure was repeated with the other anxiogenic environment. The order of presentation of the two environments was counterbalanced across animals. Additionally, a group of 6 wild-type mice were exposed only to the open field. Physiological and behavioral measures did not vary across groups. Wild type mice spent 53% of the time in the open arms of the EPM and 15% of the time in the center of the open field. The EPM and the open field were found to be anxiogenic in both wild type and 5HT1AR knockout mice. However, we were unable to detect differences between the two genotypes in classical behavioral measures of anxiety in the current cohort, likely because it was too small; group sizes of 20-25 animals are typically required to detect behavioral differences between knockouts and wildtypes in these tests (Ramboz et al., 1998). Nevertheless, we found expected differences in total path length in the open field (1061±79 and 851±83, for WTs and KOs, respectively), consistent with previous reports (Gross et al., 2002). Decreased total path length is indicative of increased responsiveness to the anxiogenic environment in the knockout mice and higher behavioral inhibition.

Exposures to the EPM were done at 200 lux. The elevated plus maze was constructed of wood painted grey and consisted of four arms, 7.6 cm wide and 28 cm long, elevated 31 cm above the floor. Two opposing arms were enclosed by 15-cm-high walls, whereas two were open except for a 1-cm-high lip at the edge. The open field consisted of a wooden round grey circular arena with 25 cm radius and 40 cm height. In order to permit a better behavior/physiology correlation, it was necessary to increase the variance in center time by altering the illumination in the open field. Therefore, half of the open field recordings were done at 20 lux, while the other half was done at 120 lux. As intended, recordings done at 20 lux increased exploration of center of the open field, and diminished the fold increase of theta power in the mPFC (1.41±0.1 and 1.0±0.13, for 120 and 20 lux, respectively). The finding that light levels affected center time (9.1±6 and 30.7±15, for 120 and 20 lux, respectively), as previously shown (Barrot et al., 2002), strongly suggests that % time spent in the center of the open field is a valid measure of anxiety in the

current cohort. Comparisons between wildtype and 5-HT1AR knockout mice were done at 20 lux. All the other analyses pooled the results from both 20 and 120 lux recordings.

The open field was clearly anxiogenic in our cohort, as the majority of mice spent less than 10% of the time exploring the brightly lit center of the open field (Figure 3.13A), in line with previous behavioral reports in mice (Fee et al., 2004) and in rats (Cannizzaro et al., 2003). Not all mice displayed robust avoidance of the open arms in the EPM. However, mice that displayed high anxiety in the EPM also did the same in the open field. Accordingly, % time spent in the center of the open field and % time spent in the open arms of the EPM were significantly correlated ($r=0.48$, $p=0.04$). This suggests that these measures are associated with individual trait-level anxiety. Moreover, % time spent in open arms was highly correlated across multiple exposures to the EPM in a subset of the animals exposed to the EPM twice ($r=0.8$, $p=0.01$). These results are consistent with the notion that the behavioral measures used in the current work reflect trait-anxiety. Although some animals were exposed to the EPM for two days, neural data from the second exposure was not analyzed.

In order to verify whether vHPC field potentials have local relevance, two mice were implanted with electrodes in the following coordinates targeting the vHPC: 3.16 mm posterior, 3.0 mm lateral and 3.2 mm depth. Electrodes were lowered across days until a dramatic increase in multiunit activity was found. The electrodes were judged to have reached the pyramidal layer in that day. Data from Figure 3.17 is from a session in the familiar environment after the pyramidal layer was reached. At the end of the experiment mice were sacrificed and perfused transcardially. Electrode position was subsequently confirmed with Nissl staining.

Data Acquisition

Recordings were obtained via a unitary gain head-stage preamplifier (HS-16; Neuralynx) attached to a fine wire cable suspended on a pulley so as not to add any weight to the animal's head. LFPs were recorded against the reference screw located above the olfactory bulb. Field potential signals were amplified, bandpass filtered (1-1000 Hz) and acquired at 1893 Hz. Multiunit activity from mPFC was recorded simultaneously from the same electrodes used to obtain LFPs;

multiunit signals were bandpass filtered (600-6000 Hz) and recorded at 32 kHz. Spikes exceeding a threshold of 400 μV were selected for analysis of phase-locking to theta (see below). Both LFP and multiunit data were acquired by a Lynx 8 programmable amplifier (Neuralynx) on a personal computer running Cheetah data acquisition software (Neuralynx). The animal's position was obtained by overhead video tracking (30 Hz) of two light-emitting diodes affixed to the head stage.

Data Analysis

Data was imported into Matlab for analysis using custom-written software. Velocity was calculated from position records and smoothed using a window of 0.33 seconds. Measurements that were found to be affected by speed, such as coherence and power spectra, were calculated from data acquired during segments of consistent movement between 7-15 cm/s. The results described were not affected by the specific speed range used. Spectral analysis of LFPs were done using Matlab's signal processing toolbox functions along with custom software. Power spectra were calculated using the Welch method with a moving window of 0.4 s, with 90% overlap, and 4000 nFFTs. Coherence was calculated with the multitaper method, using a time-bandwidth product of 30. Confidence intervals were calculated through a jackknife method across animals and tapers. These specific parameters were optimized empirically but the results were robust to changes in any given parameter. Coherence at very high frequencies (>100 Hz) was high between all brain areas. This is likely because biological oscillations in this frequency range are small relative to noise common to all recording sites under our recording conditions.

In order to calculate theta power accurately, we fitted power spectra with the sum of an exponential and a Gaussian using Matlab's cfit function from the curve fitting tool box. The area of the theta-centered Gaussian was taken as the measure of theta power. Unless otherwise stated all power spectra, coherence plots and fold power increases bar graphs shown in figures are from data collected while animals were moving between 7 and 15 cm/s.

Coherence is comprised of power correlations and consistency of phase (phase coherence). We analyzed these two measures separately for they may vary independently. To calculate power correlations across areas, theta and gamma power were calculated over time.

Individual points in the power correlation plots (Figure 3.7A) represent average theta power calculated through a multitaper spectrogram method with an NW of 2.5. A window size of 5000 samples (2.6 seconds) with no overlap between successive windows across 10 minutes of recording was used. The linear correlation coefficient for each plot was calculated and averaged across animals for each pair of brain areas. Fisher's Z-transform was calculated on the correlation coefficients to obtain a normally distributed population of values. Student's t-tests were then performed to compare the transformed r values for mPFC-dHPC and mPFC-vHPC. Power correlations, as well as theta phase difference histograms were calculated on data from the entire recording, regardless of the speed of the animal. The consistency of the phase relationship was measured by calculating the instantaneous theta phases of two signals through the Hilbert transform and then subtracting the phases of the 2 LFPs from each other. Only time points during which hippocampal theta power was greater than the mean theta power for that session were used. The phase differences obtained were then plotted as histograms, and the width of this plot at half of the peak height was used as a measure of the consistency of the phase relationship of the two signals. If two signals tend to have a constant phase relationship (i.e., the difference between the phases of the two signals tends to be constant), the phase difference histogram will display a narrow peak, independent of the absolute mean phase difference.

To measure the influence of hippocampal theta phase on mPFC gamma power, instantaneous values for theta phase and gamma amplitude were obtained using a Hilbert transform on band-pass filtered LFP data. The strength of the modulation of gamma amplitude by theta phase was measured by first normalizing to the mean gamma power and then computing the fractional modulation of gamma amplitude by theta phase.

The strength of multiunit phase-locking to theta oscillations was assessed by comparing the mean resultant length vector (MRL), which is derived from Rayleigh's z statistic of circular uniformity across environments. Only data obtained while animals were moving (velocity > 4 cm/s) were used to compute phase-locking for theta because theta power is low during immobility, preventing accurate estimation of theta phase. To determine whether spikes were phase-locked to theta, theta phases of LFPs were determined through the Hilbert transform, and

a phase was assigned to each spike based on the time of the spike's occurrence. A phase of 0 refers to the trough of the theta cycle as recorded. The magnitude of phase-locking can be measured through Rayleigh's z parameter. MRL ($MRL=(z/number\ of\ spikes)^{0.5}$) was used in comparisons instead of z because the population of MRL values has a lower variance than the z population. Higher modulation of firing by theta phase increases MRL. However, it is important to note that high MRL values can also be obtained by calculating Rayleigh's statistic on a sample with few spikes, thus only recordings with a minimum of 700 spikes in both environments were analyzed. To avoid changes in MRL due to fluctuations in firing rate, the same number of spikes was analyzed in a given multiunit recording across environments. A paired Wilcoxon's test on MRL values was used to determine if phase-locking of multiunit activity to mPFC, dHPC and vHPC theta increased in the open field relative to the familiar arena. To determine the temporal relationship between multiunit activity and theta oscillations in each area, phase locking was calculated for 40 different temporal offsets for each multiunit recording. Units with significant Bonferroni-corrected phase locking in at least one of the 40 shifts were used for the analysis in Figure 3.8 C-E.

In order to calculate changes in mPFC theta power during transitions from the closed arm to the center, spectrograms spanning 10 seconds centered at the transitions were calculated. The multitaper method was used, with 20000 nFFTs, in 2-second windows with 97% overlap, 1.5 NW and 5 tapers. Spectrograms of all transitions in all mice were averaged and plotted on Figure 3.12. For closed-center transitions, the open and center compartments were treated as one compartment. This was done as both the open arms and the center are anxiogenic compartments, with similar changes in theta power (Figure 3.12). Coherograms centered at the transitions were calculated with 0.5-second windows with 0.3-second overlap and 3700 nFFTs. These coherence values are not directly comparable to the ones shown in Figure 3.2C, as the parameters used for the estimation of coherence were different.

Statistics

Paired Wilcoxon's signed rank tests were used for comparisons involving measurements from the same animal across behavioral conditions, such as changes in theta power in anxiogenic environments relative to the familiar arena. Comparisons between populations of r^2 across environment or across brain areas were performed with paired t-tests on the Fisher's Z transformed r values. The use of t-tests in this case is warranted because the Z transform produces a normal distribution, as verified through the Lilliefors test for normality. Standard error of means (S.E.Ms) were plotted in bar graphs to show the accuracy of the estimation of the mean of the population. Two-tailed tests were used throughout.

Histology and Genotype Confirmation

Upon the completion of recording, animals were deeply anesthetized and electrolytic lesions were made to determine the position of the electrode tips. Lastly, animals were tail clipped and perfused with formalin. Brain sections were mounted on slides to visualize and photograph lesions. For 5-HT1AR knockouts and control littermates, DNA was extracted from the clipped tails to reconfirm genotype through PCR.

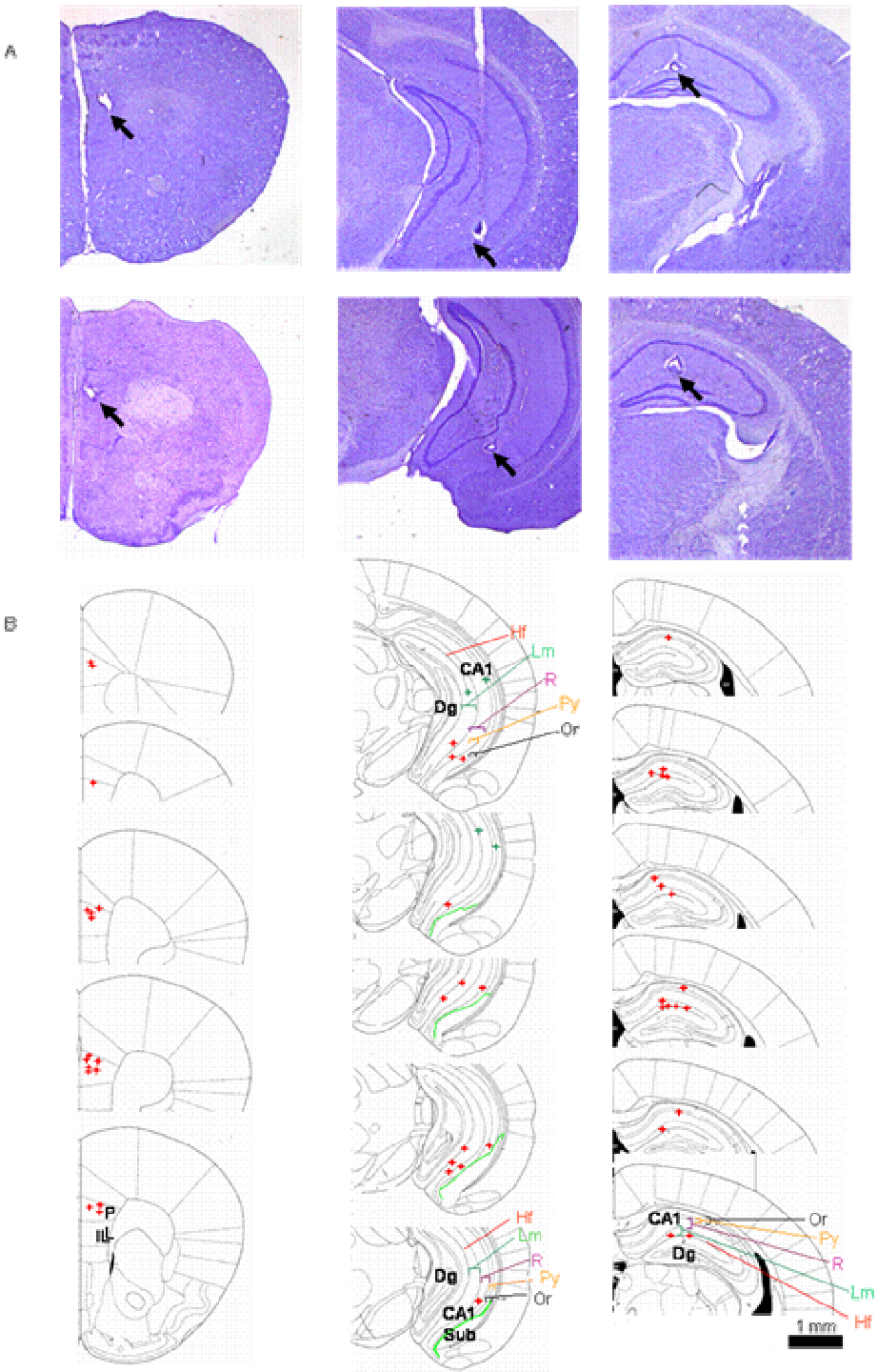

Figure 3.1. Location of electrodes. (A) Representative Nissl stained sections showing electrolytic lesions in mPFC (left column), vHPC (middle) and dHPC (right column). Lesion sites are indicated by arrows. (B) Diagrams show coronal sections arranged from most anterior (top) to most posterior lesions (bottom). Individual lesions are shown in red stars. Lesions of mHPC are shown as green stars. Hippocampal layers and sub-areas are shown for vHPC and dHPC sections. The border between subiculum and CA1 in vHPC sections is shown in green. Sub: subiculum, Dg: dentate gyrus, Hf: hippocampal fissure, Lm: lacunosum moleculare, R: stratum radiatum, Py: pyramidal layer, Or: stratum oriens, PL: prelimbic cortex, IL: infralimbic cortex.

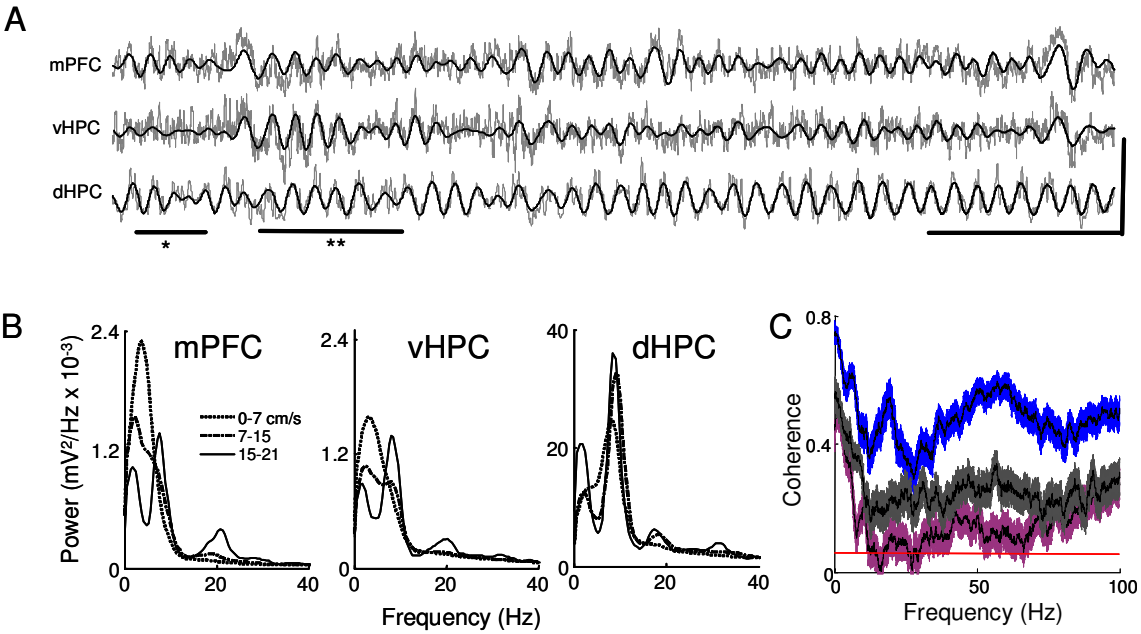

Figure 3.2- Characterization of LFPs from the mPFC, vHPC and dHPC in the familiar arena. (A) Traces of simultaneously recorded local field potentials from the mPFC, vHPC and dHPC in a mouse exploring the familiar arena. Raw traces are plotted in grey and theta filtered traces are overlaid in black. Underlines indicate a period robust theta activity in mPFC with minimal theta in the vHPC (*) and a period of robust theta-range activity in both mPFC and vHPC (**). Calibration: horizontal bar:1 s, vertical bar: 0.5 mV for mPFC and vHPC and 2.5 mV for dHPC trace. (B) Power spectra for different speed ranges for mPFC, vHPC and dHPC. Note that the peak centered at the theta range increases with higher speeds in all three areas. Also note the different scale on dHPC figure; theta power is much higher in dHPC than in vHPC and mPFC. Spectra are averages of 13 animals. (C) Coherence averaged across animals for mPFC-vHPC (blue), mPFC-dHPC (purple) and vHPC-dHPC (grey) recorded in the 7-15 cm/s speed range. Note that mPFC-vHPC coherence is higher than mPFC-dHPC for all frequencies. Shaded areas indicate 95% confidence intervals and the red line at the bottom shows the coherence expected by chance ($p<0.05$).

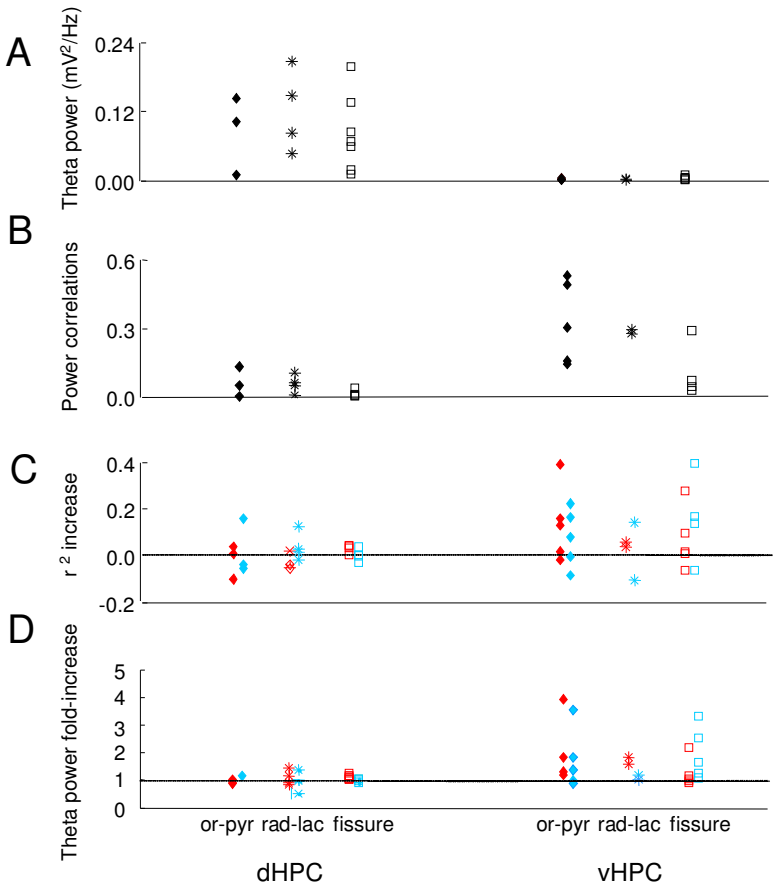

Figure 3.3- mPFC-HPC synchrony and HPC changes in theta power in the EPM and open field do not vary substantially across HPC layers. Plots of theta power for all layers of dHPC and vHPC. Power is higher in dHPC than vHPC in all layers (A). (B) Theta power correlations with mPFC for all layers of dHPC and vHPC are shown. (C) Change in theta power correlations with the mPFC for all layers of dHPC and vHPC. In all layers, mPFC-vHPC correlations increase in anxiogenic environments (C). (D) Theta power fold increases relative to the familiar environment in all layers of the dHPC, but not vHPC in both the open field and in the EPM are shown. Note that vHPC theta power is increased regardless of the location of the electrode. Or-pyr:oriens-pyramidal, rad-lac:stratum radiatum and lacunosum moleculare.

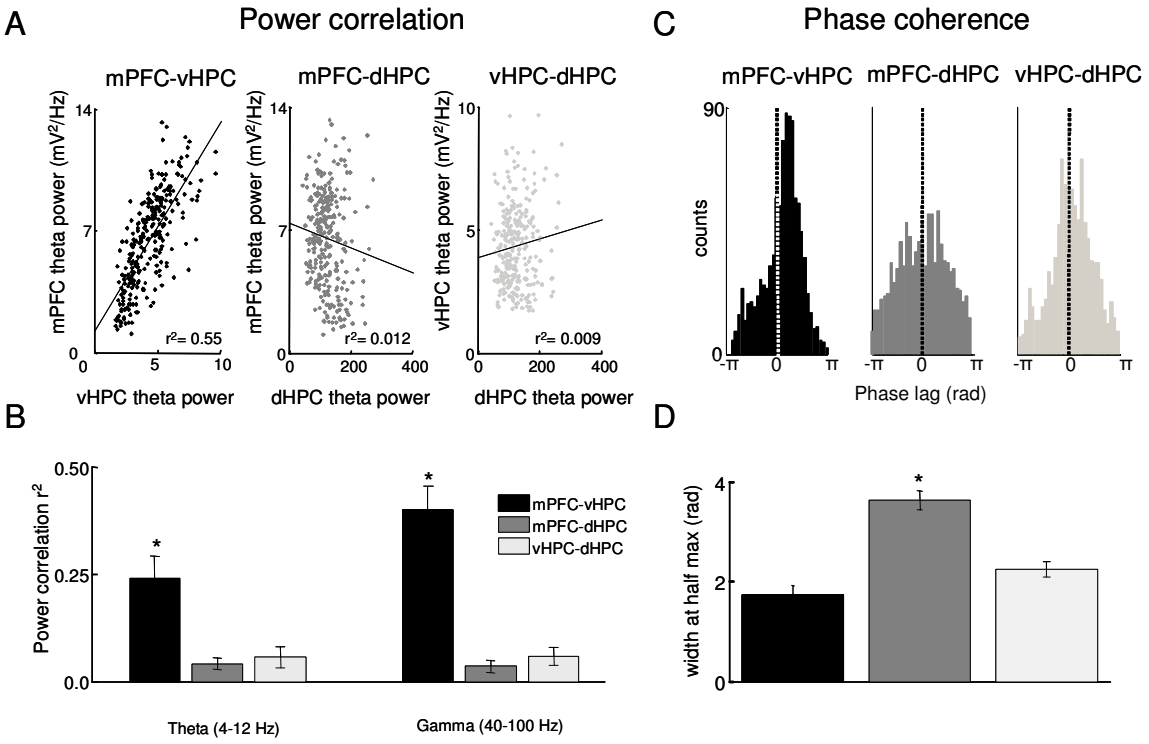

Figure 3.4- Power correlations and phase coherence across areas. (A) Representative examples of theta power correlation scatter plots for vHPC-mPFC, dHPC-mPFC and vHPC-dHPC from a 10 minute recording session in the familiar arena. Each data point represents the sum of theta power during a 2.6 s window. (B) Averages of the linear correlation coefficients of theta (left corner) and gamma (right corner) power across 13 animals for vHPC-mPFC, dHPC-mPFC and vHPC-dHPC. Error bars are ± s.e.m. *p<0.01 for paired t-tests on the Fisher's Z-transformed r values compared to mPFC-vHPC. (C) Representative histogram of theta phase differences. Instantaneous theta phase of two signals were subtracted from each other and the difference in theta phase was plotted as a histogram, for mPFC-vHPC (black), mPFC-dHPC (dark grey) and dHPC-vHPC (light grey). Narrower peaks in the histogram indicate a more consistent phase relationship. (D) Width of theta phase difference histogram at half of the peak height averaged across 13 animals for vHPC-mPFC (right panel), dHPC-mPFC (center panel) and vHPC-dHPC (left panel). Error bars are ± s.e.m. *p<0.01 for t-test comparing mPFC-vHPC to mPFC-dHPC.

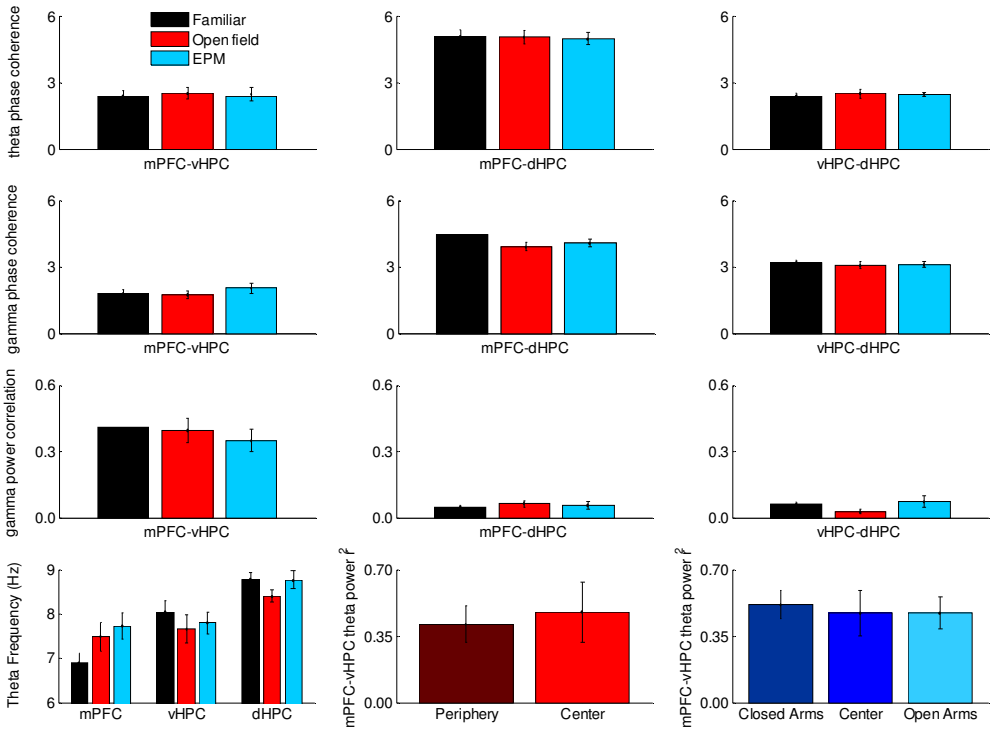

Figure 3.5-Effects of anxiety on additional measures of synchrony. (A) Theta phase coherence is not altered by open field or EPM across each of the brain region pairs. Phase coherence was estimated by measuring the width of the phase difference histogram at half of the peak height (see example in figure 2). Smaller widths indicate higher phase coherence. (B) Same as (A), but for gamma range. (C) Gamma range power correlations were not altered across each of the brain region pairs. Bar graphs show gamma power correlations across conditions. (D) Theta frequency across conditions for the mPFC, vHPC and dHPC. Note that theta frequency in the mPFC ini the familiar environment is significantly lower than in vHPC. With exposure to the EPM, mPFC theta increases, becoming closer to vHPC theta frequency. A similar increase with exposure to the open field did not reach statistical significance. (E-F) Theta power correlations between the mPFC and vHPC for sub-areas of the open field (E) and in the EPM (F). Error bars are ± s.e.m. *p<0.05 for Wilcoxon's signed rank test.

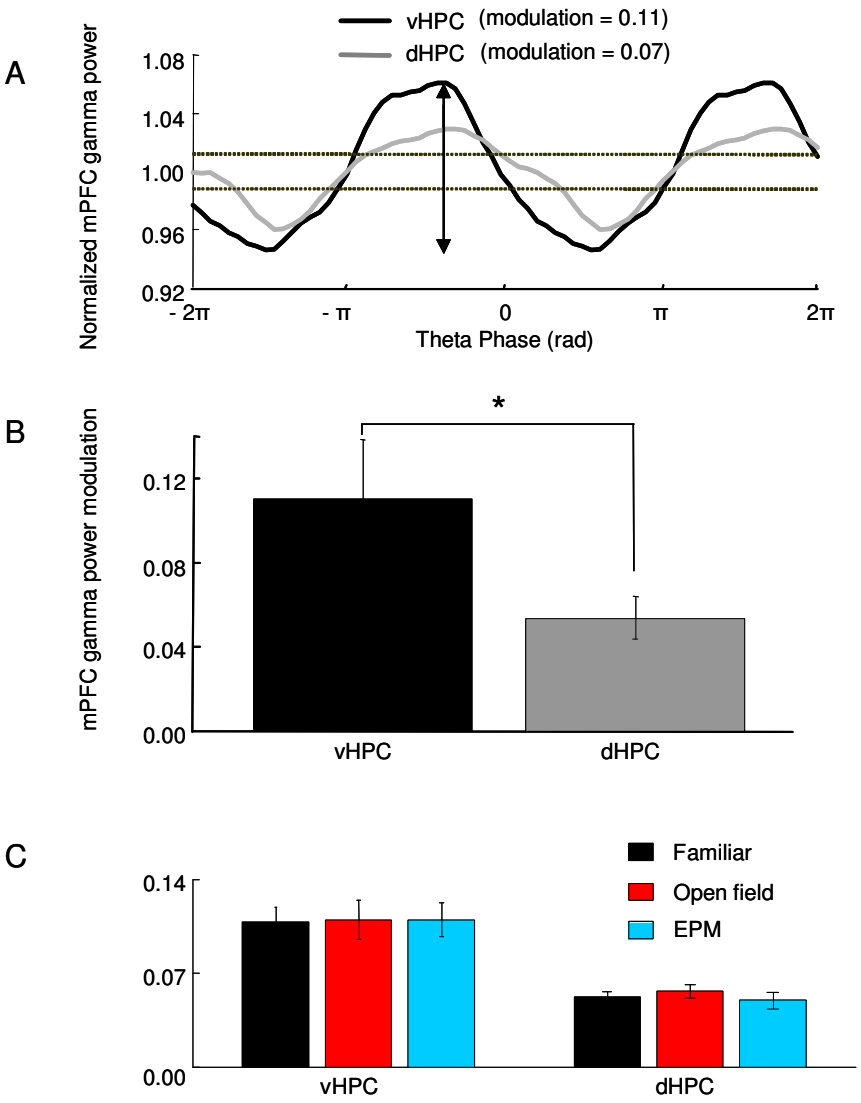

Figure 3.6- Modulation of mPFC gamma power by hippocampal theta phase. (A) Example traces showing modulation of normalized mPFC gamma power with vHPC (black trace) and dHPC (grey trace) theta phase. Modulation of gamma power by theta phase was calculated as being the peak to trough distance in the curve, as indicated by the double-headed arrow in the vHPC curve. Dotted lines indicate chance levels of modulation, obtained by shifting the mPFC signal by 5-10 seconds. (B) Modulation of mPFC gamma power by theta phase of vHPC (black bar) and dHPC (grey bar) averaged across 12 animals. mPFC gamma was more strongly modulated by vHPC theta than dHPC theta. (C) Data show modulation of gamma power in the mPFC by vHPC and dHPC theta phase in the familiar environment, the open field and the EPM. For simplicity, familiar environment data from the EPM and open field were averaged together. Error bars are ± s.e.m. *$p<0.05$ for a paired Wilcoxon's signed rank test.

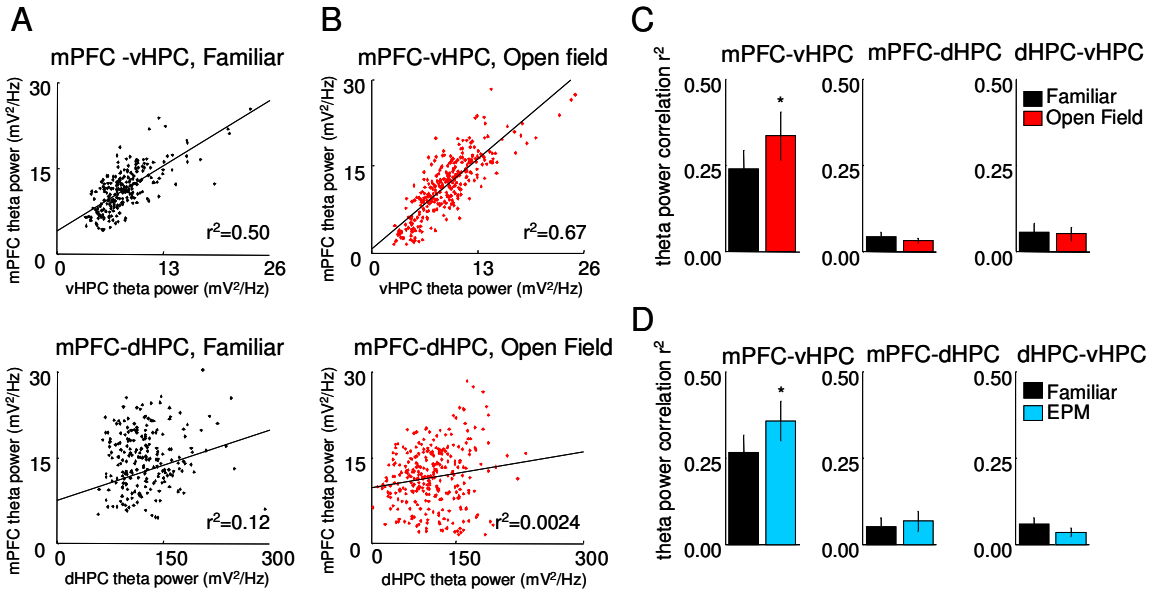

Figure 3.7- Theta power correlation between mPFC and vHPC increases in the EPM and open field. (A) Representative example of theta power correlation plot in the familiar arena between mPFC and vHPC (upper panel) and dHPC (lower panel). (B) Theta power correlation plot in the open field from the same animal as in Fig. 4a between mPFC and vHPC (upper panel) and the dHPC (lower panel). Note the increase in mPFC-vHPC linear correlation r^2 compared to Figure 4 A. Changes in averaged r^2 of theta power correlations between in the familiar arena and open field (C) and EPM D) for mPFC-vHPC (left panel), mPFC-dHPC (middle panel) and dHPC-vHPC (right panel). Bars are averages of data from 13 animals, error bars are ± s.e.m. *p<0.05 for a paired t-test for the Fisher's Z transformed r values.

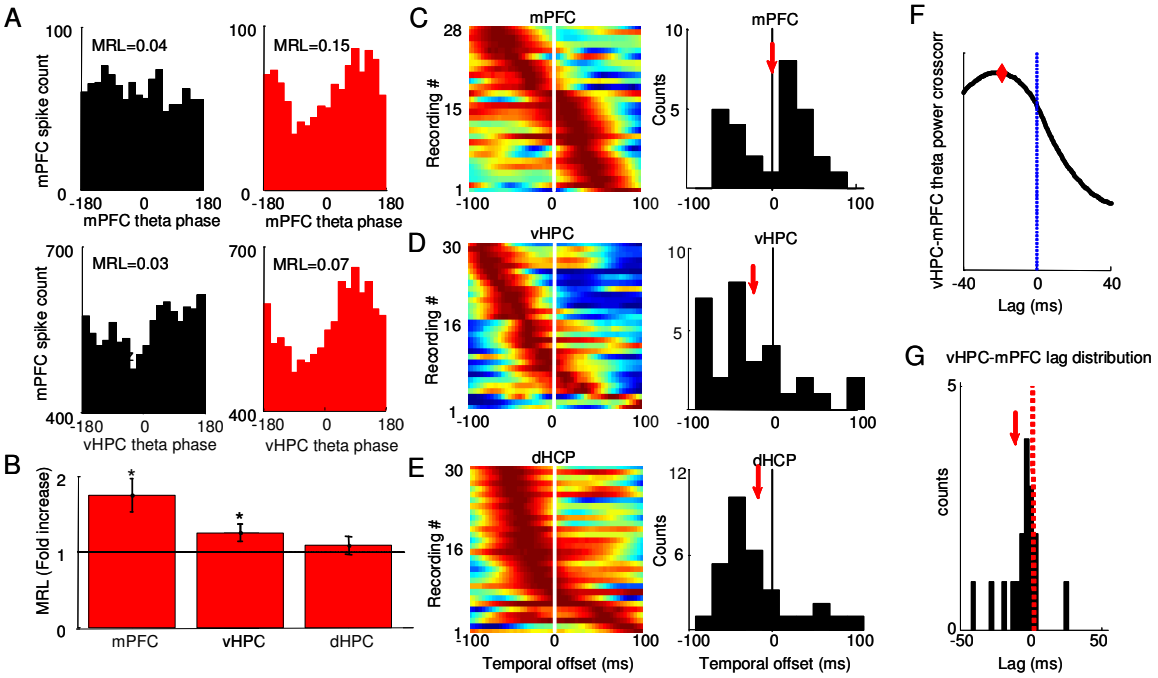

Figure 3.8- Multiunit phase-locking to mPFC and vHPC theta increases in the open field. (A) Representative examples of the distribution of preferred phases of multiunit activity recorded in the mPFC relative to local (upper panels) and vHPC (lower panels) theta oscillations in the familiar arena (black histograms) and the open field (red histograms). (B) Mean +/- S.E.M. of MRL values in the open field relative to the familiar environment for multiunit recordings to mPFC (left bar), vHPC (middle) and dHPC (right) theta oscillations. Note that the MRL in the open field is larger than in the familiar arena, indicating more robust phase-locking to both mPFC and vHPC theta oscillations. (C-E). mPFC units phase lock best to local theta of the present (C) and hippocampal theta o f the past (D,E). Color-coded plots show changes in MRL values for multiunit recordings after spikes are shifted in time relative to theta oscillations of mPFC (C), vHPC (D) and dHPC (E). Higher MRL values correspond to warmer colors. Each row corresponds to one multiunit recording. Rows are arranged according to the temporal offsets that produce maximal phase locking. Upper rows correspond to multiunit recordings that phase lock most robustly with large negative shifts, i.e., maximal phase locking to theta of the past. Histograms showing the population distribution of the temporal offsets with highest phase locking are shown on the right. The population mean is indicated by red arrows. Note that on average spikes in the mPFC are most strongly phase locked to hippocampal theta of theta of the past. Only recordings that were significantly phase locked (by Rayleigh's test for circular uniformity, Bonferroni corrected $p< 0.05/40$) in at least one temporal shift were used. n=28-30 multiunit recordings. *$p<0.05$ for a paired Wilcoxon's signed rank test on MRL values. (F) Example of crosscorrelation of mPFC and vHPC theta power. Note that the crosscorrelation peaks at a negative lag, indicating that theta power changes occur first in the vHPC and then in the mPFC. Instantaneous power was calculated through the Hilbert transform. (G) Histogram showing the distribution of lags with maximal crosscorrelation across animals. The median lag is significantly different from zero (-8 ms, $p<0.05$, signrank test). Only segments of data where vHPC theta power was greater than the mean vHPC theta power for a given session were used. The population mean is indicated by a red arrow.

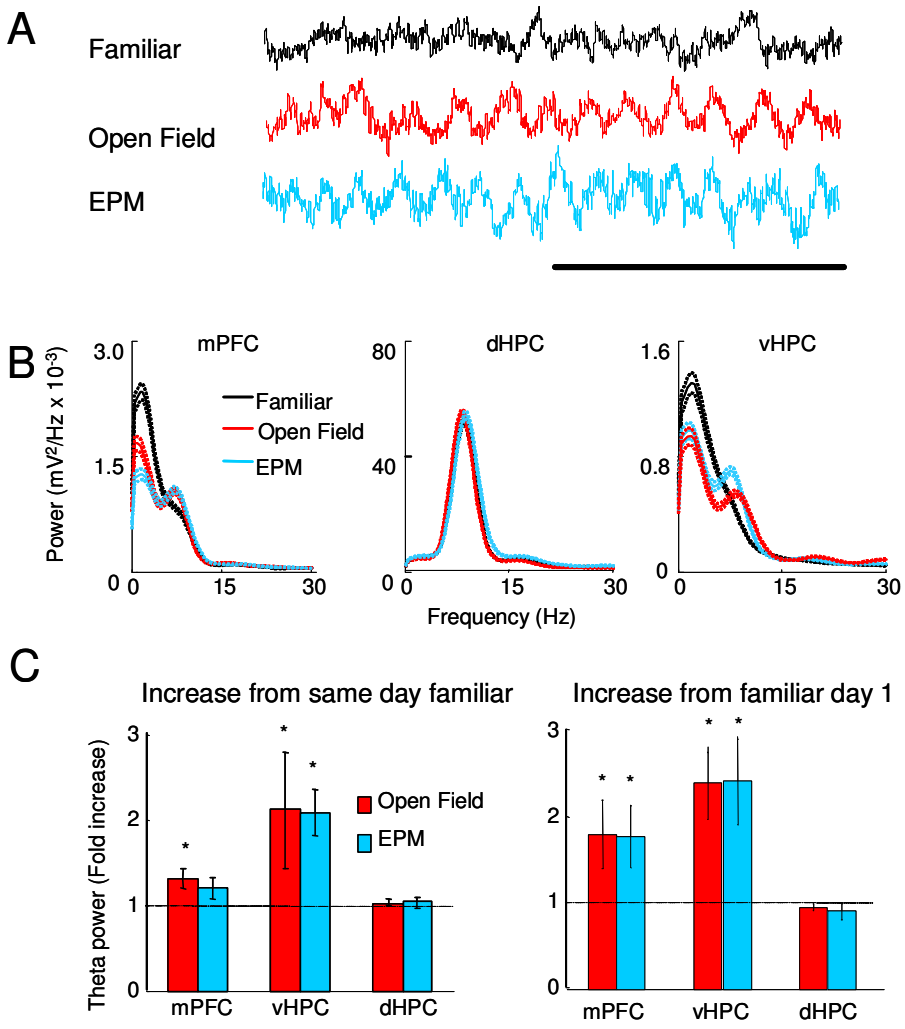

Figure 3.9- Theta power in the mPFC and dHPC increases during exposure to the EPM and open field. (A) Representative traces of mPFC LFPs recorded from the same animal in the familiar arena, open field and EPM. Calibration: 1s. (B) Examples of representative power spectra in the familiar arena (black traces), open field (red) and EPM (blue) from LFPs of the mPFC (left panel), vHPC (center) and dHPC (right). Mean power was calculated using the Welch method with s.e.m. (dashed lines) calculated across windows. (C) Left panel: Fold increases in theta power relative to the familiar arena exposures obtained in the same day as the open field (red bars) and in the EPM (blue bars) recordings. Right panel: Same as left panel, but relative to the first day of exposure to the familiar environment. All data are taken from epochs in which animals were running consistently in the 7-15 cm/s speed range.

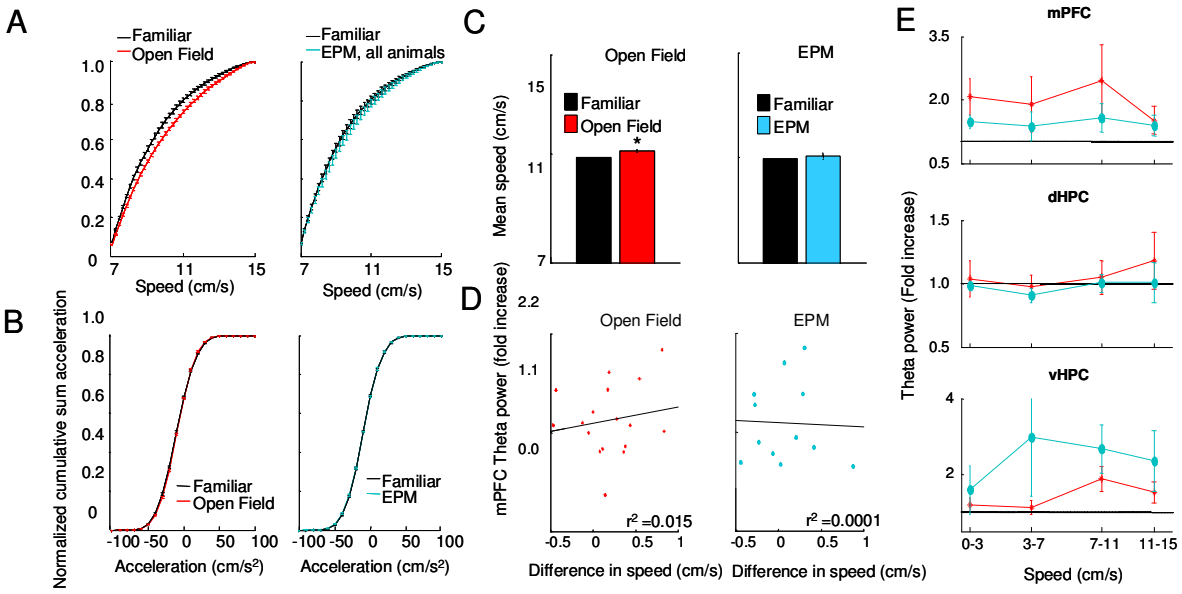

Figure 3.10- Locomotor behavior does not account for mPFC theta power increases in the open field and EPM. Cumulative sum distributions of speed (A) and acceleration (B) in the familiar environment (black), open field (red) and the EPM (blue) are shown. Speed distribution indicates a small increase in speed in the open field, but not in the EPM, compared to the familiar arena. (C) Relative to the familiar arena, mean speed in the 7-15 cm/s range is slightly increased in the open field, but not in the EPM. (D) Plots of mPFC theta power fold increase as a function of difference in mean speed from the familiar environment. Note that in both the open field (left panel) and the EPM (right panel) increases in mPFC theta power were not correlated with changes in mean speed relative to the familiar arena. (E) Plots showing theta power fold increase relative to the familiar environment for the open field (red) and EPM (blue), for the mPFC (top), vHPC (middle) and dHPC (bottom). Note that theta power is increased in the mPFC and vHPC in both anxiogenic environments at all speeds. $p<0.05$ for main effect of anxiety in a repeated measures ANOVA, both for mPFC and VHPC, in the open field and the EPM. There was no interaction effect between anxiety and speed. Error bars are ± s.e.m. n=18 and 12 for the open field and EPM, respectively. *$p<0.05$ in Wilcoxon's signed-rank test.

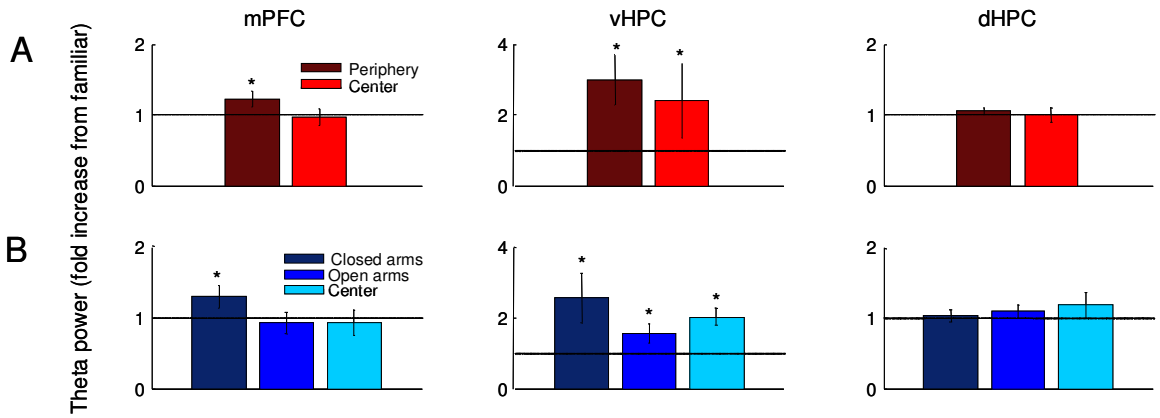

Figure 3.11- mPFC theta power is increased specifically in the safe zones of the anxiogenic arenas. (A) Theta power increases in the mPFC, vHPC and dHPC during navigation of the periphery (dark red) and center (bright red) of the open field. (B) Theta power increase in each area during navigation of the closed arms (dark blue), open arms (medium blue), and center (light blue) of the elevated plus maze. n=18 and 12 for the open field and EPM, respectively. All data are from epochs in which animals were running consistently in the 7-15 cm/s speed range. Fold increases are relative to theta power in the familiar arena exposure on the same day. Error bars are ± s.e.m. *p<0.05, for a paired Wilcoxon's signed rank test.

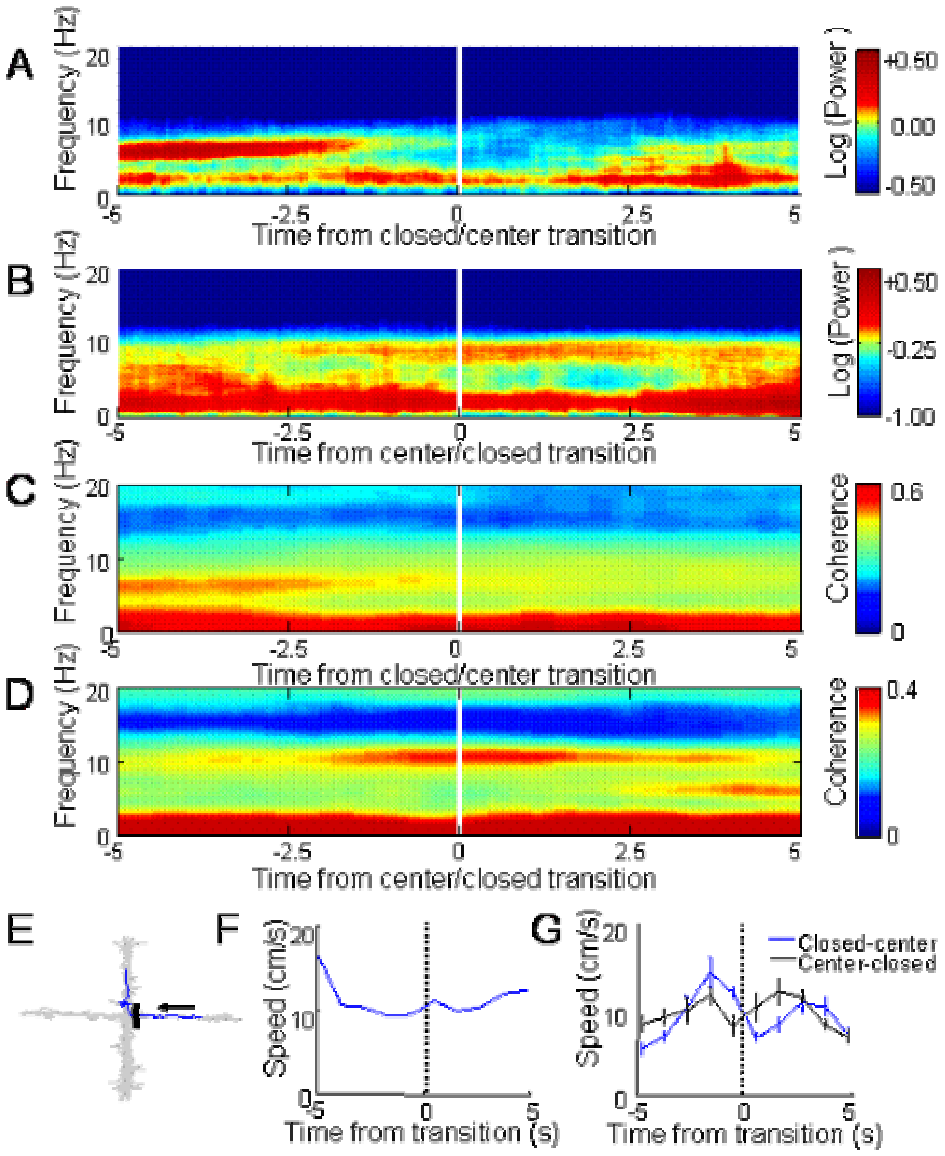

Figure 3.12- mPFC theta power and mPFC-vHPC coherence increase prior to leaving the closed arms. (A) Average mPFC spectrogram of all closed arm to center transitions in the EPM, centered at the transition point (time=0 sec). (B) Same as (A), but for center to closed arm transitions. Note sharp changes in mPFC theta power occur 2-3 s before the animal enters a new compartment of the maze. (C) Average mPFC-vHPC coherence centered at the closed to center transition. (D) Same as (C), but for center to closed transitions. (E) Example track of a closed to center transition. 10 seconds of movement (blue trace) centered at the transition is shown. Grey trace tracks the position of the mouse in the entire session. The black bar indicates the position of the transition, and the arrow shows the direction of movement. (F) Speed across time for the example transition shown in (E). (G) Average speed for both closed to center and center to closed transitions is shown.

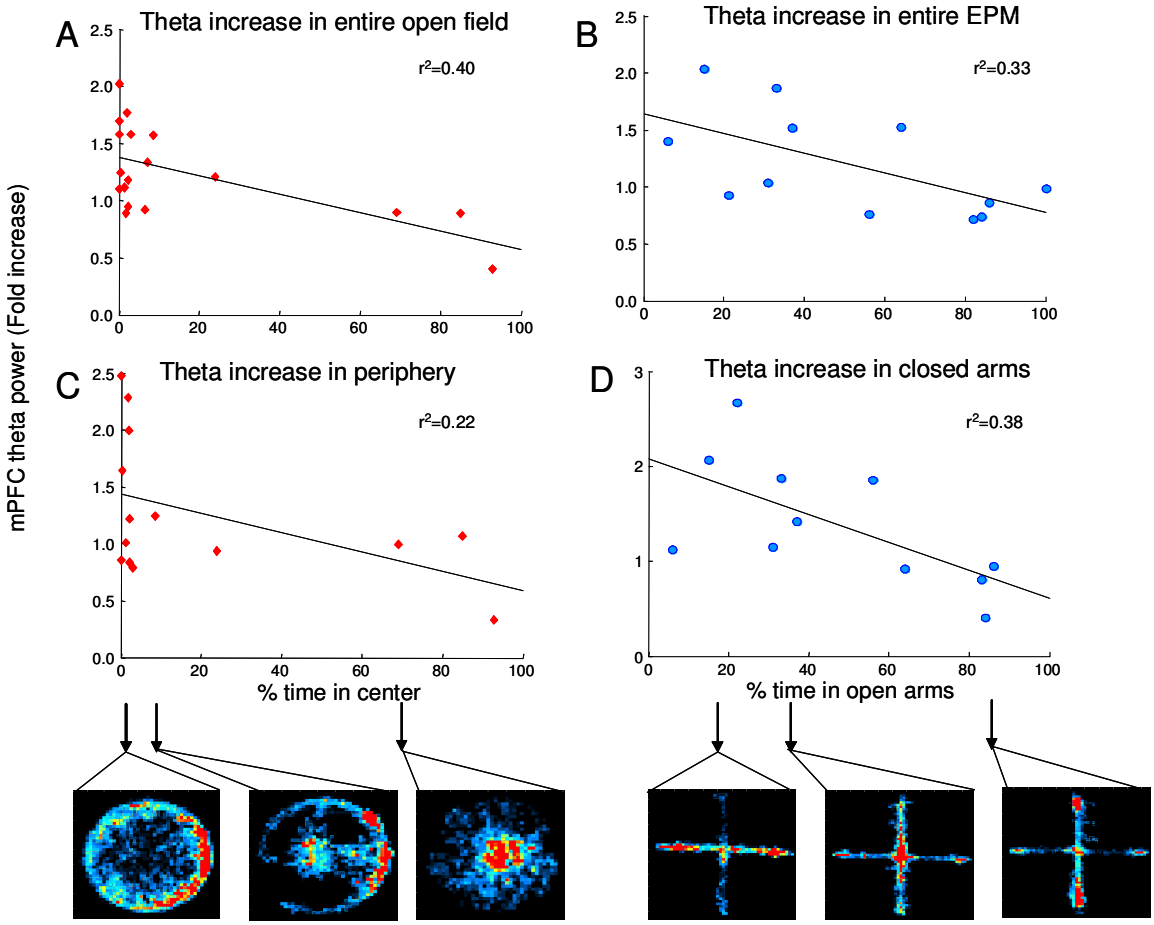

Figure 3.13- mPFC theta power increases in the EPM and the open field correlate with behavioral measures of anxiety. (A,B) Scatter plots of mPFC fold theta increase relative to the familiar arena against % time spent in the center of the open field, (A) and % time in the open arms for the EPM, (B). (C,D) Plots of fold increases in theta power in the periphery of the open field and in the closed arms of the EPM relative to the familiar environment recording of the same day, as a function of anxiety-associated behaviors in the open field (C) and the EPM (D). Lower panels show movement tracks as heat maps for selected points, indicated by arrows. In the maps of the EPM, open arms are vertically oriented. Fold theta power changes were calculated from epochs in which animals were running consistently in the 7-15 cm/s speed range.

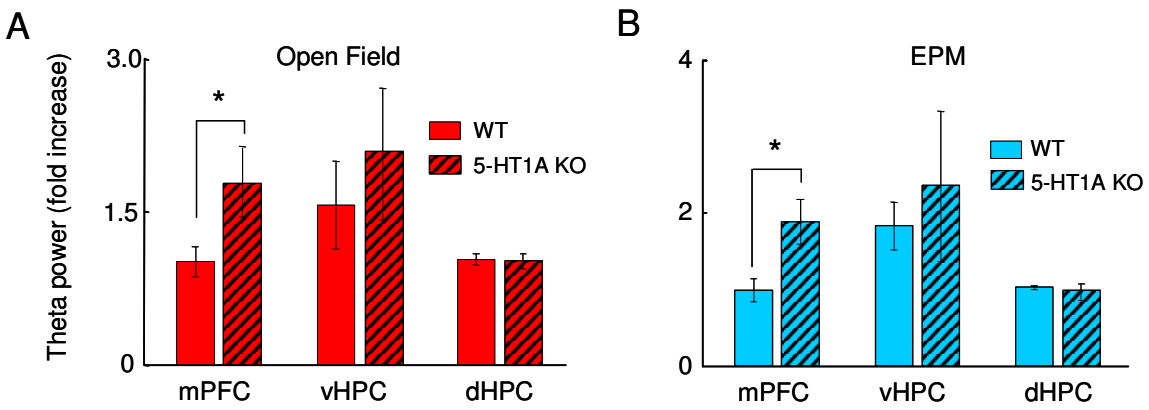

Figure 3.14- 5-HT1A knockouts (5-HT1A KO) have a higher increase in mPFC theta power in the EPM and the open field relative to wildtype (WT) mice. Bar graphs of average fold theta increase in the mPFC (left), vHPC (center) and dHPC (right), for the open field (red bars, upper panel) and EPM (blue bars, lower panel). Bars represent averages of 7 WT (clear bars) and 7 5-HT1A KO (thatched bars) mice. Error bars are ± s.e.m. *$p<0.05$ for a paired Wilcoxon's signed rank test comparing the fold theta increases of WT and 5-HT1A KO animals. Fold theta power changes were calculated from epochs in which animals were running consistently in the 7-15 cm/s speed range.

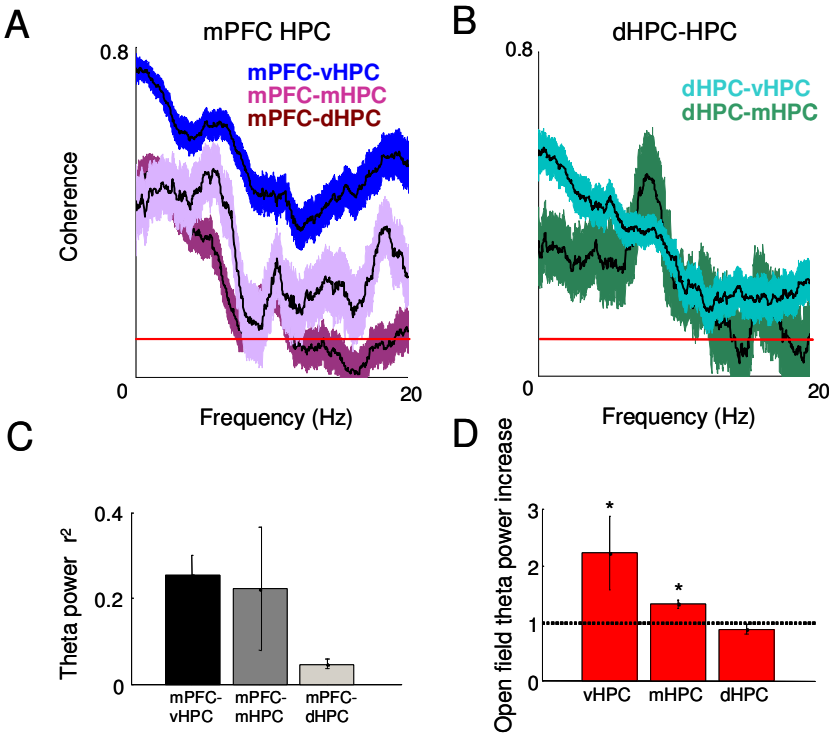

Figure 3.15- Coherence with the mPFC and changes in theta power in the middle hippocampus (mHPC) are intermediate between vHPC than dHPC. (A) Coherence plots of mPFC and dHPC, mHPC and vHPC. Note that coherence between mPFC and HPC increases gradually across the septo-temporal axis of the HPC, being largest with vHPC. (B) Coherence plots of dHPC with vHPC and mHPC. Theta range coherence with dHPC falls slightly across the long axis of the Hippocampus. (C) Theta power correlations of mPFC-vHPC, mPFC-mHPC and mPFC-dHPC. Correlations are high between mPFC-vHPC and mPFC-midHPC but not mPFC-dHPC. (D) Bar graphs showing fold increase of theta power in the open field relative to the familiar environment recording from the same day. Exposure to the open field increases theta power in the vHPC and mHPC relative to the familiar environment. All data shown is for the 7-15 cm/s speed range, except for theta power correlations (C), which were calculated for the length of the session. n=11, 4, 18 for the vHPC, mHPC and dHPC, respectively. Error bars are ± s.e.m. *p<0.05 in Wilcoxon's signed-rank test. Red lines on (A) and (B) indicate 95% significance levels.

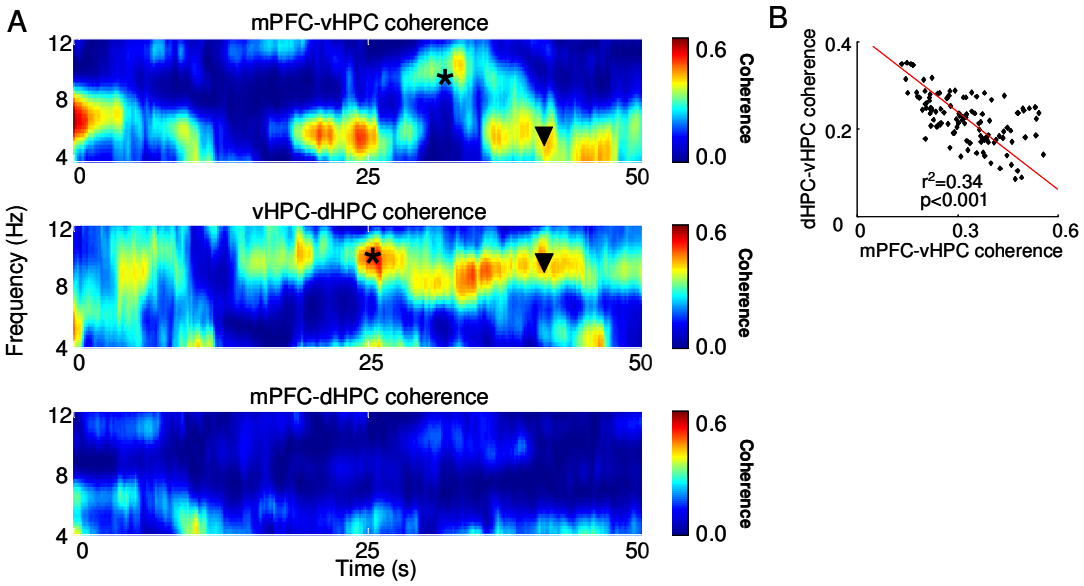

Figure 3.16- Temporal dynamics of coherence between vHPC, dHPC and mPFC. (A) Coherence over time plots of vHPC-mPFC (upper panel), mPFC-dHPC (middle panel) and vHPC-dHPC (lower panel) in the theta range. Higher coherence is indicated by warmer colors. Note that vHPC-dHPC and vHPC-mPFC coherence occurs either at different times (asterisks) or at different frequencies (arrowheads).Coherence was calculated on a moving 0.5 second window with 0.3 second overlap and 3700 nFFTs. Spectral densities were calculated using the multitaper method. (B) Plot showing dHPC-vHPC and mPFC-vHPC coherence across time during exploration of the familiar environment. Each point represents average coherence during 4 seconds. Note that dHPC-vHPC and mPFC-vHPC coherences are negatively correlated. Red line shows the linear fit for the scatter plot. Data was not filtered by speed and is a representative example obtained during a 10 minute familiar environment session.

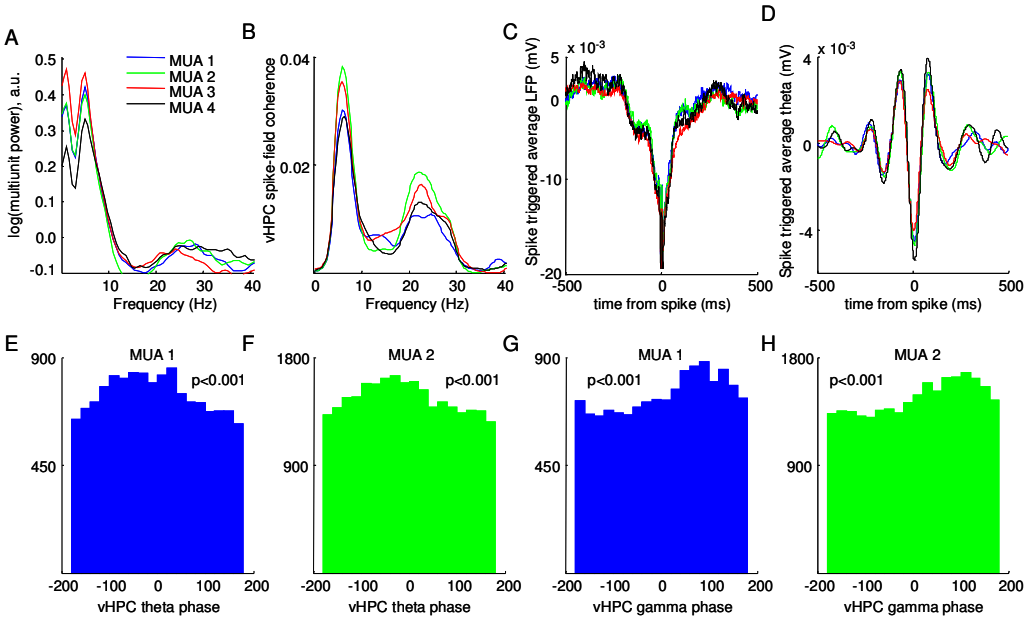

Figure 3.17- vHPC local field potential has local relevance. (A) Power spectra of vHPC multiunit activity (MUA). Four simultaneous recordings were made in the pyramidal layer of the vHPC, during exploration of the familiar environment. (B) Field potential–MUA coherence. Note a prominent peak at the theta range (7 Hz). (C) Spike-triggered average of the local field potential. Note that spikes tend to occur at the trough of the field. (D) Spike triggered average of theta-filtered field potential. (E) Distribution of preferred phases of vHPC MUA 1 relative to local theta oscillations. Note that spikes phase lock to the trough of vHPC pyramidal layer theta oscillations. (F) Same as (E), but for MUA 2. (G-H) Same as (E-F), but for gamma oscillations. (H) Same as (G), but for gamma oscillations. In (E-H) p values were calculated through the Rayleigh's test for circular uniformity.

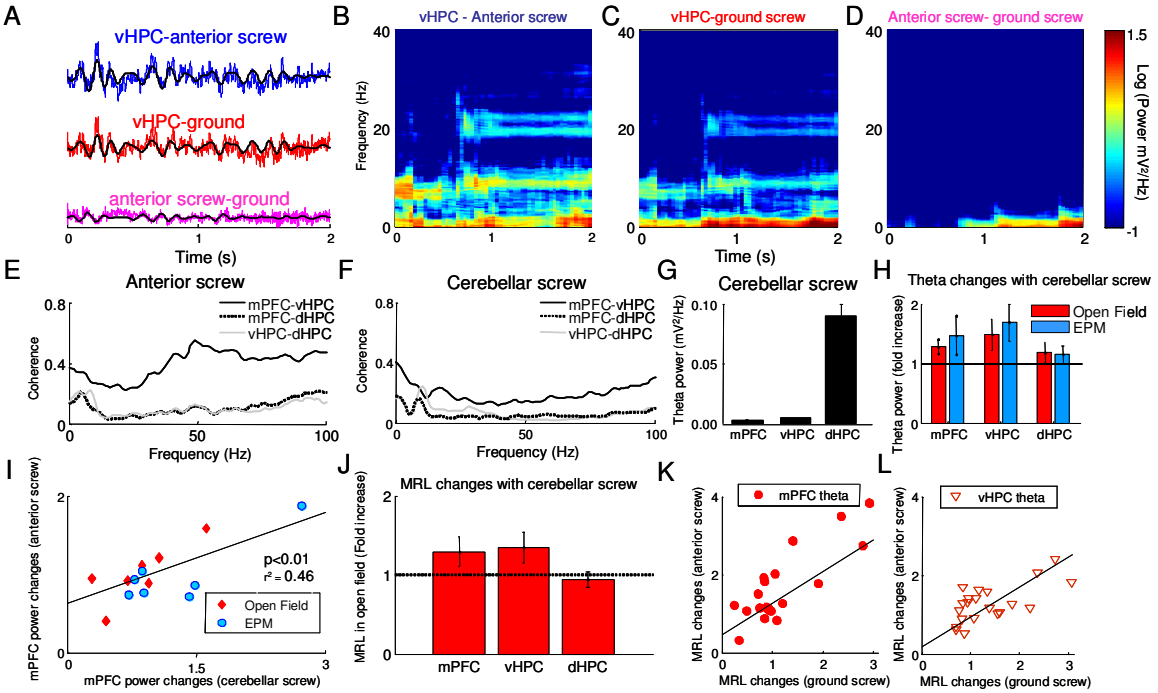

Figure 3.18- Main results are not reference-specific. (A) Representative traces showing the vHPC field potential recorded against the frontal (blue) or ground (red) screw. Note that both traces are very similar, indicating that the two references used are essentially identical. Accordingly, the trace of the frontal screw reference against the ground screw (pink) has overall smaller amplitude than the first two traces. (B-D) Spectrograms of the traces shown in (A). Note that the vHPC spectrogram has the same microstructure regardless of the reference used, as B and C are very similar. Furthermore, note that the anterior-screw against ground spectrogram (D) has no discernable theta-range oscillations. (E) Average coherence plots of mPFC-vHPC, mPFC-dHPC and dHPC-vHPC using an anterior screw as the reference. (F) Same as (E), but using the ground screw as a reference. Note that the mPFC is more coherent with vHPC than dHPC regardless of the reference used. (G) Theta power in the mPFC, vHPC and dHPC using the cerebellar screw as a recording reference. Note that theta power is highest in dHPC. (H) Plots of theta power increases relative to the familiar environment in the open field (red) and EPM (blue) using a cerebellar screw as a reference. Note that mPFC and vHPC theta power are increased. (I) Plot of mPFC theta power increases relative to the familiar arena with the LFP referenced either against the anterior or the cerebellar screw. Note that both measures are highly correlated in recordings performed with both references simultaneously. (J) Fold increase of MRL values in the open field relative to the familiar arena. The fold increases seen with this small sample size (n=13) agree with the full data set using the frontal reference, although they do not reach statistical significance. n=13 recordings with at least 700 spikes in each session. (K-L) Plots show fold increase of MRL relative to the familiar environment for both mPFC (K) and vHPC (L) theta oscillations. LFPs were simultaneously recorded against a cerebellar and a ground screw. Note that changes in MRL values are highly correlated across references. (E-I) Data plotted are from periods of consistent movement in the 7-15 cm/s range. (J-L) All data recorded at speeds above 4 cm/s were used. Error bars are ± s.e.m.

Chapter 4

Single units in the medial prefrontal cortex with anxiety-related firing patterns are preferentially influenced by ventral hippocampal activity

Single units in the medial prefrontal cortex with anxiety-related firing patterns are preferentially influenced by ventral hippocampal activity

4.1 Introduction

In rodents, anxiety is commonly studied in paradigms such as the elevated plus maze (EPM), a pharmacologically validated innate conflict-anxiety paradigm, with well-defined safe (the closed arms) and aversive areas (the closed and open arms, respectively). In such paradigms anxiety can be estimated by quantifying the avoidance of the aversive open arms (Cruz et al., 1994). Lesion studies have implicated the medial prefrontal cortex (mPFC) (Shah and Treit, 2003)in anxiety paradigms such as the EPM in rodents. Remarkably, in agreement with lesion studies, electrophysiological data also support a role for the mPFC in anxiety. For example, we have shown that mPFC theta-range power increases are correlated with the display of anxiety-like behaviors in two anxiety paradigms, the open field and the EPM (see Chapter 3). Furthermore, changes in mPFC theta power predicted changes in location of mice exploring the EPM. Although these results suggest that the mPFC is involved in anxiety, single unit recordings are needed tohave a clearer picture of how the mPFC acts during anxiety.

Most awake-behaving rodent single unit recordings performed in the mPFC are from working-memory related tasks (Gemmell et al., 2002; Jones and Wilson, 2005; Jung et al., 1998; Pratt and Mizumori, 2001; Sigurdsson et al., 2010). The most comprehensive of these studies showed that the firing rates of a large fraction of mPFC single units were modulated by behavioral demands of the task. Intriguingly, different units had distinct task-related firing patterns (i.e., some fired during consumption of reward, whereas other fired while running towards the reward ports)(Jung et al., 1998). This result suggests that mPFC unit firing is correlated with the

behavioral demands of the task being performed. However, it is not known if these paradigm-related firing properties are generated in the mPFC or if they originate in an upstream structure.

Intriguingly, there is evidence that some aspects of task-related firing in the mPFC may be inherited from the ventral hippocampus (vHPC). To this end, it was shown that single units in the mPFC(Burton et al., 2009) and the vHPC(Hok et al., 2007) display anticipatory firing before rats receive a reward, and that mPFC anticipatory firing was abolished following vHPC lesions (Burton et al., 2009) suggesting that hippocampal paradigm-related firing patterns may be propagated to the mPFC. This result indicates that mPFC paradigm-related firing may be inherited from the vHPC.

Intriguingly, the vHPC, similarly, to the mPFC, has also been shown to be required for normal anxiety-like behavior in the EPM (Kjelstrup et al., 2002). Furthermore, there is a monosynaptic unidirectional projection from the vHPC to the mPFC(Parent et al., 2009; Verwer et al., 1997), suggesting that these two areas may be part of a functional circuit with a role in anxiety. Recent results have supported this notion, as higher theta (4-12 Hz) range synchrony between the mPFC and the vHPC was found during anxiety compared to baseline conditions, both between local field potentials (LFPs) from these areas and between mPFC multiunit spikes and vHPCLFPs(Adhikari et al., 2010). Thus, LFP and multiunit results support a role for the vHPC-mPFC circuit in anxiety. However, the relationship between vHPC LFPs and mPFC single units in anxiety is unknown, as single unit recordings have not been performed in the mPFC during exploration of an anxiogenic environment.

Considering that task-related firing patterns have been observed in mPFC single units previously (Jung et al., 1998) and that results of mPFC lesion and recordings support a role for this structure in anxiety (Shah and Treit, 2003), we hypothesized that mPFC single units possess anxiety-correlated firing patterns in innate anxiety paradigms such as the EPM. Furthermore, as the vHPC-mPFC circuit has been implicated in anxiety (Adhikari et al., 2010), we predicted that mPFC single units with anxiety-correlated firing patterns would phase-lock more strongly to vHPC

theta, consistent with the notion that anxiety-related information is forwarded to the mPFC from the vHPC. To test these hypotheses, we recorded mPFC single units and vHPC LFPs in mice during exploration of the EPM. Strikingly, in the population of mPFC single units, firing rates in safe and aversive arms of the EPM were inversely correlated, suggesting that mPFC units differentiate between closed and open arms of the EPM. Importantly, these firing patterns could not be accounted for by the geometric arrangement of the arms of the EPM. Furthermore, units could differentiate between safe and aversive arms regardless of whether openness or brightness was used as the anxiogenic stimulus. Lastly, mPFC units with robust task-related firing patterns were more strongly phase-locked to vHPC theta oscillations and were more likely to follow vHPC theta of the past, in line with studies suggesting that hippocampal theta-range activity may propagate to the mPFC (Siapas et al., 2005; Sigurdsson et al., 2010). Importantly, anxiety related cells were no more likely to phase lock to dHPC theta oscillations, in accordance with studies showing that only the ventral pole of the hippocampus is involved in anxiety (Bannerman et al., 2004; Kjelstrup et al., 2002). These results further support a role for the mPFC in anxiety and suggest that mPFC units with anxiety-related firing patterns are preferentially integrated into a vHPC-mPFC circuit.

4.2 Results

mPFC single units appear to have anxiety-related firing patterns in the EPM

Lesion studies have shown that the mPFC has a role in innate anxiety in rodents (Shah and Treit, 2003). However, there are no reports of mPFC single unit recordings in rodents while animals are exploring an anxiogenic environment. To characterize the activity of mPFC single units in the EPM, 60 well-isolated cortical single units were recorded through stereotactically implanted stereotrode bundles targeting deep layers of the prelimbic cortex in 15 129/SvevTac mice. Nine units were excluded from further analysis for having less than 100 spikes. To characterize the firing patterns of mPFC single units while mice explored the EPM, spatial firing rate maps were computed for all cells. Strikingly, many of the single units had higher firing rates in specific subcompartments of the EPM such as the closed arms, open arms and center of the maze (upper

panels in Figure 4.1A, B and C, respectively). Not all units had preferred firing locations, as several units fired homogenously throughout the maze. However, all units that had well defined and robust preferred firing locations had spatial firing patterns that were correlated with anxiety-related features of the environment. For example, the unit shown in Figure 4.1A fired more strongly in the left and the right arms, both of which are closed arms, thus being locations that are similar in aversiveness. To further characterize these firing patterns, normalized firing rates (% difference from mean firing rate) were calculated in all the sub compartments (the four arms and the center) of the EPM. The unit shown in 1B, fired preferentially in both open arms, thus it has higher normalized firing rates in the up and down arms and low rates in the left and right arms (Figure 4.1D). A unit such as this one, with similar firing rates in arms of the same type, had a firing pattern that may be related to the anxiety-associated features of this environment. Conversely, a unit that fires preferentially in one open and one closed arm (Figure 4.1E), has a firing pattern unrelated to anxiety.

To characterize firing patterns in the entire population of recorded units, normalized firing rates were calculated in all compartments of the EPM for single units with more than 100 spikes. As shown in Figure 4.1, units with anxiety-correlated firing patterns have similar firing rates in arms of the same type. Thus, if a large fraction of units have anxiety-correlated firing patterns, normalized firing rates in arms of the same type would be expected to be positively correlated across the population of recorded units. Interestingly, in line with this prediction, firing in both closed arms (left and right arms in Figure 4.1D) was positively correlated ($r=+0.58$, $p<0.00001$, Figure 4.2A). Similar results were also found between firing rates in the open arms ($r=+0.40$, $p<0.003$, Figure 4.2B). These results suggest that a substantial fraction of the units have paradigm-related firing patterns in the EPM. Notably, firing rates across arms of different types were negatively correlated ($r=-0.52$, $p<0.01$, Figure 4.2C), as expected for units with anxiety-related firing patterns. Importantly, these results cannot be accounted for by novelty, as similar results were found during a second exposure to the EPM, after a rest period of 24 hours (Figure 4.3). Moreover, locomotor differences between closed and open arms exploration epochs also cannot account for the above results, as velocity and acceleration profiles did not differ between

closed and open arms (Figure 4.4). Thus, these data show that a large fraction of mPFC single units had firing patterns that were correlated to the anxiety-associated features of the EPM.

Anxiety paradigm-related firing does not depend on the geometric arrangement of EPM arms

The above data demonstrate that mPFC single units fired differently in closed and open arms of the EPM, suggesting that these units may have firing patterns related to anxiety. It is important to note, however, that the paradigm-related firing patterns shown in Figure 4.1 could be induced by other differences unrelated to anxiety between the closed and open arms. One such confound is the geometric arrangement of the arms. It is possible, for example, that a cell that is active preferentially in the open arms is actually firing not because the animal is in the open arms, but rather, because it is walking in the north-south direction. To verify if this was the case, 18 single units with more than 100 spikes were recorded from five additional mice while they explored an altered EPM the open arms were adjacent to each other rather than across from each other (Figure 4.5A). Similarly to the results obtained in the standard EPM, in the altered EPM firing rates were positively correlated between arms of the same type (Figure 4.5B and C, $r=+0.67$, $p<0.01$ for the closed arms and $r=+0.71$, $p<0.0003$ for the open arms), even though the position of the arms was changed. Furthermore, firing rates between closed and open arms were negatively correlated in the altered EPM ($r=-0.54$, $p<0.002$), in line with the results from the standard EPM.

To further confirm that the arrangement of the arms cannot account for these result, these same mice were exposed to a standard EPM after a 1 hour delay. 18/20 neurons (90%) were successfully recorded in both mazes.. Strikingly, firing rates between arms of the same type were positively correlated across the two configurations ($r=+0.43$, $p<0.04$ for the closed arms and $r=+0.53$, $p<0.01$ for the open arms).

mPFC single units can differentiate between safe and aversive arms regardless of the anxiogenic stimulus

The above results show that mPFC single units can differentiate between closed and open arms of the EPM. However, it is unclear if this is due to differences in aversiveness across the arms or differences in sensory input that are unrelated to anxiety. Unfortunately, it is impossible to control for all the sensory differences between the closed and open arms that are unrelated to anxiety. We reasoned that if the firing patterns of mPFC units are indeed associated with anxiety, units should differentiate between safe and aversive arms regardless of the particular anxiogenic stimulus used. To this end, we characterized the response of mPFC single units to openness and brightness, as both are anxiogenic, despite providing different sensory input. Anxiety induced by openness was studied in a standard EPM, with two open and two closed arms, in the dark (maze 1). Reponses to anxiety caused by brightness were explored in an EPM with four closed arms, where two arms were brightly lit (maze 2). These behavioral paradigms were both anxiogenic, as naïve mice avoided the aversive arms in both conditions (% time spent in bright closed arms = 20.3 $\pm$ 2.5 and % time spent in the dark open arms = 21.4 $\pm$ 5.3).

In both behavioral paradigms, normalized firing rates were negatively correlated between aversive and safe arms, in both paradigms (Figure 4.6 A and B, $r=-0.51$, $p<0.01$ for closed-open and $r=-0.55$-, $p<0.01$, for dark-bright arm correlations, respectively). If these firing patterns were indeed related to anxiety, it would be expected that mPFC units should respond similarly to anxiety caused different sensory stimuli. To test this prediction, correlations of normalized rate were calculated between aversive arms across mazes for all units that were recorded in both mazes. Strikingly, rates were correlated across the aversive arms of mazes 1 and 2 ($r=0.31$, $p<0.05$), even though in maze 1 aversiveness is induced by openness while in maze 2 brightness is the aversive stimulus. These results suggest that mPFC single units can differentiate between safe and aversive compartments, independently of the nature of the anxiogenic stimuli.

These results show that mPFC single units respond similarly to aversiveness induced by different anxiogenic stimuli. Furthermore, the above data show that mPFC single units can differentiate safe and aversive compartments regardless of the anxiety-inducing stimulus. Thus, these results are consistent with the notion that the paradigm-associated firing patterns observed in the EPM are associated with anxiety.

The majority of mPFC single units have task-related firing patterns

Correlations of firing rates between different arms (Figure 4.2) indicate that the population of mPFC single units is capable of representing the anxiety-related task components. However, such correlations do not quantify the extent to which the firing pattern of any given single unit is paradigm-related. To address this issue, an EPM score (see Materials and Methods) was calculated for each recorded unit. The EPM score quantifies the degree to which a unit differentiates across arms of different types (see Methods). A maximum EPM score of 1 indicates that all the differences between firing rates across arms were due to arm type; a score of zero, on the other hand, indicates that the unit fired without regard to arm type. If EPM scores can estimate the degree to which the firing pattern of a single unit is task-associated, the correlation of firing rates across arms of the same type should be higher in units with higher EPM scores. Indeed, stronger correlation in normalized firing rates in arms of the same type was observed in units with EPM scores higher then the mean score of the population, both for closed and open arms (Figure 4.7A-B). Importantly, the mean EPM score (0.205 ± 0.03) is significantly larger than zero (Wilcoxon's ranksum test, $p<0.001$), indicating that a substantial fraction of units have anxiety-correlated firing in the EPM. To determine whether these EPM scores could be obtained by chance, the significance of EPM scores was assessed by comparing the observed EPM score for each cell to a surrogate distribution generated by calculating the scores of randomly selected simulated spike times (see Methods for details). The majority (55%) of units had EPM scores significantly higher than expected by chance (see Methods). Lastly, EPM scores and spatial information content were highly correlated ($r=0.46$, $p<0.02$), indicating that a substantial fraction of spatially selective firing was due to paradigm-associated firing patterns. These results suggest that paradigm-related firing is a prominent feature of mPFC single unit activity, as the majority of units had positive EPM scores.

Single units with more robust anxiety-related firing phase lock more strongly to vHPC theta oscillations

The above results suggest that the mPFC may encode aspects of the environment related to anxiety. As anxiety modulates vHPC-mPFC theta-range synchrony (Adhikari et al., 2010), we hypothesized that mPFC single units with more robust anxiety-related firing patterns would phase-lock more strongly to vHPC theta oscillations. To investigate this hypothesis we calculated correlations between EPM scores and phase locking strength to vHPC theta oscillations, which was measured with the mean resultant length vector (MRL, see Methods). Interestingly, EPM scores and vHPC phase locking strength were strongly correlated (Figure 4.8A, $r=+0.53$, $p<0.02$), suggesting that cells that receive vHPC input are more likely to have anxiety-related firing patterns. This effect was specific for phase locking to the theta range, as it was not observed for vHPC delta (1-4 Hz) or gamma (30-80 Hz) oscillations (data not shown). As not only mPFC-vHPC theta-range synchrony, but also mPFC theta power increases have been associated with higher anxiety (Adhikari et al., 2010), we reasoned that EPM scores would also be correlated to phase locking strength to mPFC theta oscillations. Indeed, in accordance with this hypothesis, these two measures were highly correlated as well ($r=+0.57$, $p<0.01$). On the other hand, phase locking strength of mPFC single units to dHPC theta oscillations was not correlated with EPM score, in agreement with lesion (Kjelstrup et al., 2002) and physiology (Adhikari et al., 2010) studies suggesting that the dHPC is not required for normal anxiety-related behavior in the EPM.

These results suggest that mPFC single units with robust anxiety-related firing patterns are integrated into a circuit involving the mPFC and the vHPC, in which theta-range activity is propagated from the vHPC to the mPFC.

Single units that follow vHPC theta oscillations have more prominent anxiety-related firing patterns

The above results suggest that mPFC single units with robust anxiety-related firing patterns are preferentially recruited into a circuit involving the vHPC. Considering that the projection from the vHPC to the mPFC is unidirectional (Parent et al., 2009; Verwer et al., 1997), and that hippocampal theta-range activity has been shown to lead the mPFC (Sigurdsson et al., 2010), we hypothesized that mPFC single units that follow vHPC theta would have stronger anxiety-related

firing patterns (i.e., higher EPM scores) than cells that lead vHPC theta. To find which cells follow hippocampal theta activity, MRL values were calculated after shifting the spike train of each mPFC single unit in time, relative to the vHPC local field potential (LFP). The example spike train shown in Figure 4.9A follows vHPC theta, as it phase locks more robustly to the LFP after the spike train is shifted to the past (i.e., a negative time shift or lag). Similarly, the single unit in Figure 4.9B also follows vHPC theta, as the maximum MRL for this unit occurs at a negative time shift. Conversely, the single unit shown in Figure 4.9C does not follow vHPC theta, as its highest MRL value occurs at a positive lag, indicating that even though it is phase locked to vHPC theta, it is not led by vHPC theta. mPFC cells are thought to lag relative to hippocampal theta because of conduction and synaptic delays of the pathway, or due to polysynaptic phase locking. Indeed, in average, mPFC single units were maximally phase locked to vHPC theta of the past (mean shift= -13.8 $\pm$ 8.1 ms). Importantly, this mean shift is in good agreement with previous estimates of the conduction delay of the vHPC-mPFC pathway (-16 ms) (Thierry et al., 2000). Calculating MRL values for different shifts allowed the separation of mPFC single units into two groups: units that follow vHPC theta, in which the maximal MRL occurs at negative shifts, and all other units (maximal MRL occurs at zero or positive shifts). We then compared EPM scores between these two groups. Strikingly, cells such as the one in Figure 4.9B, that follow vHPC theta, had higher EPM scores compared to units that led vHPC theta (Figure 4.9D, $p<0.05$). In line with lesion studies (Bannerman et al., 2002) and our data (Chapter 3) showing that the dHPC is not involved in anxiety, units that followed dHPC did not have higher EPM scores (Figure 4.9F). These results indicate that units that follow vHPC input display stronger anxiety-related firing patterns, suggesting that these units are preferentially recruited into a circuit in which theta-range activity is propagated from the vHPC to the mPFC.

4.3 Discussion

Previous reports have suggested a role for the mPFC during anxiety. However, it was not known how the mPFC acts during anxiety. We show that a large fraction of single units in the mPFC displays task-related firing patterns in the EPM, an innate anxiety paradigm. Some cells are

active preferentially in the aversive open arms of the EPM whereas another others fire preferentially in the safer, closed arms of the maze. Importantly, these results cannot be accounted for by novelty or the specific geometric arrangement of the arms. Furthermore, similar paradigm-related firing patterns were observed when openness and brightness were separately used as anxiogenic stimuli. Strikingly, units with more robust paradigm-related firing patterns were more likely to follow vHPC theta oscillations and phase locked more strongly to vHPC theta. These results suggest that vHPC input to the mPFC may have a role in generating paradigm-related activity in an innate anxiety task, and support the involvement of the vHPC-mPFC pathway in anxiety.

Role of the mPFC in defensive behaviors

The mPFC has been implicated in numerous defensive behaviors in rodents, such as anxiety (Shah and Treit, 2004), extinction of fear conditioning (Vidal-Gonzalez et al., 2006) and aggression (Sustkova-Fiserova et al., 2009). Involvement in such a wide array of tasks suggests that the mPFC may have numerous unrelated functions. However, a more careful analysis of the results of mPFC lesions and drug infusion studies indicate that the mPFC increases behavioral inhibition. To this end, it has been shown that mPFC lesions decrease prepulse inhibition (Yee, 2000), and diminish anxiety-related behaviors in the Vogel test (Resstel et al., 2008)and the EPM (Shah and Treit, 2004). Furthermore, electric stimulation of the dorsal mPFC (prelimbic cortex) has been shown to increase the expression of conditioned fear (Vidal-Gonzalez et al., 2006), suggesting that the mPFC influences defensive behaviors. Interestingly, previous reports on mPFC activity in the theta range during anxiety also suggest that the mPFC plays a role in increasing behavioral inhibition, as it was shown that increases in mPFC theta power correlate with anxiety-related behaviors in the EPM and the open field (Adhikari et al., 2010). Thus, both lesion and physiology studies suggest the mPFC may modulate the display of defensive behaviors.

Anatomically, the mPFC is in a good position to evaluate the aversiveness of the environment and influence defensive behaviors. Areas related to contextual representation, such

as the rhinal cortices and the hippocampus project to the mPFC(Hoover and Vertes, 2007), suggesting that the mPFC would be ideally situated to evaluate abstract features of the environment, such as aversiveness. The mPFC may then influence anxiety through its projections to areas directly associated with defensive behaviors, such as the amygdala (Vertes, 2004).

Strikingly, in line with the notion that the mPFC has a role in anxiety, we found that a large fraction of single units in the mPFC had paradigm-related firing in the EPM. Some units fired preferentially in the aversive open arms, while other units fired mostly in the safer closed arms. Importantly, units tended to maintain the same preference of firing in a specific arm type even when the arms were re-arranged relative to each other. This finding demonstrates that the observed task-related firing is associated with arm type, and cannot be accounted for by the specific geometric arrangement of the arms. Furthermore, cells could differentiate between aversive and safe arms regardless of openness or brightness being the anxiogenic stimulus, in agreement with the notion that mPFC single unit firing may reflect the aversiveness of the environment. The finding that firing rates were negatively correlated between open and closed arms even when the maze is in the dark demonstrates that the findings shown in Figure 4.2, in which mice explored the EPM under moderate illumination, cannot be accounted for by differences in visual input between the closed and open arms. Importantly, spatial information content and EPM firing scores were positively correlated, indicating that a significant portion of spatial selectivity in firing was related to the task. It is noteworthy that previous findings on task-related firing patterns of mPFC units were all obtained in tasks in which rodents have been over-trained (Fanselow and Kim, 1994; Jung et al., 1998), and that the current work is the first to demonstrate paradigm-related firing in an innate anxiety paradigm.

It is important to consider that the observed paradigm-related firing in the EPM may not necessarily be associated with anxiety, as it may be caused by other states such as arousal or stress, which generally accompany anxiety. Further experiments are needed to evaluate if the paradigm-related firing in the EPM displayed by mPFC units is related to aversiveness. Nevertheless, the existence of putative anxiety-related mPFC cells is intriguing from a mechanistic viewpoint, as it is unclear what could be the role of these cells. One possibility is that

the number of currently active paradigm-related cells may be used to evaluate the aversiveness of the environment, such that if a large fraction of closed-arm cells were active, the environment would be considered safe. Another possibility is that cells that fire preferentially in aversive environments may increase activation of the amygdala, leading to the display of appropriate behaviors.

The vHPC-mPFC circuit during anxiety

Previous reports showed that lesions of either the vHPC (Kjelstrup et al., 2002)or the mPFC(Shah and Treit, 2003) decrease the display of anxiety-related behaviors in the EPM. Intriguingly, the presence of a projection from the vHPC to the mPFC suggests that the mPFC may be influenced by hippocampal input. In accordance with this idea, it has been shown that mPFC units phase lock more robustly to hippocampal theta oscillations after shifting the spike train into the past, by a temporal offset that presumably reflects the synaptic and conduction delay of the pathway (Siapas et al., 2005). Furthermore, mPFC cells are more likely to fire after hippocampal principal cells fire (Siapas et al., 2005). Lastly, in urethane-anesthetized rats (Taxidis et al., 2010), hippocampal theta activity was found to predict mPFC activity in the theta range. Interestingly, hippocampal input to the mPFC has been proposed to play a role in anxiety as well. To this end, it was shown that vHPC-mPFC synchrony in the theta range increases in two anxiety paradigms, the EPM and the open field. Remarkably, changes in theta-range vHPC-mPFC coherence partially predicted whether a mouse would move from the closed arm into the open arm (Adhikari et al., 2010). These results show that it is likely that hippocampal theta oscillations influence mPFC activity. Moreover, these results are consistent with the notion that the hippocampal input to the mPFC has a role in anxiety. Intriguingly, hippocampal theta oscillations have been linked to anxiety by studies that have shown that anxiolytic drugs such as benzodiazepines decrease the magnitude of hippocampal theta oscillations(McNaughton and Gray, 2000). Furthermore, vHPC theta power increases during exploration of the EPM (Adhikari et al., 2010).

The current findings support involvement of the vHPC-mPFC circuit in anxiety. Remarkably, we found that mPFC units with stronger EPM-related firing patterns were more

robustly phase-locked to vHPC theta oscillations. Furthermore, units that followed vHPC theta oscillations also had stronger paradigm-related firing, indicating that mPFC-vHPC synchrony in the theta range may be involved in anxiety. Interestingly, some mPFC single units lead vHPC theta (i.e., phase locked more robustly to vHPC theta of the future). This indicates that feedback from the mPFC to the hippocampus may have a role in pacing vHPC theta oscillations. The role of such feedback activity is unclear. Nevertheless, these findings are consistent with the idea that vHPC input in the theta range has contextual information that is used by the mPFC to evaluate the aversiveness of the environment. The mPFC might then modulate the activity of downstream target areas associates with viscero-motor processes and defensive behaviors.

Intriguingly, higher phase-locking of mPFC spikes to hippocampal theta has been found not only in anxiety, but also in working memory tasks, such as the T-maze(Sigurdsson et al., 2010). In a related working memory task it was demonstrated that the highest coherence between the mPFC and the dHPC occurs at the choice point of a Y-maze (Benchenane et al., 2010). These findings suggest that mPFC-HPC synchrony may reflect decision-making processes, in which the mPFC utilizes contextual information from the hippocampus to guide behavior during exploration of the EPM, the Y-maze and T-maze, as in all of these tasks a rodent must evaluate the environment and the relevant behavioral demands before selecting which arm of the maze to enter.

The present results suggest that cells that are more influenced by vHPC input are more likely to display paradigm -associated firing in the EPM, indicating that these firing patterns may be inherited from the vHPC. Indeed, In accordance with this idea, it was reported that vHPC, but not dHPC, units can differentiate between the open and closed arms of an eight arm-radial maze task (Royer et al., 2010), suggesting that perhaps the paradigm-related firing in the EPM displayed by the mPFC is inherited from the vHPC. Simultaneous recording of single units from both of these structures during exploration of the EPM is necessary to investigate this idea. Although the present findings suggest that theta range vHPC input to the mPFC has a role in anxiety, perturbations of the vHPC input through optogenetic approaches are necessary to test this hypothesis.

4.4 Materials and Methods

Animals

Three to six month old male 129Sv/Ev mice were obtained from Taconic (Germantown, NY, USA). Twenty mice were used for the simultaneous mPFC, dHPC and vHPC recordings. The procedures described here were conducted in accordance with National Institutes of Health regulations and approved by the Columbia University and New York State Psychiatric Institute Institutional Animal Care and Use Committees.

Microdrive Construction

Microdrives were built as described previously (Adhikari et al., 2010). Briefly, Custom microdrives were constructed using interface boards (EIB-16, Neuralynx, Bozeman MT) fastened to machine screws (SHCX-080-6, Small Parts, Inc, Miramar, FL). Stereotrodes implanted in the mPFC were constructed by wounding two four-inch pieces of 25 μM Formvar-coated tungsten micro wire (California Fine Wire, Grover Beach, CA) around each other at 100 RPM for 6 minutes. Stereotrodes (4-6 per animal) were fastened to a cannula attached to the interface board, allowing them to be advanced by turning the machine screws. Hippocampal electrodes were stereotactically placed and cemented directly to the skull during surgery.

Surgery

Surgical procedures have been described elsewhere (Adhikari et al., 2010). Briefly, animals were deeply anesthetized with ketamine and xylazine (165 and 5.5 mg/kg, in saline) and supplemented with inhaled isoflurane (0.5-1%) in oxygen. Mice were secured in a stereotactic apparatus (Kopf Instruments, Tujunga, CA) while resting on a heating pad. Anterior-posterior and medial-lateral coordinates were measured from bregma, while depth was calculated relative to brain surface. Tungsten wire electrodes were implanted in the dHPC CA1 (1.94 mm posterior, 1.5 mm lateral and 1.4 mm depth), vHPC CA1 (3.16 mm posterior, 3.0 mm lateral and 4.2 mm depth) and mPFC

(+1.65 mm anterior, 0.5 mm lateral and 1.5 mm depth). These coordinates resulted in electrode tips located near the fissure or in the stratum lacunosum-moleculare for the hippocampal electrodes, and in the deep layers of the prelimbic cortex for the mPFC electrodes. The stereotrodes in the microdrive were then lowered to the mPFC with a micromanipulator and cemented to the skull. Animals were monitored postoperatively and given analgesics (Carprofen, 5 mg/kg S.C.) as necessary.

Behavioral Protocol

Animals were permitted to recover for at least one week or until regaining pre-surgery body weight. Mice were then food restricted to 85% body weight. During food restriction animals were familiarized to the recording setup and handling by being tethered to the head stage preamplifier in their home cages for 5-7 daily sessions of 20 minutes each. Upon reaching their target weight, mice were exposed to either to standard or to one of the altered versions of the EPM for 10 minutes. A resting period of one hour separated the two EPM exposures in experiments in which recordings from the same single unit were obtained in two different EPM configurations.

The EPM was chosen for this work because it is a standard anxiety paradigm with pharmacological validity (Cruz et al., 1994; Pellow and File, 1986). Furthermore, contrary to other anxiety paradigms such as the open field, the EPM has well-defined boundaries between the more aversive (open arms) and the safe areas (closed arms). Lastly, normal anxiety-related behavior in the EPM has been shown to require both the mPFC(Shah and Treit, 2003) and the vHPC(Kjelstrup et al., 2002). Exposures to the standard EPM were done at 200 lux. The elevated plus maze was constructed of wood painted grey and consisted of four arms, 7.6 cm wide and 28 cm long, elevated 31 cm above the floor. 15-cm-high walls enclosed two opposing arms, whereas two arms were open, except for a 1-cm-high lip at the edge. Time spent in open arms was highly correlated across multiple exposures to the EPM in a subset of the animals exposed to the EPM twice ($r=0.8$, $p<0.01$), Furthermore, in a subset of mice exposed to both the EPM and the open field (an anxiety paradigm in which the center is the aversive area), time spent in the open arms

of the EPM and center of the open field were highly correlated ($r=0.45$, $p<0.05$). These data suggest that behavioral measures used in the current work reflect trait-anxiety.

The altered EPM used for the analysis in Figure 4.5 has identical dimensions, but the arrangement of the arms is altered, such that open arms are adjacent to each other (Figure 4.5A). Animals exposed to the altered EPM were also exposed to the standard EPM in the same day, with an intervening rest period of at least one hour between EPM exposures. The order of presentation of the mazes was counterbalanced across animals.

To verify if animals displayed anxiety in the experiments shown in Figure 4.6, naïve mice were exposed to both the standard EPM in the dark and the EPM with four closed arms with two brightly lit (600 lux) arms. In both cases naïve mice ($n=5$ for each maze) avoided the aversive arms (% time spent in bright arms = 20.3 ± 2.5 and % time spent in open arms = 21.4 ± 5.3). Furthermore, mPFC theta power was higher in the safe arms of all the EPM configurations used (Figure 4.10), in agreement with previous reports of mPFC theta power being higher in the periphery of the open field and in the closed arms of the EPM (Adhikari et al., 2010). These results show that anxiety can be induced in 129Sv/Ev mice with openness and brightness separately.

Data Acquisition

MPFC stereotrodes were advanced by turning machine screws attached to the interface board until at least four well-isolated single units could be recorded. Recordings were obtained via a unitary gain head-stage preamplifier (HS-16; Neuralynx) attached to a fine wire cable suspended on a pulley to counter-weight the cable. Field potential signals from hippocampal and cortical sites were recorded against a screw implanted in the anterior portion of the skull. LFPs were amplified; bandpass filtered (1-1000 Hz) and acquired at 1893 Hz. Spikes were recorded only from the mPFC. Spikes exceeding 40 μV were bandpass-filtered (600-6000 Hz) and recorded at 32 kHz. Both LFP and spiking data were acquired by a Lynx 8 programmable amplifier (Neuralynx) on a personal computer running Cheetah data acquisition software (Neuralynx). The

animal's position was obtained by overhead video tracking (30 Hz) of two light-emitting diodes affixed to the head stage.

Data Analysis

Data was imported into Matlab for analysis using custom-written software. Velocity was calculated from position records and smoothed using a window of 0.33 seconds.
Clustering of spikes was performed offline manually with SpikeSort 3D (Neuralynx). Cluster isolation quality was assessed by calculating L ratio and isolation distance measurements for all clusters. Well-isolated clusters have low L ratio and high isolation distance values. The computation of these measures has been described in detail previously (Schmitzer-Torbert et al., 2005). Cluster isolation quality measures (Figure 4.11 mean and median L ratio = 0.13 ± 0.03 and 0.021, and mean and median isolation distance = 61.2 ± 10.2 and 35, respectively) were similar to those of previously published reports (Schmitzer-Torbert et al., 2005). Importantly, cluster isolation quality was not correlated with EPM scores (Figure 4.11 or phase locking, indicating that cells with low EPM scores or weak phase locking are not poorly isolated. Mean firing rates (2 ± 0.59 Hz) and waveform features were similar to previous reports (Bartho et al., 2004), and suggest that the majority of the neurons are putative pyramidal cells. None of the results shown were correlated with firing rates, waveform features or cortical layer, thus the results from all cells were pooled together.

To assure that a good estimate of firing rates in all compartments of the EPM could be obtained, only cells with more than 100 spikes were used in all analysis, unless otherwise stated. Out of 79 units 69 had more than 100 spikes in the 10-minute EPM exploration session. Importantly, the results did not change if other values were selected for the minimum number of spikes, provided that this number was above 50 spikes. Furthermore, only data from mice that explored all arms of the maze were used in all the analyses.
EPM scores were computed to quantify the degree to which the firing pattern of a single unit is anxiety-related. EPM scores were calculated through the following formula:
Score= (A-B) / (A+B), where

$A=0.25*(|F_L-F_U|+|F_L-F_D|+|F_R-F_U|+|F_R-F_D|)$ and

$B=0.5*(|F_L-F_R|+|F_U-F_D|)$.

F_L, F_R, F_U and F_D are the % difference from mean firing rate in left, right, up and down arms, respectively. The term A is the average difference in normalized firing rate between arms of different types, while B is the mean difference in normalized firing rate for arms of the same type. A cell that has a firing pattern that is strongly related to the task has similar firing rates in arms of the same type (resulting in a small B) and big differences in firing between arms of different types (resulting in a large value for A). Accordingly, the maximum score of 1 indicates no difference in firing rates across arms of the same type (B=0). Negative scores indicate that firing rates are more similar across arms of different types than across arms of the same type. Importantly, EPM scores cannot be accounted for by overt changes in running speed throughout compartments of the EPM, as there are no differences in speed across arms (Figure 4.4). Moreover, mPFC single unit firing was not robustly correlated with speed (mean r^2 for correlation between firing and speed=0.03 ± 0.001 for all cells analyzed). After computing the EPM score for each cell, the score's significance was calculated. To this end, for a given cell with *n* spikes, a simulated distribution of scores was generated by calculating the EPM score of *n* randomly chosen LFP timestamps 500 times. The significance of the experimentally observed EPM score was calculated by Wilcoxon's test by comparing it to the simulated distribution.

In order to calculate the information content I between the firing rate R and the location X, spatial information was computed as described previously (Cacucci et al., 2007),through the following formula,

$$I(R/X)=\sum_i p(x_i)f(x_i)\log 2\frac{f(x_i)}{F}$$

where for each pixel *i*, $p(x_i)$, $f(x_i)$ are the probability of occupying pixel x_i and the firing rate in x_i, while *F* is the mean firing rate in the whole environment.

To determine whether spikes were phase-locked to theta, theta phases of LFPs were determined through the Hilbert transform, and a phase was assigned to each spike based on the time of the spike's occurrence. A phase of 0 refers to the trough of the theta cycle as recorded.

$$MRL=\sqrt{\frac{z}{n}},$$

The magnitude of phase locking can be measured through mean resultant length vector (MRL) values. MRL can be calculated from the z statistic provided by Raleigh's test for circular uniformity by where *n* is the total number of spikes. MRL ranges from 0 to 1, where 1 represents perfect phase locking. To avoid changes in MRL due to differences in firing rate, the same number of spikes per cell (1000 spikes) was used to compute phase locking in all scatter plots containing data from multiple single units. As all cells used had more than 1000 spikes, MRL values were calculated on 500 sub samples of 1000 randomly selected spikes from each cluster that had at least 1000 spikes. The mean of these 500 MRL values were used as the MRL value for a given cluster.

In order to characterize the temporal relationship between single unit spike trains and theta oscillations in each area, phase locking was calculated for 40 different temporal offsets for each single unit spike train. Cells that were led by theta oscillations phase-locked more robustly after the spike train was shifted to the past relative to the LFP. EPM scores were compared between cells that were and weren't led by theta oscillations from each area.

Importantly, all the results reported were independent of the mPFC and vHPC layer in which the electrode tip was located. It is also noteworthy that the LFP recordings reported in the current work did not change appreciably when recorded against another reference. Furthermore, strong phase locking of mPFC spikes to local delta, gamma and theta oscillations indicate that the recorded LFPs have local relevance. Similar phase locking results were also found in an additional cohort (n=2), in which vHPC spikes and LFPS were simultaneously recorded (data not shown). These data strongly suggest that the LFPs recorded reflected local synaptic activity and were not significantly contaminated by volume-conduction or by noise from the reference used.

Histology

At the end of the experiment animals were anesthesized with ketamine and xylazine and lesioned in hippocampal and mPFC recording sites by passing a 50 μA current for 10 seconds. Mice were then perfusedtranscardially with saline and 10% formaline and post-fixed in 30% sucrose. Brain

sections were mounted on slides to visualize and photograph lesions. Only data from animals with lesions in the intended locations were analyzed.

Statistics

Paired Wilcoxon's signed rank non-parametric tests were used throughout, unless otherwise stated. Two-tailed tests were used at all times. All correlations and their associated p values were calculated through Spearman's non-parametric correlation. Importantly, all the correlations reported in the current work as being significant with Spearman's method were also significant with Pearson's method. Spearman's correlation coefficient was used instead of the more widely used Pearson's r because it is less sensitive to outliers. Furthermore, a high Spearman's correlation will be obtained whenever two variables have a strong monotonic relationship between them, even if it is not linear. On the other hand, Pearson's r only quantifies linear relationships. Nevertheless, Spearman's and Pearson's correlations were in good agreement with each other in the current work as all of the significant correlations were predominantly linear. Standard errors of means (S.E.Ms) were plotted in bar graphs to show the accuracy of the estimation of the mean of the population.

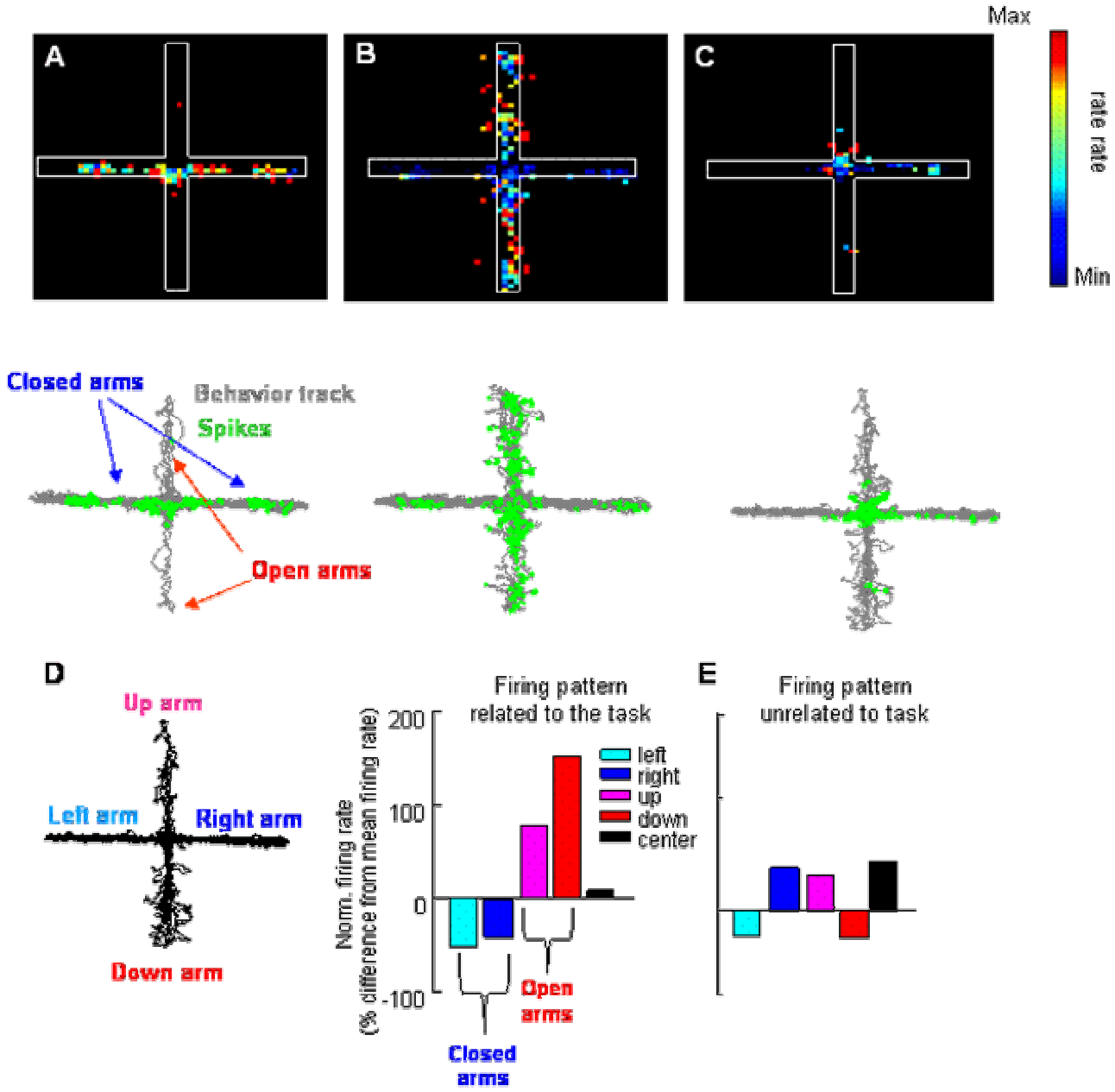

Figure 4.1-mPFC single units appear to have anxiety-related firing in the EPM.(A) Upper Panel: Example of spatial firing rate map from an mPFC single unit with anxiety-related firing. Average firing rates are color-coded (higher firing rates are indicated by warmer colors) for each pixel of a ten-minute exposure to the EPM. Note that this unit fires preferentially in the closed arms of the EPM. Lower panel: Importantly, spikes (green circles) were observed almost exclusively in the closed arms even though the mouse explored the entire maze, as shown by the behavior track, in grey. (B) and (C) Spatial firing rate maps for units that fired preferentially in the open arms and in the center of the EPM. (D) Left panel: In order to quantify differences in firing

rate across the maze normalized firing rates (% difference from mean firing rate) were calculated in five sub compartments of the maze (the four arms and the center). Thus, a unit that fires homogenously in the whole maze would have a normalized firing rate of zero in all compartments. Right panel: Bar graph displaying normalized firing rates for the single unit shown in (B). Units with task-related firing patterns have similar firing rates in arms of the same type. Accordingly, this unit has high firing rates in both open arms (up arm and down arm) and low firing rates in both closed arms (left and right arms). (E) Same as (D, right panel), but for a unit that does not have an anxiety-related firing pattern.

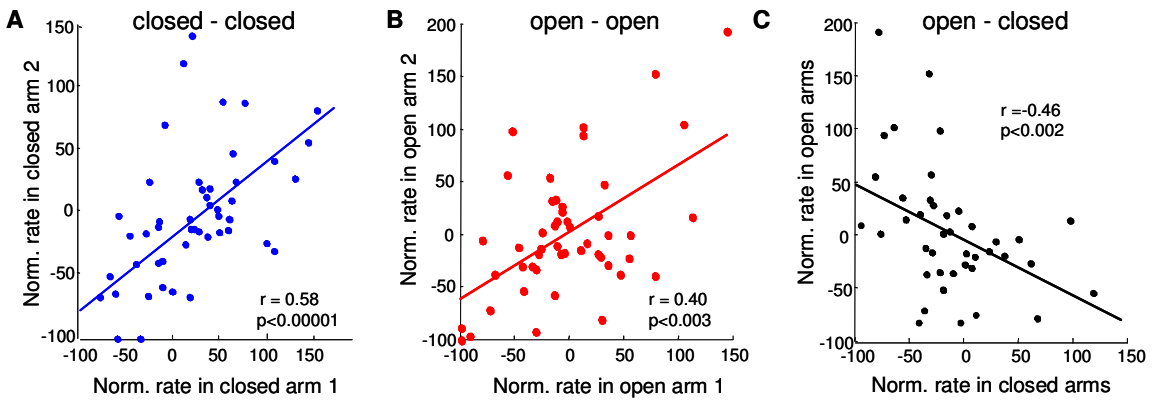

Figure 4.2-mPFC single units have similar firing rates in arms of the same type in the EPM.(A) Scatter plot of normalized firing rates (% difference form mean rate) across both closed arms (right and left arms). Each point represents one single unit. Note that normalized rates in the left and right arms are strongly positively correlated (r=0.58, p<0.0001, n=69 cells). (B) Same as (A), but for open arms (up and down arms). Firing rates are also positively correlated between the open arms of the maze (r= 0.40, p<0.003). (C) Same as (A), but for one closed and one open arm. Strikingly, normalized firing rates are negatively correlated across closed and open arms (r= -0.46, p<0.001).

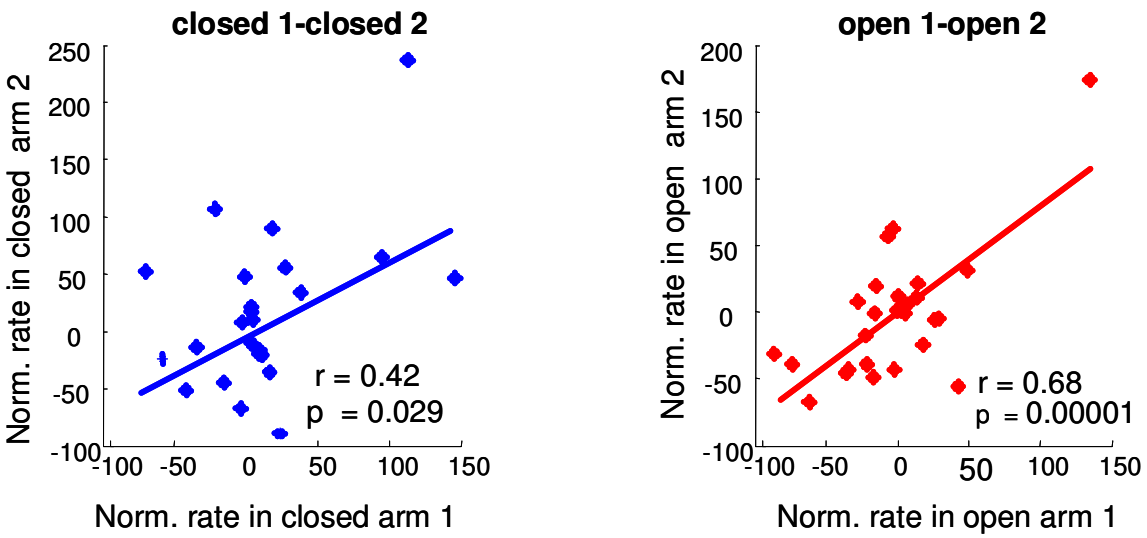

Figure 4.3-Anxiety-related firing patterns in the EPM are not related to novelty. Left Panel: Scatter plot of normalized firing rates for mPFC single units in both closed arms during a second ten-minute exposure to the EPM, a day after the original exposure. Right panel: Same as left panel, but for firing in both open arms. Note that firing rates are positively correlated among arms of the same type even during the second exposure to the EPM.

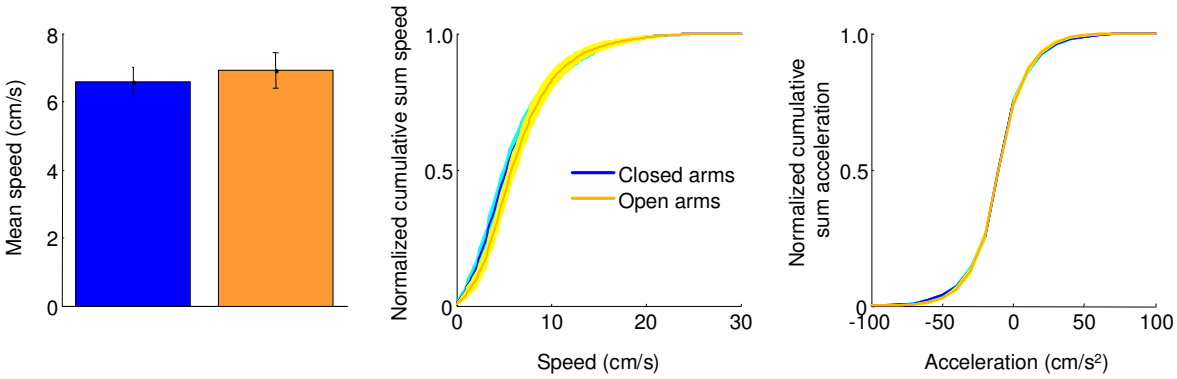

Figure 4.4-Locomotor behavior does not vary across arms of the EPM. Left Panel: Mean speed across animals in the closed and open arms (p=0.56). Middle panel: Cumulative sum distribution of speed in the closed and open arms. Right panel: Cumulative sum distribution of acceleration. Speed and acceleration profiles are entirely overlapping across open and close arms, indicating that there is no overall change in locomotor behavior across arm types in the EPM. Shaded areas in the cumulative distributions are ± S.E.Ms across animals.

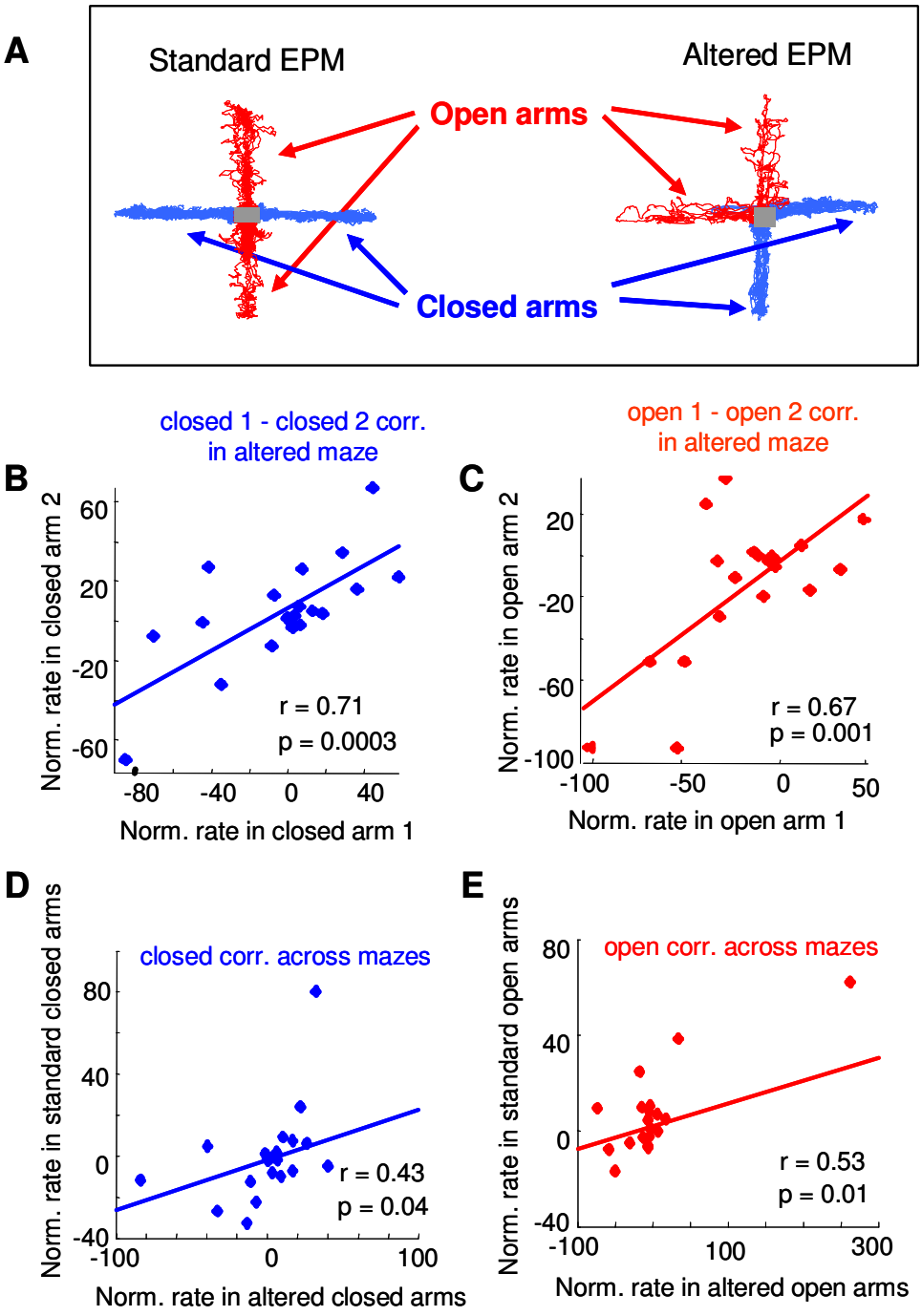
A
Standard EPM
Altered EPM
Open arms
Closed arms
B
closed 1 - closed 2 corr.
in altered maze
Norm. rate in closed arm 2
Norm. rate in closed arm 1
r = 0.71
p = 0.0003
C
open 1 - open 2 corr.
in altered maze
Norm. rate in open arm 2
Norm. rate in open arm 1
r = 0.67
p = 0.001
D
closed corr. across mazes
Norm. rate in standard closed arms
Norm. rate in altered closed arms
r = 0.43
p = 0.04
E
open corr. across mazes
Norm. rate in standard open arms
Norm. rate in altered open arms
r = 0.53
p = 0.01

Figure 4.5-Anxiety-related firing patterns do not depend on the geometric arrangement of the arms.(A) An altered EPM was built to assess if the firing patterns of mPFC single units is dependent on the particular geometric characteristics of the standard EPM. In the standard EPM (left) arms of the same type are opposed to each other. Conversely, in the altered EPM, arms of the same type are adjacent to each other. (B) Scatter plot of normalized rates (% difference from mean firing rate) across closed arms (right and down arms, shown in blue in A, right panel) of the altered EPM. (C) Same as (B), but for the open arms (up and left arms). Note that normalized firing rates are strongly positively correlated between arms of the same type in the altered EPM, both for closed arms ($r=0.71$, $p<0.003$, $n=21$ cells) and for open arms ($r=0.67$, $p<0.001$, $n=21$ cells). (D) Scatter plot of normalized rates for firing in the closed arms in the standard and altered EPM. (E) Same as (D), but for open arms. Firing rates are positively correlated across arms of the same type even across mazes, both for open ($r=0.53$, $p<0.01$, $n=21$ cells) and closed arms ($r=0.43$, $p<0.04$). The correlation in (E) is significant even if the point on the upper right corner is excluded ($r=0.46$, $p=0.04$).

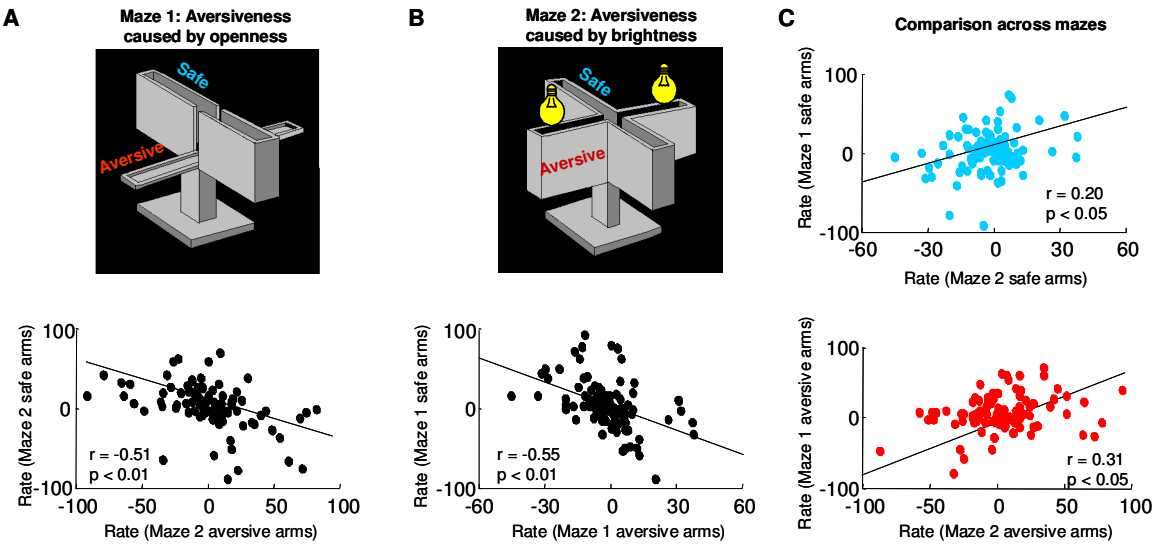

Figure 4.6-mPFC single units respond similarly to different anxiogenic stimuli. (A) Upper panel: Depiction of maze 1. In this condition, the openness of the open arms are the only anxiogenic stimuli which differs across safe and aversive arms. As mice explored this maze in the dark, all the arms had 0 Lux illumination. Lower panel: Correlations of normalized firing rates firing rates across arms of maze 1, which is a standard EPM kept in the dark. Firing rates across closed and open arms were negatively correlated ($r=-0.51$, $p<0.01$). (B) Upper panel: Depiction of maze 2. In this condition, brightness is the sole aversive stimulus that differs across safe and aversive arms. Illumination was kept at 600 Lux for the aversive arms and less than 5 Lux for safe arms. There are no open areas in maze 2, as all the arms were closed. Lower panel: Correlations of normalized firing rates firing rates across arms of maze 2. Firing rates across closed and open arms were negatively correlated ($r=-0.55$, $p<0.01$). (C) Correlations of normalized firing rates across mazes for safe arms and aversive arms. Rates were correlated across safe arms of mazes 1 and 2 ($r=0.20$, $p<0.05$). Rates were also positively correlated between aversive arms of maze 1 and 2 ($r=0.31$, $p<0.05$), even though the aversive stimulus in maze 1 and 2 is different.

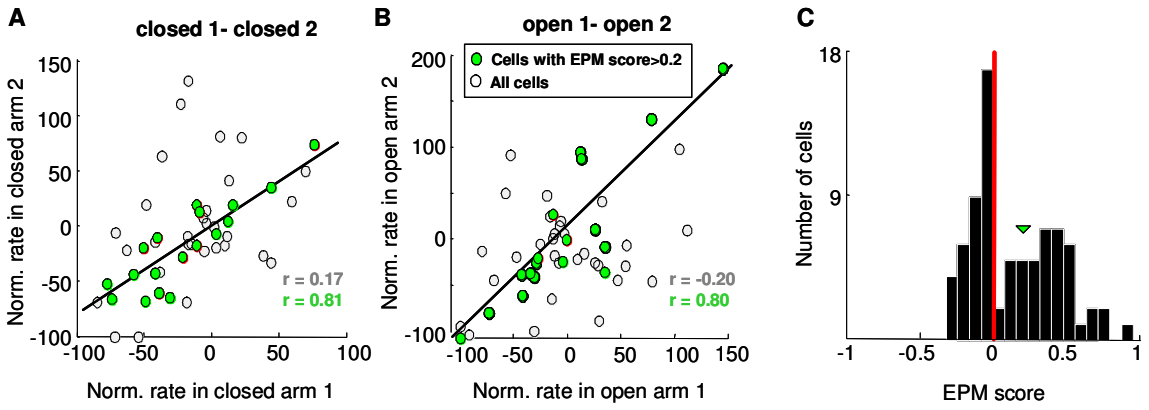

Figure 4.7-mPFC units with anxiety-related firing patterns are over-represented in the population.(A) Scatter plot of normalized firing rates (% difference from mean firing rate) of single units in both closed arms is shown in Figure 4.2A. To quantify the degree to which firing patterns are task-related, EPM scores (see methods) were calculated for all single units. An EPM score of 1 indicates perfect task-relatedness (there is zero difference between firing rates in arms of the same type), whereas a score of zero indicates homogenous firing throughout the maze. Cells with negative scores have high differences in firing across arms of the same type. Units with EPM scores higher than the mean score (0.205) are shown in green, while other units are depicted with grey circles. (B) Same as (A), but for firing rates in the open arms. Note that normalized spiking rates of the units with high EPM scores are more strongly correlated between arms of the same type, both for closed and open arms. Correlation values for grey and green circles are plotted in their respective colors. (C) Histogram showing the distribution of EPM scores for all the single units. The distribution peaks around zero, as many units fire homogenously in all compartments of the maze. Nevertheless, several units have strong task-related patterns, as many units have high EPM scores. Note that no units have robust anti-task related firing patterns, as no units have large negative EPM scores. The green arrowhead indicates the mean EPM score (0.205).

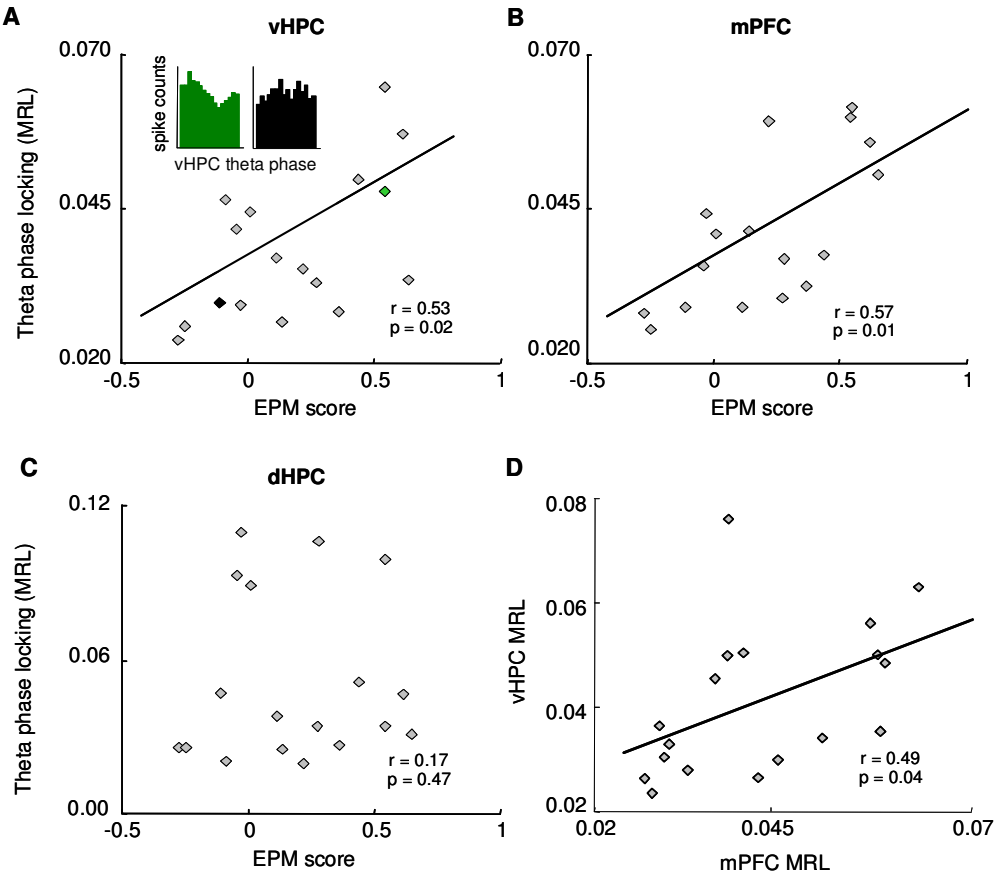

Figure 4.8-mPFC units with more prominent anxiety-related firing patterns are more robustly phase-locked to vHPC and mPFC theta oscillations.(A) Scatter plot of EPM scores against phase locking strength to vHPC theta oscillations. Robustness of phase locking was assessed through the mean resultant length (MRL) vector (see methods). Note that cells with strong phase locking to vHPC theta oscillations (i.e., larger MRL values) tend to have prominent anxiety-related firing patterns (high EPM scores). Insets show examples of the distribution of preferred phases of spikes of two mPFC single units relative to vHPC theta oscillations. These units are shown in the main scatter plot with points of the same color as their respective phase distribution histograms. The green unit has high MRL and EPM score values (EPM score=0.54, MRL=0.04), whereas the black unit has low values for both of these measures (EPM score=-0.02, MRL=0.024).(B) and (C) Same as (A), but for phase locking to mPFC and dHPC theta oscillations. EPM scores are positively correlated with phase locking to theta oscillations from the vHPC ($r=0.53$, $p<0.02$) and mPFC ($r=0.57$, $p<0.01$), but not the dHPC ($p<0.47$). (D) Scatter plot of phase locking strength to vHPC and mPFC theta oscillations. Note that MRL values for vHPC and mPFC theta oscillations are positively correlated ($r=0.49$, $p<0.04$).

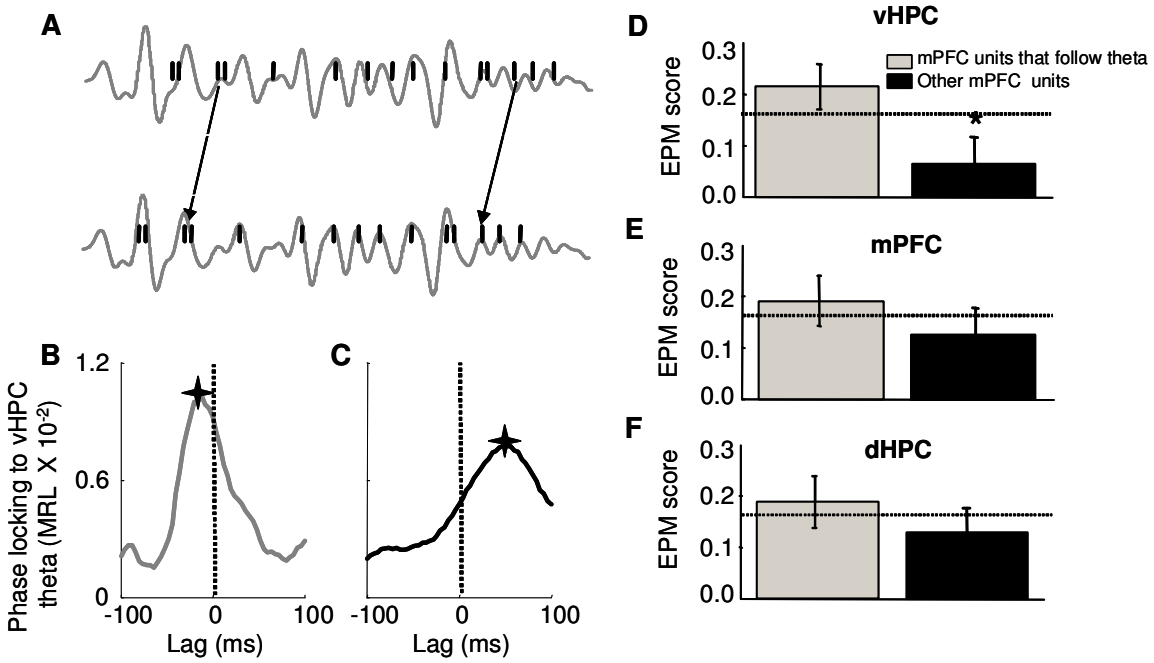

Figure 4.9-mPFC units that follow vHPC theta oscillations have more robust task-related firing patterns.(A) Upper panel: this simulated spike train is not phase locked to the theta-filtered trace shown. Lower panel: Shifting the spike train to the past reveals very robust phase locking, thus this spike train follows the theta trace shown. Conversely, if it phase-locked best at zero or after being shifted into the future, the spike train would not be led by vHPC theta. (B) and (C) Effect of shifting the spike train of two representative mPFC single units on the strength of phase-locking (MRL) to vHPC theta oscillations. The unit in (B) follows vHPC theta, as the maximal MRL value is observed at a negative lag (-12 ms), while the unit in (C) does not follow vHPC theta. A star marks the position of the maximum MRL and a dashed line was plotted at zero lag for reference. (D) EPM scores for units that follow vHPC theta (grey) and all other units (black). Units that followed vHPC theta had significantly higher EPM scores (*$p<0.05$, Wilcoxon's test). (E) and (F) Same as (D), but for mPFC and dHPC theta oscillations. Units that followed mPFC or dHPC theta oscillations did not have higher EPM scores.

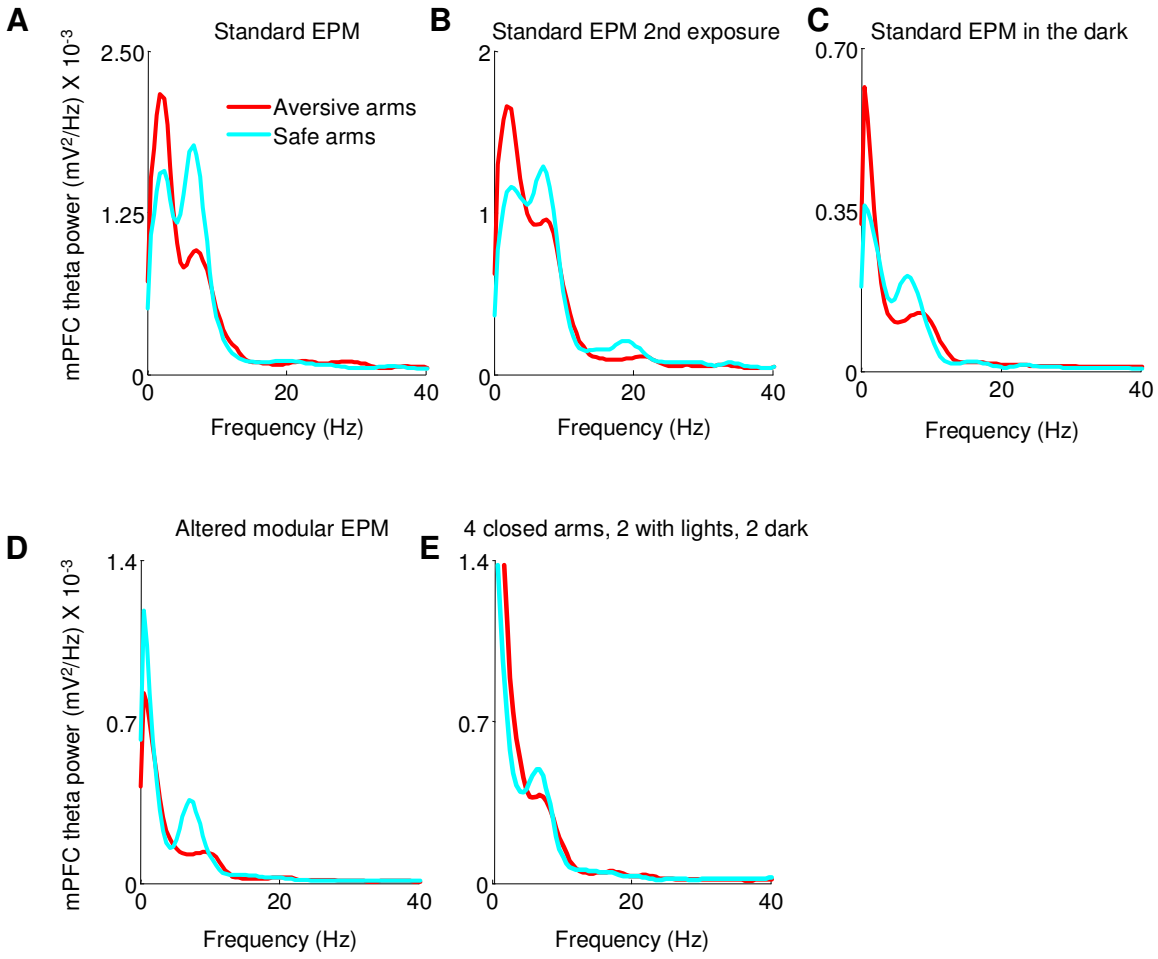

Figure 4.10-mPFC theta power is higher in the safe compartment of all EPM configurations. mPFC theta power is increased in the safe arms compared to the aversive arms, as seen in representative power spectra from the standard EPM at 200 Lux (A), the 2nd exposure to the EPM (B), the EPM at zero lux (C), the altered configuration in which arms of the same type are adjacent to each other, as illustrated in Figure 3 (C) and in the EPM with 4 closed arms in which two arms are brightly lit (E).

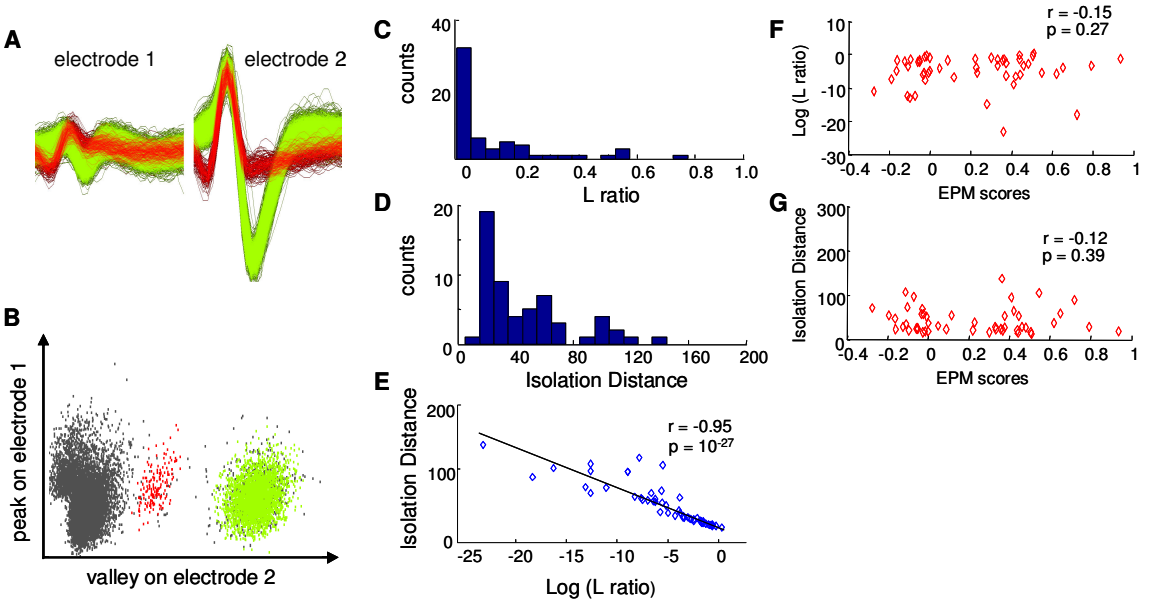

Figure 4.11-Isolation of single unit clusters.(A) Representative examples of spikes from two single units simultaneously recorded through the same stereotrode. (B) Scatter plot of peak on electrode 1 against valley on electrode 2. The spikes from these two single units form clusters that are well isolated from each other and from the noise cluster (grey points). (C and D) Distribution of L Ratio (mean L ratio =0.13 ± 0.03) and isolation distance (mean isolation distance = 61.2 ± 10.2) values for all single unit clusters. L ratio and isolation distance are measures of cluster isolation quality. Lower L ratio values and higher isolation distance values indicate well-isolated cluster. (E) Scatter plot of isolation distance and log (L ratio) for all clusters. Note the strong correlation, indicating that these two measures of cluster quality are in agreement with each other, (F) Scatter plot of L ratio against EPM scores for all the clusters. (G) Same as (F), but for isolation distances. Both measures of cluster quality are uncorrelated with EPM scores, demonstrating that clusters with low EPM scores do no tend to be poorly isolated units.

Chapter 5

Discussion

5. Discussion

5.1. Summary of Principal Findings

Results from lesion experiments indicate that the mPFC and the vHPC are implicated in anxiety. Interestingly, these two structures are anatomically connected, as the vHPC projects to the mPFC, suggesting that these areas may form a circuit in which vHPC input affects mPFC activity. Considering these reports, we hypothesized that vHPC-mPFC theta-range synchrony would increase during anxiety and that electrophysiological correlates of anxiety would exist in the activity of both structures. Initially we sought to find evidence consistent with the idea that vHPC input may affect mPFC activity. To do so, we developed a method to estimate the lag between brain areas using LFP recordings. This method, when applied to recordings of the vHPC and the mPFC obtained during exploration of a familiar environment, indicated that there is a lag in the theta range between these areas, comparable to the conduction delay of the pathway. Furthermore, mPFC activity only followed vHPC activity consistently in the theta-range, in line with previous reports of simultaneous hippocampal-cortical recordings suggesting that specifically theta-range activity may be propagated from the hippocampus to the mPFC (Siapas et al., 2005; Sigurdsson et al., 2010).

After establishing that vHPC theta leads the mPFC, we characterized the synchrony between the hippocampus and the mPFC in mice exploring a non-anxiogenic familiar environment. In agreement with anatomy studies demonstrating that only the ventral pole of the hippocampus projects robustly to the mPFC, we found that mPFC activity was highly synchronized to vHPC, but not dHPC activity. Strikingly, vHPC-mPFC theta power correlations increased in the EPM and in the open field relative to the familiar environment, suggesting that functional connectivity between these areas may be involved in anxiety. Importantly, higher vHPC-mPFC synchrony was also reflected in local activity, as phase locking of mPFC spikes to vHPC theta was higher in the open field than in the familiar environment. Consistent with a role for theta oscillations in anxiety, increases in mPFC theta power in anxiogenic arenas correlated

with behavioral measures of anxiety. Intriguingly, mPFC theta power was higher in the safer zones of the anxiogenic environments, suggesting a role for mPFC theta in behavioral inhibition. In agreement with this notion, changes in mPFC theta power predicted changes in the position of the animal in the EPM, as mPFC theta power increased immediately before the mouse entered the closed arms. These results are consistent with the idea that propagation of activity in the theta range from the vHPC to the mPFC may be involved in anxiety-related behaviors in mice.

To further characterize mPFC activity during anxiety we recorded single units during exploration of the EPM. Intriguingly a large fraction of units displayed paradigm-related firing, being active preferentially in the open or in the closed arms of the maze. Importantly, these firing patterns could not be accounted for by the geometric arrangement of the arms. Lastly, units with more prominent task-related firing phase locked more strongly to vHPC theta oscillations, and were more likely to follow them compared to units firing patterns unrelated to the task. These results suggest that a large fraction of mPFC units may encode aspects of the environment related to its aversiveness, and that part of the contextual information necessary for such paradigm-related firing may originate in vHPC input.

In summary, these data are consistent with a model in which contextual information from the vHPC is propagated to the mPFC through theta oscillations. This contextual information may be used to evaluate the aversiveness of the environment, allowing the mPFC to adequately regulate the activity of downstream areas involved with defensive behaviors.

In order to discuss these findings in the context of the existing literature, we will first examine evidence in both, the current and previous work, indicating a role for the mPFC and the vHPC in defensive behaviors. We will also consider how the present work, along with published studies, further supports the view that the vHPC, but not dHPC, is involved in anxiety-related behaviors. We then discuss the significance of the vHPC-mPFC pathway during anxiety. To do so, first we evaluate whether existing data support the notion that vHPC input can drive mPFC activity in rodents. Next, we discuss the significance and possible role of the vHPC input to the mPFC during anxiety in light of what is known about the neural activity of these areas. We argue that although there are few reports on the influence of the vHPC input on the mPFC, existing data

are consistent with the idea that aspects of task-related firing in the mPFC may be inherited from the vHPC. Next, we consider possible roles for the increase in vHPC-mPFC theta-range synchrony and higher theta power in this circuit we observed during anxiety. We suggest that our data are in agreement with a model in which theta range synchrony between the vHPC and the mPFC leads to more effective driving of downstream target areas directly involved with defensive behaviors, such as the amygdala, which in turn will modulate behavior appropriately. We then further expand on this idea and speculate, based on current and previous findings, that the vHPC and the mPFC may be part of a large network of structures, comprising a circuit in which complex interplay between various areas influences behavior during exploration of aversive environments. We argue that future studies with simultaneous recordings in other areas of this putative anxiety circuit are needed to further understanding of the neural circuitry of anxiety. However, there are various shortcomings associated with anxiety paradigms that may hinder efforts of future electrophysiology studies in these paradigms. Thus, lastly, we discuss strategies to overcome and minimize the impact of some of these shortcomings, based on approaches that were successful in the present work.

5.2. Role of the mPFC in defensive behaviors

The involvement of the mPFC in innate anxiety has been assessed by studying the effect of mPFC lesions on a wide variety of anxiety paradigms. It has been shown that mPFC lesions increase the exploration of the open arms of the EPM (Shah and Treit, 2003) and the center of the open field (Lacroix et al., 1998; Lacroix et al., 2000). Furthermore, excitoxic mPFC lesions induce animals to interact longer with unfamiliar rats in the social interaction test (Gonzalez et al., 2000; Shah and Treit, 2003). In line with a role for the mPFC in social inhibition, there are reports of higher aggressiveness in rats with lower levels of mPFC GABA (Sustkova-Fiserova et al., 2009). Moreover, rats with excitotoxic mPFC lesions are also less likely to bury a shock-delivering probe in the shock-probe burying test (Shah and Treit, 2003). Lastly, rats with mPFC lesions have shorter latencies to eat food in the hyponeophagia test (Gonzalez et al., 2000). It is noteworthy that some previous studies have reported increased anxiety-like behaviors in the

open field and EPM (Holson, 1986; Jinks and McGregor, 1997), after electrical lesions of the mPFC, contradicting the results found by groups that used excitoxic lesions. It is likely that this discrepancy arises because electrolytic lesions destroy fibers of passage, making the interpretation of the results less clear. Nevertheless, considering only the results from excitoxic mPFC lesions from various groups, it seems that the mPFC generally increases both anxiety-related responses and behavioral inhibition.

The anatomical connections of the mPFC also suggest that this structure may have a role in defensive behaviors. The mPFC has access to highly processed contextual information due to inputs from the rhinal cortices and the hippocampus (Hoover and Vertes, 2007). The mPFC may use this contextual information to evaluate the aversiveness of the environment to appropriately modulate the activity of downstream areas related to defensive behaviors, such as the amygdala and the periaqueductal grey (Vertes, 2004).

Our results are in agreement with the hypothesis that the mPFC influences the display of defensive behaviors. Consistent with a role for this area in anxiety, a large fraction of single units in the prelimbic cortex appears to have firing patterns correlated with the anxiety-associated features of the EPM. The majority of single units from this area fire preferentially in the safe or aversive arms of the EPM. Interestingly, units can differentiate safe and aversive arms of the maze regardless of whether openness or brightness is used as the anxiogenic stimuli, indicating that the observed firing patterns may be associated with anxiety and not to unrelated differences in sensory input across safe and aversive arms. It is unclear what the function of such firing patterns is. Perhaps if a large number of "open arm" units become active the mPFC increases activation of amygdala output, leading to the display of appropriate defensive behaviors. It is tempting to hypothesize that open and closed arm-preferring units may have different connectivities, such that open arm units excite areas involved with increased display of anxiety-like behaviors, while closed arm units would have the opposite effect.

However, it is important to consider that the mPFC single unit results were obtained from mice that spent a reasonable time exploring all four arms of the maze, as otherwise it would not be possible to assess the firing rates of units in all compartments of the maze. Thus, these mice

did not avoid the open arms completely. Consequently, the presence of paradigm-related units in these mice suggests that these units may not mediate anxiety-like behaviors such as robust avoidance of the open arms. One possibility is that these units are involved in representing the aversiveness of the environment, but not in selecting or initiating the appropriate behavioral response. To investigate this issue further it would be interesting to investigate whether there is any correlation across animals between the aversion to the open arms and the fraction of units that prefer to fire in the open arms. Unfortunately, this analysis is not possible with the current dataset as the number of cells recorded per animal was too small. Although intriguing from a mechanistic perspective, the specific function of mPFC paradigm-related units in the EPM cannot be ascertained with existing data. Nevertheless, these results support a role for the mPFC in anxiety.

Involvement of the mPFC in anxiety was supported not only by single unit activity, but also by results obtained from mPFC LFPs. Here, we show that theta power in the mPFC is correlated with behavioral measures of anxiety in the EPM and the open field and that mPFC theta power is highest in the safe areas of the EPM. Intriguingly, mPFC theta power decreases immediately before the animal leaves the closed arms, suggesting that the mPFC may have a role in guiding behavior in the EPM. It is currently unclear how mPFC theta power fluctuations affect behavior during exploration of anxiety paradigms. Considering that the mPFC does not directly control defensive behaviors, it is likely that the effects of mPFC activity on behavior are mediated through downstream targets of the mPFC, such as the amygdala. Perhaps during periods with high mPFC theta power the amygdala receives a strong drive from the mPFC, as many mPFC projection neurons will be synchronized in high theta power epochs. A subsequent drop in mPFC theta power would then result in less activity of amygdala output neurons, inhibiting the display of anxiety/fear -related behaviors. In agreement with the view that mPFC theta may modulate amygdala activity during defensive behaviors, preliminary results from our group show that mPFC-lateral amygdala theta-range coherence increases during testing of fear conditioning (Likhtik et al., personal communication). A decrease in behavioral inhibition due to modulation of amygdala activity could in turn result in entry into the open arms, consistent with our finding of

mPFC theta power dropping prior to entry into the open arms. Consistent with this idea, stimulation of the mPFC has been shown to excite basolateral amygdala neurons (Likhtik et al., 2005). It is also possible that the mPFC modulates behavior through its projection to the BNST (Vertes, 2004), which is a structure with a role in modulating defensive behaviors elicited by innately aversive stimuli, such as bright light (Walker and Davis, 1997). Further studies with simultaneous recordings in these areas are needed to test if the mPFC leads the amygdala or the BNST while animals are in the closed arms of the EPM.

Differentiation of the mPFC along the dorso-ventral axis

Anatomy studies show that the mPFC can be divided into subregions with differential connectivities. The ventral mPFC, or infralimbic cortex projects strongly to the lateral septum, the bed nucleus of the stria terminalis and the basomedial amygdala (Vertes, 2004), suggesting a role in visceromotor control. On the other hand, the dorsal mPFC, or prelimbic cortex projects robustly to the agranular insular cortex, claustrum, nucleus accumbens, the paraventricular, mediodorsal, and reuniens nuclei of thalamus (Vertes, 2004), indicating involvement in limbic and cognitive functions. These studies indicate that specific subregions of the mPFC have different functions, which are likely to be reflected in the neural activity of these structures.

Although a functional differentiation across the dorso-ventral axis of the mPFC probably exists, most studies of awake-behaving rodents pool together data from the prelimbic and infralimbic cortices (Jones and Wilson, 2005; Siapas et al., 2005). However, recent reports found evidence that the prelimbic and infralimbic cortices have different roles in extinction of fear conditioning. It was shown that stimulation of the infralimbic cortex decreases freezing during extinction while stimulation of the prelimbic cortex had the opposite effect (Vidal-Gonzalez et al., 2006). These results suggest that the prelimbic, but not the infralimbic cortex increases the display of defensive behaviors. This idea is in agreement with the known connectivity of these regions to the amygdala, as the prelimbic cortex is thought to activate cells in the central nucleus of the amygdala through its projections to the basolateral amygdala. On the other hand, the infralimbic projects to intercalated nuclei in the amygdala, (Vertes, 2004) which inhibit activity of

the central nucleus. Supporting this dissociation between the prelimbic and infralimbic cortex it has been shown that stimulation of the prelimbic cortex excites neurons in the basolateral amygdala (Likhtik et al., 2005), while stimulation of the infralimbic cortex decreases the excitability of neurons in the central nucleus of the amygdala (Quirk et al., 2003). Thus, both electrophysiology and anatomy data indicate the prelimbic cortex is a pro-anxiogenic area.

Prelimbic cortex in anxiety

In the present study, mPFC recordings were obtained from the prelimbic cortex, an area that may be involved with increasing fear/anxiety-related behaviors. Our results agree with the hypothesis that the prelimbic cortex is a pro-anxiogenic area, as higher theta power increases in this structure were correlated with behavioral measures of anxiety in the open field and in the EPM. Furthermore, 5-HT1A receptor knockout mice, which are known to display higher anxiety in these paradigms, had higher increases in prelimbic theta power in the open field and the EPM compared to WT mice. These data show that prelimbic theta power correlated with anxiety-like behaviors. If, however, prelimbic theta power has a role in the display or in the generation of these behaviors, theta power would be expected to change prior to the occurrence of such behaviors. Remarkably, in line with this prediction, we found that prelimbic theta power decreased immediately before mice left the safe closed arms of the EPM. Importantly, all of these results are consistent with previous anatomy and physiology studies, which also suggest that the prelimbic cortex is involved defensive behaviors.

However, it is not known whether in anxiety paradigms the prelimbic and infralimbic cortex have opposing functions, as shown for extinction of fear conditioning (Vidal-Gonzalez et al., 2006). Published reports do not address this issue, as studies evaluating the effect of mPFC lesions in anxiety paradigms lesioned the entire mPFC (Lacroix et al., 1998; Shah and Treit, 2003). Studies with smaller lesions, targeting the prelimbic and the infralimbic cortices specifically are needed to clarify this question. It is also not known if the neural activity in these areas differ during anxiety, as there are no reports of simultaneous recordings in the infralimbic and prelimbic cortices in anxiety. Remarkably, preliminary data from our group with multisite recording probes

spanning the prelimbic and infralimbic cortices indicate that, in the theta range, recording sites are more coherent within an area than across areas (Sigurdsson et al., unpublished data). This indicates that the differentiation between the infra and prelimbic cortices found in microstimulation and anatomy studies may be reflected in the LFPs from these areas. Comparisons of simultaneously recorded single unit activity between these areas would be even more informative. It would be interesting to investigate how single units from the infralimbic cortex fire in the EPM. If these mPFC subregions indeed have different roles in anxiety, perhaps the infra- and prelimbic cortices may have different numbers of cells that fire preferentially in safe and aversive portions of the environment. It is also possible that a larger fraction of infralimbic units have paradigm-related firing in anxiety tasks, as the infralimbic receives more limbic input than the prelimbic cortex (Hoover and Vertes, 2007).

5.3 vHPC and dHPC functional differentiation in anxiety

Various lines of evidence suggest that the dHPC and vHPC have different functions. For example, anatomical data show that the dHPC projects robustly to areas involved with spatial representation, such as the mammillary complex and the dorsal entorhinal cortex, while the vHPC projects more strongly to limbic areas, such as the hypothalamus and the amygdala (Swanson and Cowan, 1977). These results suggest that the dHPC is preferentially involved in spatial navigation, whereas the vHPC may have a role in mood regulation and functions. Interestingly, lesion studies support this idea, as it has been shown that dHPC, but not vHPC lesions affect spatial working memory tasks. On the other hand, vHPC, but not dHPC lesions decrease the avoidance of the aversive open arms of the EPM (Bannerman et al., 2002). These data also support a role for the ventral, but not dorsal hippocampus in anxiety-related behaviors.

Although both lesion and anatomy studies suggest that the vHPC is involved in anxiety, no recordings have been obtained in the vHPC or its dorsal counterpart in innate anxiety paradigms. Here we report several results suggesting that vHPC, but not dHPC, theta-range activity may have a role in anxiety. First, mPFC units with stronger paradigm-associated firing in the EPM tend to follow vHPC, but not dHPC theta. Second, phase locking of mPFC units to vHPC

theta is correlated with the strength of task-related firing in the EPM. Third, vHPC theta power and vHPC-mPFC theta synchrony increases during anxiety. In agreement with our data, previous reports also suggest that modulation of theta-synchrony with hippocampal downstream targets may play a role in the modulation of defensive behaviors. To this end, it has been shown that hippocampal-amygdala theta-range activity becomes more synchronized during testing of fear conditioning (Seidenbecher et al., 2003). In summary, the current results are consistent with previous reports indicating that hippocampal theta activity may have a relevant role in defensive behaviors, and further support the idea that the ventral, but not dorsal, pole of the hippocampus is involved in anxiety, as demonstrated by lesion studies (Bannerman et al., 2004).

In the present work, we have identified vHPC theta-range activity as a possible neural correlate of defensive behaviors. However, to better understand how the vHPC acts during anxiety and how its activity differs from that of the dHPC in aversive environments, it is necessary to record single unit activity in these areas in anxiety paradigms. Although there are no reports of single unit recordings from these areas during anxiety, dHPC and vHPC single units have been recorded in foraging and working memory tasks. In agreement with lesion and anatomy studies, which indicate the existence of a functional differentiation along the long axis of the hippocampus. single unit studies found various differences between vHPC and dHPC single unit activity. For example, compared to dHPC units, vHPC units display more robust task-related firing patterns (Royer et al., 2010). Furthermore, place fields are larger in the vHPC than in the dHPC, and a disproportionately high number of vHPC place fields occur near reward locations (Kjelstrup et al., 2008). Thus, previous reports suggest that vHPC activity differs from the dHPC and is more likely to reflect task-related firing than dHPC activity. As all of these recordings were obtained during foraging tasks, it is not known whether or how vHPC and dHPC unit activity differ during anxiety. Although there are no reports of vHPC activity in the EPM, it has been shown that in an eight-arm radial maze task vHPC cells can differentiate open arms from closed arms (Royer et al., 2010), indicating that vHPC units may also differentiate between the close and open arms of an EPM. Thus, existing data suggest that vHPC units may display task-related firing patterns in anxiety

paradigms. Future studies in which dorsal and ventral hippocampus units are simultaneously recorded are necessary to investigate this issue.

5.4. vHPC input to the mPFC

Can vHPC input robustly affect mPFC activity in awake-behaving rodents?

Much of the rationale, analysis and interpretation of the results described in the current work rely on the assumption that vHPC activity can significantly influence mPFC spiking in awake-behaving rodents. Previous studies are consistent with this idea, as it has been demonstrated that hippocampal theta-range activity leads the mPFC, both in anesthetized (Taxidis et al., 2010) and awake-behaving rodents (Sigurdsson et al., 2010). Furthermore, measures showing that the mPFC lags behind hippocampal activity in the theta range were found both in cortical LFPs (Chapter 2) and in spikes (Siapas et al., 2005). However, it is important to note that although lagging relative to hippocampal activity suggests that the hippocampus affects the mPFC, it does not prove this contention. These results could arise due to input from a third area that projects both to the hippocampus and to the mPFC with a longer conduction lag to the latter. Thus, although data from awake-behaving rodents are consistent with the idea that vHPC activity can affect the mPFC, these data do not conclusively demonstrate this contention, because the effect of perturbing the vHPC input to the mPFC has never been investigated in awake-behaving rodents.

Nevertheless, importantly, direct influence of mPFC activity by hippocampal input has been reported in anesthetized mice, as stimulation of hippocampal inputs was shown to drive mPFC single unit (Tierney et al., 2004) and LFP responses (Laroche et al., 1990). These results are in agreement with the hypothesis that the hippocampus can robustly modulate cortical activity.

Thus, the assumption underlying the rationale and interpretation of the current work, that vHPC input can affect the mPFC in awake-behaving rodents, is reasonably well supported, although not conclusively confirmed by existing data.

Possible role for the vHPC input to the mPFC

In order to evaluate the functional consequence of vHPC input to the mPFC it is first necessary to understand vHPC activity. As there are very few reports on recordings from the vHPC, a clear understanding of vHPC activity has not emerged yet. Existing reports consistently show that place fields in the vHPC are much larger than those in the dHPC (Jung et al., 1994; Kjelstrup et al., 2008; Royer et al., 2010). The most straightforward interpretation of this finding is that large place fields represent the larger environment in which the animal is. Thus, while dHPC units may represent in which corner of the maze a rat is in, vHPC units may represent the room in which the rat is currently located. Although this may be one of the functions of the large place fields displayed by vHPC units, previous reports suggest that vHPC unit firing also reflects task-related features, as vHPC place fields tend to occur near reward ports (Kjelstrup et al., 2008). Furthermore, vHPC units can differentiate between open and closed arms of an 8-arm radial maze and are more likely than dHPC units to have direction-sensitive firing patterns (Royer et al., 2010). These findings suggest that vHPC units are more strongly modulated by behavioral paradigm-related features than units from the dHPC are.

However, it is not known how vHPC units fire in the EPM, which is a paradigm in which normal behavior is known to require the vHPC. Nevertheless, it is likely that some vHPC units can differentiate between open and closed arms of the EPM, as similar firing patterns have been observed in an 8-arm radial maze with two open arms (Royer et al., 2010). Preliminary recordings of vHPC single units from mice exploring the EPM performed by our group also suggests that a significant fraction of vHPC units may differentiate between open and closed arms in this environment (Gordon et al, personal communication). These results support the notion that vHPC units have a large-scale spatial representation of space and that these cells are sensitive to behavioral demands of the task.

What would be the function of the vHPC input to the mPFC, considering that vHPC units have large place fields and reflect ongoing task-related behaviors? Contrary to findings on hippocampal units, previous reports of mPFC unit-firing have not found evidence of spatially

selective place fields in the mPFC (Gemmell et al., 2002). Rather, a substantial fraction of mPFC units have firing patterns that are correlated with specific task demands, such as reaching the reward zones, returning to the start position of the trial, etc (Gemmell et al., 2002; Jung et al., 1998; Pratt and Mizumori, 2001). The current work is consistent with these previous reports, as several units had paradigm-related firing patterns in the EPM, firing preferentially either in the more aversive or in the safer subcompartments of the EPM. These results suggest that mPFC task-related firing patterns may be partially inherited from the vHPC. Our own results are consistent with this idea, as mPFC units with more robust paradigm-related firing in the EPM were more phase locked to vHPC theta and were more likely to follow vHPC theta. Remarkably, we found that the mPFC only followed vHPC activity in the theta range (Figure 2.10), suggesting that not all hippocampal activity is propagated to the mPFC. This finding supports the idea that vHPC contextual information may be transmitted to the mPFC, as vHPC units with higher spatial information were also more strongly phase locked to local theta (Royer et al., 2010). Thus, the current work is consistent with the idea that some aspects of paradigm-associated firing from the vHPC may be inherited by the mPFC.

Intriguingly, in agreement with the current work, some previous reports have found evidence of hippocampal task-related firing patterns being propagated to the mPFC. First, it was shown that hippocampal units fire in anticipation of reward, while a rat is waiting in a specified position for a food pellet (Hok et al., 2007). Next, it was found that mPFC units display similar anticipatory firing in the same task. Lastly, it was demonstrated that anticipatory firing in the mPFC was abolished following hippocampal lesions (Burton et al., 2009), strongly suggesting that hippocampal paradigm-related firing patterns may be propagated to the mPFC.

Similar studies have not been performed in anxiety tests, so it is not known if the paradigm-related firing displayed by mPFC units in the EPM is generated by vHPC input. Stronger support for this hypothesis may come from studies in which single units are simultaneously recorded from the vHPC and the mPFC. If, indeed, paradigm-associated firing in the EPM displayed by mPFC units reflects vHPC inputs, then, on average, mPFC units that fire preferentially in the open arms would tend to fire immediately after vHPC units that have similar

firing patterns. Another approach to address this issue is to silence the vHPC input to the mPFC, either through muscimol infusions or through optogenetic approaches. Silencing vHPC input would be expected to lead to a loss of paradigm-related firing in mPFC units. Thus, although existing evidence is consistent with the notion that vHPC input may be partly responsible for generating task-related firing patterns displayed by mPFC units in anxiety paradigms, future studies in which vHPC input to the mPFC is manipulated are necessary to settle this question.

5.5 The vHPC-mPFC circuit during anxiety

We consistently found in two anxiety paradigms that vHPC and mPFC theta power increases during anxiety. There are no reports on correlates of mPFC theta power with behavior, and although there has been speculation on the significance of hippocampal theta power, there is no consensus on what are the specific correlates of increased hippocampal theta magnitude with behavior. Nevertheless, generally, increases in hippocampal theta power in awake-rodents have been observed in states associated with higher alertness, such as exploratory behavior, but not in repetitive behaviors such as grooming (Buzsaki, 2002). It is thus not surprising that an increase in hippocampal theta power was observed during anxiety, which is also a state associated with higher alertness. Higher theta power during such states may create a suitable condition to induce the plasticity necessary for encoding the memory of the current environment. In line with this idea, it has been shown that LTP in the hippocampus is most effective if two electrical stimuli are delivered separated by 200 ms (Larson and Lynch, 1986), which is equivalent to one cycle of a 5 Hz theta oscillation. Furthermore, LTP can be induced with only one thetanic train if it is given at the trough of the pyramidal layer theta cycle (Larson and Lynch, 1986) which is the window at which hippocampal units are most likely to fire (Buzsaki, 2002). These data suggest that the higher vHPC theta power during anxiety may have a role in inducing plasticity within CA1 cell ensembles. Alternatively, it is also possible that higher vHPC theta oscillations during anxiety are only a byproduct of the hippocampal network being in a different state, perhaps due to altered concentration of neuromodulators. In agreement with this idea, hippocampal 5-HT receptors have been shown to modulate theta magnitude (Hirose et al., 1990).

Although it is currently not possible to ascertain the functional consequence of increased vHPC theta power during anxiety, existing data are consistent with the hypothesis that increases in vHPC theta power may be involved in driving downstream target structures more effectively. To this end it has been shown that hippocampal theta may be propagated to many vHPC downstream targets, such as the mPFC (Sigurdsson et al., 2010), nucleus accumbens (Nason Jr et al., unpublished data), dorsal striatum (DeCoteau et al., 2007) and amygdala (Seidenbecher et al., 2003). It is reasonable to suppose that higher vHPC theta power results in more synchronous theta range output from vHPC projection neurons. Accordingly, we found that vHPC multiunit activity is very robustly phase locked to local theta oscillations (Figure 3.17). High theta power and higher theta phase locking of vHPC units may drive downstream target areas more robustly in two ways: First, areas such as the mPFC and the amygdala would become more phase locked to vHPC theta. Second, the observed increased synchrony between mPFC and vHPC theta may lead to more effective driving of areas that receive projections simultaneously from both the mPFC and the vHPC. Such areas include the amygdala, the periaqueductal grey, which is very strongly associated with freezing, and the ventral entorhinal cortex, an area implicated in innate anxiety (Steffenach et al., 2005). The function of higher theta range synchrony between the mPFC and the vHPC cannot be ascertained with existing data. Nevertheless, the results are consistent with a model in which modulation of convergent downstream targets more directly associated with defensive behaviors, such as the amygdala, due to synchronous input from the vHPC and the mPFC may have a role in guiding behavior during anxiety.

It is important to point out that these results do not indicate whether in the HPC-mPFC pathway there is any advantage of modulating synchrony specifically in the theta range instead of other frequency ranges, such as the delta (1-4 Hz) or gamma (30-100 Hz) bands. The finding that mPFC activity only lags the vHPC consistently in the theta range (Chapter 2) suggests that synchrony in the theta range may have some advantageous feature over synchrony in other frequency bands. One possible advantage of the theta range is that phase locking of cells in the HPC and the mPFC to theta offers a favorable temporal window to drive common downstream targets more effectively compared to the delta or gamma ranges. Modulation of synchrony in the

gamma range in the HPC-mPFC circuit due to ongoing behavioral demands is unlikely to occur, as gamma oscillations are generally coherent only across short distances, both in the cortex (Sirota et al., 2008) and in the hippocampus (Gloveli et al., 2005). Phase locking to delta oscillations also does not provide an optimal temporal window, as the delta cycle is around 500 milliseconds long. Such a long window is not favorable for effective temporal summation of EPSPs on common downstream targets of the HPC and the mPFC. On the other hand, a 12 Hz theta cycle is around 80 milliseconds long, suggesting that input synchronized in the theta-range may allow for optimal temporal summation of EPSPs in convergent downstream targets of the vHPC and the mPFC, such as the amygdala. In agreement with this idea, it has been shown that paired-pulses tend to produce facilitation if the interval between pulses is short, whereas generally depression is observed if the pulses are more than 300 ms apart (Debanne et al., 1996). Although supported by some experimental evidence, it is not known if the function of modulation of HPC-mPFC theta synchrony due to behavioral demands is to drive convergent downstream target areas. Further studies, with simultaneous recordings in the HPC, mPFC and a behaviorally relevant downstream area (such as the rhinal cortices in a navigation task or the amygdala in trace fear conditioning), are required to address this issue.

Lastly, it is noteworthy that although vHPC-mPFC synchrony increases during anxiety, coherence between these areas is already reasonably high during exploration of the non-anxiogenic familiar environment. This finding may indicate that the vHPC is constantly updating the mPFC with contextual information, regardless of the anxiogenicity of the environment. In anxiety-provoking environments, this contextual information may reflect the aversiveness of the environment, while in a task such as the 8-arm radial maze it may represent the contextual information relevant to the behavioral demands associated with the ongoing task phase. Such flexible representations of associated with behavioral demands is supported by the anatomy of the vHPC, as it not only receives highly processed contextual information from the rhinal cortices, but is also connected to areas that may be involved with emotional valence and mood regulation, such as the nucleus accumbens and the amygdala (Witter et al., 1989).

Circuits related to anxiety: beyond the vHPC and the mPFC

The current work indicates that the vHPC-mPFC pathway, and that theta-range activity in this circuit in particular, may be important for anxiety-related behaviors. To this end, we show that vHPC-mPFC synchrony in the theta range increases during exploration of the open field and EPM, and that changes in vHPC-mPFC theta coherence can partially predict the future location of a mouse exploring the EPM. The results from mPFC single-unit activity in the EPM also support a role for the vHPC-mPFC circuit in anxiety, as mPFC units with stronger paradigm-related firing patterns were more phase-locked to vHPC theta and were more likely to follow vHPC theta.

These results suggest involvement of the vHPC-mPFC pathway in innate anxiety-related behaviors in mice. However, lesion studies have demonstrated that many other brain structures are required for normal anxiety in the EPM and in the open field. These structures include the mediodorsal thalamus (Chauveau et al., 2005), the amygdala (Green and Vale, 1992), the medial septum (Degroot and Treit, 2004), the ventral entorhinal cortex (Steffenach et al., 2005) and the bed nucleus of the stria terminalis (Walker et al., 2009), among others. Intriguingly, tracing studies show that most of these structures are directly connected to the vHPC and the mPFC (Cenquizca and Swanson, 2007; Vertes, 2004; Witter et al., 1989). This suggests that the mPFC and the vHPC may be part of larger circuit involved in the modulation of anxiety.

Strikingly, some groups have shown that these areas modulate defensive behaviors distinctly in different tests. For instance, bed nucleus of the stria terminalis lesions show that this structure is required for light-enhanced startle, but not fear enhanced startle (Walker and Davis, 1997). Conversely, the amygdala is implicated only in fear, but not light, potentiated startle (Walker and Davis, 1997). It has also been shown that in the same test, two members of this putative anxiety-related circuit may modulate anxiety in different directions. For example, in the EPM, lesions of the dorso-medial thalamus decrease exploration of the open arms (Chauveau et al., 2005), while lesions of the medial septum induce the opposite result (Degroot and Treit, 2004). These data indicate that complex interactions between these areas are likely to influence defensive behaviors in rodents, as these structures appear to have different roles in each paradigm.

Remarkably, there is some evidence indicating that the interplay between these areas may be partly mediated by theta-range activity, similarly to the results we found in the vHPC-mPFC pathway. To this end, previous reports have shown that many of these structures are associated with hippocampal theta oscillations. For example, it is known that entorhinal and medial septal input are involved in the generation of currents associated with CA1 theta oscillations (Buzsaki, 2002). The amygdala, on the other hand, while not being involved in generating hippocampal theta, has been shown to display increased theta-range synchrony with the hippocampus during fear conditioning (Seidenbecher et al., 2003). Thus, previous reports indicate that several structures implicated in anxiety are synchronized to some extent to hippocampal theta oscillations.

Therefore, existing data are reasonably consistent with the hypothesis that modulation of theta-range synchrony across a large network of structures may have a role in modulating innate anxiety-related behaviors in rodents. Future studies with simultaneous recordings from multiple structures of this putative circuit are needed to clarify this issue.

5.6 Electrophysiology during anxiety

Anxiety-related mood disorders are highly prevalent, and non-pathological anxiety states are adaptive and useful for both humans and other animals. Consequently, it is not surprising that there is considerable interest in studying the neurobiology of anxiety. Accordingly, many studies investigating the neural underpinnings of anxiety have been conducted. For example, the roles of specific genes involved in anxiety-like behavior, such as the 5-HT1A receptor, have been extensively studied by assessing the behavior of knockout mice in anxiety paradigms (Ramboz et al., 1998). Moreover, several attempts to identify brain structures implicated in anxiety have been made, through lesion (Shah and Treit, 2003), inactivation (Sanders and Shekhar, 1995), drug infusion (Engin and Treit, 2007), and immediate early gene marker activation studies (Kung et al.). Although these studies have been instrumental in furthering knowledge of both normal and pathological anxiety states, a thorough understanding of anxiety is not possible without recordings of neural activity obtained during exploration of anxiety paradigms.

Intriguingly, despite the wealth of knowledge that electrophysiological data obtained from animals in anxiety paradigms could bring, very few reports exist on neural activity during anxiety in rodents. This is likely because compared to many behavioral paradigms, such as working memory tasks or tone fear conditioning; innate anxiety paradigms do not seem amenable to electrophysiology. Contrary to many other behavioral paradigms, innate anxiety tests have no inherent temporal structure built in, as there are no trials or task phases. Further complicating the issue, behavioral variability across animals is likely to be much larger in anxiety paradigms compared to tests in which animals have been trained extensively. Lastly, multiple exposures to the same anxiety paradigm are not desirable, as anxiety-related behaviors generally differ across subsequent exposures. This severely limits the amount of data it is possible to obtain from one animal. Lastly, in anxiety tasks it is often difficult to parse out whether the electrophysiological data collected is indeed related to anxiety, and not to novelty, arousal or sensory input unrelated to anxiety.

The current work shows that it is possible to obtain useful and interpretable electrophysiological data from anxiety paradigms and illustrates some strategies through which the shortcomings associated with such recordings may be dealt with.

Although it is true that there is no consistent temporal structure to physiology data during anxiety, behavioral landmarks can be used as useful timestamps to study the temporal dynamics of the data. For example, in the current study, changes in mPFC theta power were analyzed immediately before the animal transitioned from safe to aversive zones in the maze. Other potential useful behavioral landmarks include dips in the open arms and freezing behaviors.

The issue of behavioral variability across animals cannot be fully controlled. Nevertheless, it is possible to show that the effect of interest is independent of changes in speed or acceleration, as done here to show that theta power increases in the vHPC in the EPM compared to the familiar environment regardless of the speed of the animal. Furthermore, the physiology from an anxiety paradigm may be compared to that obtained in a control non-anxiogenic environment in which overall locomotor behavior is the same.

Due to the nature of anxiety paradigms, data collected over multiple exposures are not comparable, decreasing the amount of data that can be collected per animal. However, current microdrive technology allows for high-density recordings in which around 10 single units in a mouse or dozens of units in a rat can be recorded simultaneously. The use of multi-site silicon probes also greatly increases the single-unit yield per animal. These technical advances significantly increase the amount of data that can be obtained from one rodent.

Another significant issue in analyzing data from anxiety paradigms is how to assure that the observed effect is related to anxiety, and not to other factors, such as novelty or arousal. It is noteworthy that this is an issue not only with electrophysiology, but also with most types of data obtained from anxiety paradigms. Several steps were taken in the current work to deal with this problem. These same approaches may prove to be helpful in future studies. One indication that the observed effect is related to anxiety may come from correlating the magnitude of the effect to behavioral measures of anxiety across animals. In this work, for example, we show that mPFC theta power increases correlate with % time spent in the open arms of the EPM. Another approach is to show that the effect of interest varies as expected when the anxiety provoking stimuli are increased or decreased in intensity. To this end, we show that mPFC theta power changes are smaller if the open field is kept in the dark, instead of being illuminated with bright lights. One may also attempt to verify if the effect of interest varies across safe and aversive sub areas of the same anxiogenic arena. The use of these approaches ought to increase considerably the strength of the association of the measured effects with anxiety.

The most difficult obstacle in interpreting data from anxiety paradigms is to show that the effect of interest is related to anxiety, and not to specific sensory stimuli present in the anxiety paradigm used. This problem is also present in other types of data obtained in anxiety paradigms. For example, if a particular line of knockout mouse avoids the center of the open field more than wild type mice, is that enough evidence to suggest that the knockout strain is more anxious in the EPM? Although some studies have made similar claims, there are many confounds in this approach. It is possible, for example, that the eyes of the knockout mice are overtly sensitive to bright lights, and that is the reason why this strain avoids the more brightly illuminated center. We

feel that the most straightforward way of dealing with this issue is to verify if the effect of interest is present regardless of the specific sensory nature of the anxiogenic stimuli used. Accordingly, we showed that that the population of cells can distinguish between safe and aversive compartments, independently of whether anxiety is caused by lights or openness.

We hope that these approaches will serve to decrease the aversion many electrophysiologists have towards obtaining recordings in anxiety paradigms, as a more complete understanding of the neural underpinnings of anxiety cannot occur without knowledge of brain activity during high anxiety states.

References

Adhikari, A., Topiwala, M.A., and Gordon, J.A. (2010). Synchronized activity between the ventral hippocampus and the medial prefrontal cortex during anxiety. Neuron *65*, 257-269.

Aguilar, R., Gil, L., Flint, J., Gray, J.A., Dawson, G.R., Driscoll, P., Gimenez-Llort, L., Escorihuela, R.M., Fernandez-Teruel, A., and Tobena, A. (2002). Learned fear, emotional reactivity and fear of heights: a factor analytic map from a large F(2) intercross of Roman rat strains. Brain Res Bull *57*, 17-26.

Alonso, J.M., and Martinez, L.M. (1998). Functional connectivity between simple cells and complex cells in cat striate cortex. Nat Neurosci *1*, 395-403.

Amaral, D.G., Dolorfo, C., and Alvarez-Royo, P. (1991). Organization of CA1 projections to the subiculum: a PHA-L analysis in the rat. Hippocampus *1*, 415-435.

Astolfi, L., Cincotti, F., Mattia, D., Marciani, M.G., Baccala, L.A., de Vico Fallani, F., Salinari, S., Ursino, M., Zavaglia, M., and Babiloni, F. (2006). Assessing cortical functional connectivity by partial directed coherence: simulations and application to real data. IEEE Trans Biomed Eng *53*, 1802-1812.

Baccala, L.A., and Sameshima, K. (2001). Partial directed coherence: a new concept in neural structure determination. Biol Cybern *84*, 463-474.

Bagdy, G., Graf, M., Anheuer, Z.E., Modos, E.A., and Kantor, S. (2001). Anxiety-like effects induced by acute fluoxetine, sertraline or m-CPP treatment are reversed by pretreatment with the 5-HT2C receptor antagonist SB-242084 but not the 5-HT1A receptor antagonist WAY-100635. Int J Neuropsychopharmacol *4*, 399-408.

Bannerman, D.M., Deacon, R.M., Offen, S., Friswell, J., Grubb, M., and Rawlins, J.N. (2002). Double dissociation of function within the hippocampus: spatial memory and hyponeophagia. Behav Neurosci *116*, 884-901.

Bannerman, D.M., Rawlins, J.N., McHugh, S.B., Deacon, R.M., Yee, B.K., Bast, T., Zhang, W.N., Pothuizen, H.H., and Feldon, J. (2004). Regional dissociations within the hippocampus--memory and anxiety. Neurosci Biobehav Rev *28*, 273-283.

Barrot, M., Olivier, J.D., Perrotti, L.I., DiLeone, R.J., Berton, O., Eisch, A.J., Impey, S., Storm, D.R., Neve, R.L., Yin, J.C., *et al.* (2002). CREB activity in the nucleus accumbens shell controls gating of behavioral responses to emotional stimuli. Proc Natl Acad Sci U S A *99*, 11435-11440.

Bartho, P., Hirase, H., Monconduit, L., Zugaro, M., Harris, K.D., and Buzsaki, G. (2004). Characterization of neocortical principal cells and interneurons by network interactions and extracellular features. J Neurophysiol *92*, 600-608.

Belzung, C., and Griebel, G. (2001). Measuring normal and pathological anxiety-like behaviour in mice: a review. Behav Brain Res *125*, 141-149.

Benchenane, K., Peyrache, A., Khamassi, M., Tierney, P.L., Gioanni, Y., Battaglia, F.P., and Wiener, S.I. (2010). Coherent Theta Oscillations and Reorganization of Spike Timing in the Hippocampal- Prefrontal Network upon Learning. Neuron *66*, 921-936.

Bourin, M., and Hascoet, M. (2003). The mouse light/dark box test. Eur J Pharmacol *463*, 55-65.

Britton, D.R., and Britton, K.T. (1981). A sensitive open field measure of anxiolytic drug activity. Pharmacol Biochem Behav *15*, 577-582.

Burgos-Robles, A., Vidal-Gonzalez, I., Santini, E., and Quirk, G.J. (2007). Consolidation of fear extinction requires NMDA receptor-dependent bursting in the ventromedial prefrontal cortex. Neuron *53*, 871-880.

Burton, B.G., Hok, V., Save, E., and Poucet, B. (2009). Lesion of the ventral and intermediate hippocampus abolishes anticipatory activity in the medial prefrontal cortex of the rat. Behav Brain Res *199*, 222-234.

Burwell R.D. and Witter, M.P. (2002). Basic anatomy of the parahippocampal region in monkeys and rats (New York: Oxford University Press).

Burwell, R.D., Witter, M.P., and Amaral, D.G. (1995). Perirhinal and postrhinal cortices of the rat: a review of the neuroanatomical literature and comparison with findings from the monkey brain. Hippocampus *5*, 390-408.

Buzsaki, G. (2002). Theta oscillations in the hippocampus. Neuron *33*, 325-340.

Buzsaki, G., Buhl, D.L., Harris, K.D., Csicsvari, J., Czeh, B., and Morozov, A. (2003). Hippocampal network patterns of activity in the mouse. Neuroscience *116*, 201-211.

Cacucci, F., Wills, T.J., Lever, C., Giese, K.P., and O'Keefe, J. (2007). Experience-dependent increase in CA1 place cell spatial information, but not spatial reproducibility, is dependent on the autophosphorylation of the alpha-isoform of the calcium/calmodulin-dependent protein kinase II. J Neurosci *27*, 7854-7859.

Cadotte, A.J., Demarse, T.B., Mareci, T.H., Parekh, M., Talathi, S.S., Hwang, D.U., Ditto, W.L., Ding, M., and Carney, P.R. (2010). Granger causality relationships between local field potentials in an animal model of temporal lobe epilepsy. J Neurosci Methods.

Cannizzaro, C., Martire, M., Cannizzaro, E., Monastero, R., Gagliano, M., Mineo, A., and Provenzano, G. (2003). Effects of 8-OH-DPAT on open field performance of young and aged rats prenatally exposed to diazepam: a tool to reveal 5-HT1A receptor function. Eur Neuropsychopharmacol *13*, 209-217.

Canteras, N.S., Simerly, R.B., and Swanson, L.W. (1992). Connections of the posterior nucleus of the amygdala. J Comp Neurol *324*, 143-179.

Cenquizca, L.A., and Swanson, L.W. (2007). Spatial organization of direct hippocampal field CA1 axonal projections to the rest of the cerebral cortex. Brain Res Rev *56*, 1-26.

Chauveau, F., Celerier, A., Ognard, R., Pierard, C., and Beracochea, D. (2005). Effects of ibotenic acid lesions of the mediodorsal thalamus on memory: relationship with emotional processes in mice. Behav Brain Res *156*, 215-223.

Choleris, E., Thomas, A.W., Kavaliers, M., and Prato, F.S. (2001). A detailed ethological analysis of the mouse open field test: effects of diazepam, chlordiazepoxide and an extremely low frequency pulsed magnetic field. Neurosci Biobehav Rev *25*, 235-260.

Corcoran, K.A., and Quirk, G.J. (2007). Activity in prelimbic cortex is necessary for the expression of learned, but not innate, fears. J Neurosci *27*, 840-844.

Crawley, J.N. (1985). Exploratory behavior models of anxiety in mice. Neurosci Biobehav Rev *9*, 37-44.

Cruz, A.P., Frei, F., and Graeff, F.G. (1994). Ethopharmacological analysis of rat behavior on the elevated plus-maze. Pharmacol Biochem Behav *49*, 171-176.

Csicsvari, J., Jamieson, B., Wise, K.D., and Buzsaki, G. (2003). Mechanisms of gamma oscillations in the hippocampus of the behaving rat. Neuron *37*, 311-322.

Davis, M. (1997). Neurobiology of fear responses: the role of the amygdala. J Neuropsychiatry Clin Neurosci *9*, 382-402.

de Angelis, L., and File, S.E. (1979). Acute and chronic effects of three benzodiazepines in the social interaction anxiety test in mice. Psychopharmacology (Berl) *64*, 127-129.

Deacon, R.M., Bannerman, D.M., and Rawlins, J.N. (2002). Anxiolytic effects of cytotoxic hippocampal lesions in rats. Behav Neurosci *116*, 494-497.

Debanne, D., Guerineau, N.C., Gahwiler, B.H., and Thompson, S.M. (1996). Paired-pulse facilitation and depression at unitary synapses in rat hippocampus: quantal fluctuation affects subsequent release. J Physiol *491 (Pt 1)*, 163-176.

DeCoteau, W.E., Thorn, C., Gibson, D.J., Courtemanche, R., Mitra, P., Kubota, Y., and Graybiel, A.M. (2007). Learning-related coordination of striatal and hippocampal theta

rhythms during acquisition of a procedural maze task. Proc Natl Acad Sci U S A *104*, 5644-5649.

Degroot, A., and Treit, D. (2004). Anxiety is functionally segregated within the septo-hippocampal system. Brain Res *1001*, 60-71.

Dekeyne, A., Brocco, M., Adhumeau, A., Gobert, A., and Millan, M.J. (2000). The selective serotonin (5-HT)1A receptor ligand, S15535, displays anxiolytic-like effects in the social interaction and Vogel models and suppresses dialysate levels of 5-HT in the dorsal hippocampus of freely-moving rats. A comparison with other anxiolytic agents. Psychopharmacology (Berl) *152*, 55-66.

Dong, H.W., Swanson, L.W., Chen, L., Fanselow, M.S., and Toga, A.W. (2009). Genomic-anatomic evidence for distinct functional domains in hippocampal field CA1. Proc Natl Acad Sci U S A *106*, 11794-11799.

Drapier, D., Bentue-Ferrer, D., Laviolle, B., Millet, B., Allain, H., Bourin, M., and Reymann, J.M. (2007). Effects of acute fluoxetine, paroxetine and desipramine on rats tested on the elevated plus-maze. Behav Brain Res *176*, 202-209.

Dulawa, S.C., Holick, K.A., Gundersen, B., and Hen, R. (2004). Effects of chronic fluoxetine in animal models of anxiety and depression. Neuropsychopharmacology *29*, 1321-1330.

Durand, M., Berton, O., Aguerre, S., Edno, L., Combourieu, I., Mormede, P., and Chaouloff, F. (1999). Effects of repeated fluoxetine on anxiety-related behaviours, central serotonergic systems, and the corticotropic axis axis in SHR and WKY rats. Neuropharmacology *38*, 893-907.

Duvarci, S., Bauer, E.P., and Pare, D. (2009). The bed nucleus of the stria terminalis mediates inter-individual variations in anxiety and fear. J Neurosci *29*, 10357-10361.
Engin, E., and Treit, D. (2007). The role of hippocampus in anxiety: intracerebral infusion studies. Behav Pharmacol *18*, 365-374.

Fanselow, M.S., and Dong, H.W. Are the dorsal and ventral hippocampus functionally distinct structures? Neuron *65*, 7-19.

Fanselow, M.S., and Kim, J.J. (1994). Acquisition of contextual Pavlovian fear conditioning is blocked by application of an NMDA receptor antagonist D,L-2-amino-5-phosphonovaleric acid to the basolateral amygdala. Behav Neurosci *108*, 210-212.

Fee, J.R., Sparta, D.R., Knapp, D.J., Breese, G.R., Picker, M.J., and Thiele, T.E. (2004). Predictors of high ethanol consumption in RIIbeta knock-out mice: assessment of anxiety and ethanol-induced sedation. Alcohol Clin Exp Res *28*, 1459-1468.

File, S.E., Gonzalez, L.E., and Andrews, N. (1996). Comparative study of pre- and postsynaptic 5-HT1A receptor modulation of anxiety in two ethological animal tests. J Neurosci *16*, 4810-4815.

File, S.E., and Hyde, J.R. (1979). A test of anxiety that distinguishes between the actions of benzodiazepines and those of other minor tranquilisers and of stimulants. Pharmacol Biochem Behav *11*, 65-69.

File, S.E., and Seth, P. (2003). A review of 25 years of the social interaction test. Eur J Pharmacol *463*, 35-53.

Frankland, P.W., Bontempi, B., Talton, L.E., Kaczmarek, L., and Silva, A.J. (2004). The involvement of the anterior cingulate cortex in remote contextual fear memory. Science *304*, 881-883.

Gemmell, C., Anderson, M., and O'Mara, S.M. (2002). Deep layer prefrontal cortex unit discharge in a cue-controlled open-field environment in the freely-moving rat. Behav Brain Res *133*, 1-10.

Gloveli, T., Dugladze, T., Rotstein, H.G., Traub, R.D., Monyer, H., Heinemann, U., Whittington, M.A., and Kopell, N.J. (2005). Orthogonal arrangement of rhythm-generating microcircuits in the hippocampus. Proc Natl Acad Sci U S A *102*, 13295-13300.

Gonzalez, L.E., Rujano, M., Tucci, S., Paredes, D., Silva, E., Alba, G., and Hernandez, L. (2000). Medial prefrontal transection enhances social interaction. I: behavioral studies. Brain Res *887*, 7-15.

Gordon, J.A., and Hen, R. (2004). The serotonergic system and anxiety. Neuromolecular Med *5*, 27-40.

Gordon, J.A., Lacefield, C.O., Kentros, C.G., and Hen, R. (2005). State-dependent alterations in hippocampal oscillations in serotonin 1A receptor-deficient mice. J Neurosci *25*, 6509-6519.

Gorman, J.M., Kent, J.M., and Coplan, J.D. (2002). Current and emerging therapeutics of anxiety and stress disorders. In Neuropsychopharmacology: The fifth generation of progress, K.L. Davis, D.S. Charney, J.T. Coyle, and C. Nemeroff, eds. (Philadelphia: Lippincott Williams and Wilkins).

Gourevitch, B., Bouquin-Jeannes, R.L., and Faucon, G. (2006). Linear and nonlinear causality between signals: methods, examples and neurophysiological applications. Biol Cybern *95*, 349-369.

Green, S., and Vale, A.L. (1992). Role of amygdaloid nuclei in the anxiolytic effects of benzodiazepines in rats. Behav Pharmacol *3*, 261-264.

Gregoriou, G.G., Gotts, S.J., Zhou, H., and Desimone, R. (2009). High-frequency, long-range coupling between prefrontal and visual cortex during attention. Science *324*, 1207-1210.

Griebel, G., Blanchard, D.C., and Blanchard, R.J. (1996). Evidence that the behaviors in the Mouse Defense Test Battery relate to different emotional states: a factor analytic study. Physiol Behav *60*, 1255-1260.

Griebel, G., Cohen, C., Perrault, G., and Sanger, D.J. (1999). Behavioral effects of acute and chronic fluoxetine in Wistar-Kyoto rats. Physiol Behav *67*, 315-320.

Griebel, G., Moreau, J.L., Jenck, F., Misslin, R., and Martin, J.R. (1994). Acute and chronic treatment with 5-HT reuptake inhibitors differentially modulate emotional responses in anxiety models in rodents. Psychopharmacology (Berl) *113*, 463-470.

Grillon, C., Levenson, J., and Pine, D.S. (2007). A single dose of the selective serotonin reuptake inhibitor citalopram exacerbates anxiety in humans: a fear-potentiated startle study. Neuropsychopharmacology *32*, 225-231.

Gross, C., Zhuang, X., Stark, K., Ramboz, S., Oosting, R., Kirby, L., Santarelli, L., Beck, S., and Hen, R. (2002). Serotonin1A receptor acts during development to establish normal anxiety-like behaviour in the adult. Nature *416*, 396-400.

Harris, K.D., Csicsvari, J., Hirase, H., Dragoi, G., and Buzsaki, G. (2003). Organization of cell assemblies in the hippocampus. Nature *424*, 552-556.

Heisler, L.K., Chu, H.M., Brennan, T.J., Danao, J.A., Bajwa, P., Parsons, L.H., and Tecott, L.H. (1998). Elevated anxiety and antidepressant-like responses in serotonin 5-HT1A receptor mutant mice. Proc Natl Acad Sci U S A *95*, 15049-15054.

Hermer-Vazquez, R., Hermer-Vazquez, L., Srinivasan, S., and Chapin, J.K. (2007). Beta- and gamma-frequency coupling between olfactory and motor brain regions prior to skilled, olfactory-driven reaching. Exp Brain Res *180*, 217-235.

Hirose, A., Tsuji, R., Shimizu, H., Tatsuno, T., Tanaka, H., Kumasaka, Y., and Nakamura, M. (1990). Inhibition by 8-hydroxy-2-(di-n-propylamino) tetralin and SM-3997, a novel anxiolytic drug, of the hippocampal rhythmical slow activity mediated by 5-hydroxytryptamine1A receptors. Naunyn Schmiedebergs Arch Pharmacol *341*, 8-13.
Hok, V., Lenck-Santini, P.P., Roux, S., Save, E., Muller, R.U., and Poucet, B. (2007). Goal-related activity in hippocampal place cells. J Neurosci *27*, 472-482.

Holdefer, R.N., Miller, L.E., Chen, L.L., and Houk, J.C. (2000). Functional connectivity between cerebellum and primary motor cortex in the awake monkey. J Neurophysiol *84*, 585-590.

Holson, R.R. (1986). Mesial prefrontal cortical lesions and timidity in rats. I. Reactivity to aversive stimuli. Physiol Behav *37*, 221-230.

Hoover, W.B., and Vertes, R.P. (2007). Anatomical analysis of afferent projections to the medial prefrontal cortex in the rat. Brain Struct Funct *212*, 149-179.

Hyman, J.M., Zilli, E.A., Paley, A.M., and Hasselmo, M.E. (2005). Medial prefrontal cortex cells show dynamic modulation with the hippocampal theta rhythm dependent on behavior. Hippocampus *15*, 739-749.

Ishizuka, N. (2001). Laminar organization of the pyramidal cell layer of the subiculum in the rat. J Comp Neurol *435*, 89-110.

Jinks, A.L., and McGregor, I.S. (1997). Modulation of anxiety-related behaviours following lesions of the prelimbic or infralimbic cortex in the rat. Brain Res *772*, 181-190.

Jones, M.W., and Wilson, M.A. (2005). Theta rhythms coordinate hippocampal-prefrontal interactions in a spatial memory task. PLoS Biol *3*, e402.

Jung, M.W., Qin, Y., McNaughton, B.L., and Barnes, C.A. (1998). Firing characteristics of deep layer neurons in prefrontal cortex in rats performing spatial working memory tasks. Cereb Cortex *8*, 437-450.

Jung, M.W., Wiener, S.I., and McNaughton, B.L. (1994). Comparison of spatial firing characteristics of units in dorsal and ventral hippocampus of the rat. J Neurosci *14*, 7347-7356.

Kantor, S., Graf, M., Anheuer, Z.E., and Bagdy, G. (2001). Rapid desensitization of 5-HT(1A) receptors in Fawn-Hooded rats after chronic fluoxetine treatment. Eur Neuropsychopharmacol *11*, 15-24.

Kishi, T., Tsumori, T., Yokota, S., and Yasui, Y. (2006). Topographical projection from the hippocampal formation to the amygdala: a combined anterograde and retrograde tracing study in the rat. J Comp Neurol *496*, 349-368.

Kjelstrup, K.B., Solstad, T., Brun, V.H., Hafting, T., Leutgeb, S., Witter, M.P., Moser, E.I., and Moser, M.B. (2008). Finite scale of spatial representation in the hippocampus. Science *321*, 140-143.

Kjelstrup, K.G., Tuvnes, F.A., Steffenach, H.A., Murison, R., Moser, E.I., and Moser, M.B. (2002). Reduced fear expression after lesions of the ventral hippocampus. Proc Natl Acad Sci U S A *99*, 10825-10830.

Klemenhagen, K.C., Gordon, J.A., David, D.J., Hen, R., and Gross, C.T. (2006). Increased fear response to contextual cues in mice lacking the 5-HT1A receptor. Neuropsychopharmacology *31*, 101-111.

Kondo, Y., and Sakuma, Y. (2005). The medial amygdala controls the coital access of female rats: a possible involvement of emotional responsiveness. Jpn J Physiol *55*, 345-353.

Kung, J.C., Chen, T.C., Shyu, B.C., Hsiao, S., and Huang, A.C. Anxiety- and depressive-like responses and c-fos activity in preproenkephalin klockout mice: oversensitivity hypothesis of enkephalin deficit-induced posttraumatic stress disorder. J Biomed Sci *17*, 29.

Kurt, M., Arik, A.C., and Celik, S. (2000). The effects of sertraline and fluoxetine on anxiety in the elevated plus-maze test in mice. J Basic Clin Physiol Pharmacol *11*, 173-180.

Lacroix, L., Broersen, L.M., Weiner, I., and Feldon, J. (1998). The effects of excitotoxic lesion of the medial prefrontal cortex on latent inhibition, prepulse inhibition, food hoarding, elevated plus maze, active avoidance and locomotor activity in the rat. Neuroscience *84*, 431-442.

Lacroix, L., Spinelli, S., Heidbreder, C.A., and Feldon, J. (2000). Differential role of the medial and lateral prefrontal cortices in fear and anxiety. Behav Neurosci *114*, 1119-1130.

Laroche, S., Jay, T.M., and Thierry, A.M. (1990). Long-term potentiation in the prefrontal cortex following stimulation of the hippocampal CA1/subicular region. Neurosci Lett *114*, 184-190.

Larson, J., and Lynch, G. (1986). Induction of synaptic potentiation in hippocampus by patterned stimulation involves two events. Science *232*, 985-988.

Lavenex, P., Lavenex, P.B., and Amaral, D.G. (2007). Spatial relational learning persists following neonatal hippocampal lesions in macaque monkeys. Nat Neurosci *10*, 234-239.

Le Van Quyen, M., Foucher, J., Lachaux, J., Rodriguez, E., Lutz, A., Martinerie, J., and Varela, F.J. (2001). Comparison of Hilbert transform and wavelet methods for the analysis of neuronal synchrony. J Neurosci Methods *111*, 83-98.

Lecrubier, Y. (2007). Widespread underrecognition and undertreatment of anxiety and mood disorders: results from 3 European studies. J Clin Psychiatry *68 Suppl 2*, 36-41.
LeDoux, J. (2003). The emotional brain, fear, and the amygdala. Cell Mol Neurobiol *23*, 727-738.

LeDoux, J.E. (2000). Emotion circuits in the brain. Annu Rev Neurosci *23*, 155-184.

Leonardo, E.D., Richardson-Jones, J.W., Sibille, E., Kottman, A., and Hen, R. (2006). Molecular heterogeneity along the dorsal-ventral axis of the murine hippocampal CA1 field: a microarray analysis of gene expression. Neuroscience *137*, 177-186.

Likhtik, E., Pelletier, J.G., Paz, R., and Pare, D. (2005). Prefrontal control of the amygdala. J Neurosci *25*, 7429-7437.

Lindsey, B.G., Hernandez, Y.M., Morris, K.F., and Shannon, R. (1992). Functional connectivity between brain stem midline neurons with respiratory-modulated firing rates. J Neurophysiol *67*, 890-904.

Lister, R.G. (1987). The use of a plus-maze to measure anxiety in the mouse. Psychopharmacology (Berl) *92*, 180-185.

Maren, S. (1999). Neurotoxic or electrolytic lesions of the ventral subiculum produce deficits in the acquisition and expression of Pavlovian fear conditioning in rats. Behav Neurosci *113*, 283-290.

Maren, S., Aharonov, G., and Fanselow, M.S. (1997). Neurotoxic lesions of the dorsal hippocampus and Pavlovian fear conditioning in rats. Behav Brain Res *88*, 261-274.

McNamara, R.K., and Skeleton, R.W. (1993). Effects of intracranial infusions of chlordiazepoxide on spatial learning in the Morris water maze. I. Neuroanatomical specificity. Behav Brain Res *59*, 175-191.

McNaughton, N., and Gray, J.A. (2000). Anxiolytic action on the behavioural inhibition system implies multiple types of arousal contribute to anxiety. J Affect Disord *61*, 161-176.

Mendlowicz, M.V., and Stein, M.B. (2000). Quality of life in individuals with anxiety disorders. Am J Psychiatry *157*, 669-682.

Moller, C., Wiklund, L., Sommer, W., Thorsell, A., and Heilig, M. (1997). Decreased experimental anxiety and voluntary ethanol consumption in rats following central but not basolateral amygdala lesions. Brain Res *760*, 94-101.

Montgomery, K.C. (1955). The relation between fear induced by novel stimulation and exploratory behavior. J Comp Physiol Psychol *48*, 254-260.

Moser, E.I., Kropff, E., and Moser, M.B. (2008). Place cells, grid cells, and the brain's spatial representation system. Annu Rev Neurosci *31*, 69-89.

Parent, M.A., Wang, L., Su, J., Netoff, T., and Yuan, L.L. (2009). Identification of the Hippocampal Input to Medial Prefrontal Cortex In Vitro. Cereb Cortex.

Parks, C.L., Robinson, P.S., Sibille, E., Shenk, T., and Toth, M. (1998). Increased anxiety of mice lacking the serotonin1A receptor. Proc Natl Acad Sci U S A *95*, 10734-10739.

Paz, R., Bauer, E.P., and Pare, D. (2009). Measuring correlations and interactions among four simultaneously recorded brain regions during learning. J Neurophysiol *101*, 2507-2515.

Pellow, S., Chopin, P., File, S.E., and Briley, M. (1985). Validation of open:closed arm entries in an elevated plus-maze as a measure of anxiety in the rat. J Neurosci Methods *14*, 149-167.

Pellow, S., and File, S.E. (1986). Anxiolytic and anxiogenic drug effects on exploratory activity in an elevated plus-maze: a novel test of anxiety in the rat. Pharmacol Biochem Behav *24*, 525-529.

Pesold, C., and Treit, D. (1995). The central and basolateral amygdala differentially mediate the anxiolytic effects of benzodiazepines. Brain Res *671*, 213-221.

Petrovich, G.D., Canteras, N.S., and Swanson, L.W. (2001). Combinatorial amygdalar inputs to hippocampal domains and hypothalamic behavior systems. Brain Res Brain Res Rev *38*, 247-289.

Pitkanen, A., Pikkarainen, M., Nurminen, N., and Ylinen, A. (2000). Reciprocal connections between the amygdala and the hippocampal formation, perirhinal cortex, and postrhinal cortex in rat. A review. Ann N Y Acad Sci *911*, 369-391.

Popa, D., Duvarci, S., Popescu, A.T., Lena, C., and Pare, D. (2010). Coherent amygdalocortical theta promotes fear memory consolidation during paradoxical sleep. Proc Natl Acad Sci U S A *107*, 6516-6519.

Pothuizen, H.H., Zhang, W.N., Jongen-Relo, A.L., Feldon, J., and Yee, B.K. (2004). Dissociation of function between the dorsal and the ventral hippocampus in spatial learning abilities of the rat: a within-subject, within-task comparison of reference and working spatial memory. Eur J Neurosci *19*, 705-712.

Pratt, W.E., and Mizumori, S.J. (2001). Neurons in rat medial prefrontal cortex show anticipatory rate changes to predictable differential rewards in a spatial memory task. Behav Brain Res *123*, 165-183.

Prut, L., and Belzung, C. (2003). The open field as a paradigm to measure the effects of drugs on anxiety-like behaviors: a review. Eur J Pharmacol *463*, 3-33.

Puumala, T., and Sirvio, J. (1998). Changes in activities of dopamine and serotonin systems in the frontal cortex underlie poor choice accuracy and impulsivity of rats in an attention task. Neuroscience *83*, 489-499.

Quintero, S., Mellanby, J., Thompson, M.R., Nordeen, H., Nutt, D., McNaughton, N., and Gray, J.A. (1985). Septal driving of hippocampal theta rhythm: role of gamma-aminobutyrate-benzodiazepine receptor complex in mediating effects of anxiolytics. Neuroscience *16*, 875-884.

Quirk, G.J., and Beer, J.S. (2006). Prefrontal involvement in the regulation of emotion: convergence of rat and human studies. Curr Opin Neurobiol *16*, 723-727.

Quirk, G.J., Likhtik, E., Pelletier, J.G., and Pare, D. (2003). Stimulation of medial prefrontal cortex decreases the responsiveness of central amygdala output neurons. J Neurosci *23*, 8800-8807.

Ramboz, S., Oosting, R., Amara, D.A., Kung, H.F., Blier, P., Mendelsohn, M., Mann, J.J., Brunner, D., and Hen, R. (1998). Serotonin receptor 1A knockout: an animal model of anxiety-related disorder. Proc Natl Acad Sci U S A *95*, 14476-14481.

Ramos, A., Berton, O., Mormede, P., and Chaouloff, F. (1997). A multiple-test study of anxiety-related behaviours in six inbred rat strains. Behav Brain Res *85*, 57-69.

Rao, S., and Zisook, S. (2009). Anxious depression: clinical features and treatment. Curr Psychiatry Rep *11*, 429-436.

Resstel, L.B., Souza, R.F., and Guimaraes, F.S. (2008). Anxiolytic-like effects induced by medial prefrontal cortex inhibition in rats submitted to the Vogel conflict test. Physiol Behav *93*, 200-205.

Rodgers, R.J. (1997). Animal models of 'anxiety': where next? Behav Pharmacol *8*, 477-496; discussion 497-504.

Roy-Byrne, P.P., Davidson, K.W., Kessler, R.C., Asmundson, G.J., Goodwin, R.D., Kubzansky, L., Lydiard, R.B., Massie, M.J., Katon, W., Laden, S.K., and Stein, M.B. (2008). Anxiety disorders and comorbid medical illness. Gen Hosp Psychiatry *30*, 208-225.

Royer, S., Sirota, A., Patel, J., and Buzsaki, G. (2010). Distinct representations and theta dynamics in dorsal and ventral hippocampus. J Neurosci *30*, 1777-1787.

Rush, A.J., Trivedi, M.H., Wisniewski, S.R., Nierenberg, A.A., Stewart, J.W., Warden, D., Niederehe, G., Thase, M.E., Lavori, P.W., Lebowitz, B.D.*, et al.* (2006). Acute and longer-term outcomes in depressed outpatients requiring one or several treatment steps: a STAR*D report. Am J Psychiatry *163*, 1905-1917.

Sanders, S.K., and Shekhar, A. (1995). Anxiolytic effects of chlordiazepoxide blocked by injection of GABAA and benzodiazepine receptor antagonists in the region of the anterior basolateral amygdala of rats. Biol Psychiatry *37*, 473-476.

Schmitt, U., and Hiemke, C. (1998). Combination of open field and elevated plus-maze: a suitable test battery to assess strain as well as treatment differences in rat behavior. Prog Neuropsychopharmacol Biol Psychiatry *22*, 1197-1215.

Schmitzer-Torbert, N., Jackson, J., Henze, D., Harris, K., and Redish, A.D. (2005). Quantitative measures of cluster quality for use in extracellular recordings. Neuroscience *131*, 1-11.

Seidenbecher, T., Laxmi, T.R., Stork, O., and Pape, H.C. (2003). Amygdalar and hippocampal theta rhythm synchronization during fear memory retrieval. Science *301*, 846-850.

Shah, A.A., Sjovold, T., and Treit, D. (2004). Inactivation of the medial prefrontal cortex with the GABAA receptor agonist muscimol increases open-arm activity in the elevated plus-maze and attenuates shock-probe burying in rats. Brain Res *1028*, 112-115.

Shah, A.A., and Treit, D. (2003). Excitotoxic lesions of the medial prefrontal cortex attenuate fear responses in the elevated-plus maze, social interaction and shock probe burying tests. Brain Res *969*, 183-194.

Shah, A.A., and Treit, D. (2004). Infusions of midazolam into the medial prefrontal cortex produce anxiolytic effects in the elevated plus-maze and shock-probe burying tests. Brain Res *996*, 31-40.

Siapas, A.G., Lubenov, E.V., and Wilson, M.A. (2005). Prefrontal phase locking to hippocampal theta oscillations. Neuron *46*, 141-151.

Siemiatkowski, M., Sienkiewicz-Jarosz, H., Czlonkowska, A.I., Bidzinski, A., and Plaznik, A. (2000). Effects of buspirone, diazepam, and zolpidem on open field behavior, and brain [3H]muscimol binding after buspirone pretreatment. Pharmacol Biochem Behav *66*, 645-651.

Sigurdsson, T., Stark, K.L., Karayiorgou, M., Gogos, J.A., and Gordon, J.A. (2010). Impaired hippocampal-prefrontal synchrony in a genetic mouse model of schizophrenia. Nature *464*, 763-767.

Silva, R.C., and Brandao, M.L. (2000). Acute and chronic effects of gepirone and fluoxetine in rats tested in the elevated plus-maze: an ethological analysis. Pharmacol Biochem Behav *65*, 209-216.

Sirota, A., and Buzsaki, G. (2005). Interaction between neocortical and hippocampal networks via slow oscillations. Thalamus Relat Syst *3*, 245-259.

Sirota, A., Montgomery, S., Fujisawa, S., Isomura, Y., Zugaro, M., and Buzsaki, G. (2008). Entrainment of neocortical neurons and gamma oscillations by the hippocampal theta rhythm. Neuron *60*, 683-697.

Snider, R.K., Kabara, J.F., Roig, B.R., and Bonds, A.B. (1998). Burst firing and modulation of functional connectivity in cat striate cortex. J Neurophysiol *80*, 730-744.

Steffenach, H.A., Witter, M., Moser, M.B., and Moser, E.I. (2005). Spatial memory in the rat requires the dorsolateral band of the entorhinal cortex. Neuron *45*, 301-313.

Sustkova-Fiserova, M., Vavrova, J., and Krsiak, M. (2009). Brain levels of GABA, glutamate and aspartate in sociable, aggressive and timid mice: an in vivo microdialysis study. Neuro Endocrinol Lett *30*, 79-84.

Swanson, L.W., and Cowan, W.M. (1977). An autoradiographic study of the organization of the efferent connections of the hippocampal formation in the rat. J Comp Neurol *172*, 49-84.

Szabadics, J., Lorincz, A., and Tamas, G. (2001). Beta and gamma frequency synchronization by dendritic gabaergic synapses and gap junctions in a network of cortical interneurons. J Neurosci *21*, 5824-5831.

Taube, J.S. (2007). The head direction signal: origins and sensory-motor integration. Annu Rev Neurosci *30*, 181-207.

Taxidis, J., Coomber, B., Mason, R., and Owen, M. (2010). Assessing cortico-hippocampal functional connectivity under anesthesia and kainic acid using generalized partial directed coherence. Biol Cybern *102*, 327-340.

Thierry, A.M., Gioanni, Y., Degenetais, E., and Glowinski, J. (2000). Hippocampo-prefrontal cortex pathway: anatomical and electrophysiological characteristics. Hippocampus *10*, 411-419.

Thompson, C.L., Pathak, S.D., Jeromin, A., Ng, L.L., MacPherson, C.R., Mortrud, M.T., Cusick, A., Riley, Z.L., Sunkin, S.M., Bernard, A.*, et al.* (2008). Genomic anatomy of the hippocampus. Neuron *60*, 1010-1021.

Tierney, P.L., Degenetais, E., Thierry, A.M., Glowinski, J., and Gioanni, Y. (2004). Influence of the hippocampus on interneurons of the rat prefrontal cortex. Eur J Neurosci *20*, 514-524.

To, C.T., and Bagdy, G. (1999). Anxiogenic effect of central CCK administration is attenuated by chronic fluoxetine or ipsapirone treatment. Neuropharmacology *38*, 279-282.

Treit, D., Aujla, H., and Menard, J. (1998). Does the bed nucleus of the stria terminalis mediate fear behaviors? Behav Neurosci *112*, 379-386.

Veening, J.G., Swanson, L.W., and Sawchenko, P.E. (1984). The organization of projections from the central nucleus of the amygdala to brainstem sites involved in

central autonomic regulation: a combined retrograde transport-immunohistochemical study. Brain Res *303*, 337-357.

Vertes, R.P. (2004). Differential projections of the infralimbic and prelimbic cortex in the rat. Synapse *51*, 32-58.

Verwer, R.W., Meijer, R.J., Van Uum, H.F., and Witter, M.P. (1997). Collateral projections from the rat hippocampal formation to the lateral and medial prefrontal cortex. Hippocampus *7*, 397-402.

Vidal-Gonzalez, I., Vidal-Gonzalez, B., Rauch, S.L., and Quirk, G.J. (2006). Microstimulation reveals opposing influences of prelimbic and infralimbic cortex on the expression of conditioned fear. Learn Mem *13*, 728-733.

Walker, D.L., and Davis, M. (1997). Double dissociation between the involvement of the bed nucleus of the stria terminalis and the central nucleus of the amygdala in startle increases produced by conditioned versus unconditioned fear. J Neurosci *17*, 9375-9383.

Walker, D.L., Miles, L.A., and Davis, M. (2009). Selective participation of the bed nucleus of the stria terminalis and CRF in sustained anxiety-like versus phasic fear-like responses. Prog Neuropsychopharmacol Biol Psychiatry *33*, 1291-1308.

Whishaw, I.Q., Gharbawie, O.A., Clark, B.J., and Lehmann, H. (2006). The exploratory behavior of rats in an open environment optimizes security. Behav Brain Res *171*, 230-239.

Winterhalder, M., Schelter, B., Hesse, W., Schwab, K., Leistritz, L., Klan, D., Bauer, R., Timmer, J., and Witte, H. (2005). Comparison directed of linear signal processing techniques to infer interactions in multivariate neural systems. Signal Processing *85*, 2137-2160.

Witter, M.P., Groenewegen, H.J., Lopes da Silva, F.H., and Lohman, A.H. (1989). Functional organization of the extrinsic and intrinsic circuitry of the parahippocampal region. Prog Neurobiol *33*, 161-253.

Yee, B.K. (2000). Cytotoxic lesion of the medial prefrontal cortex abolishes the partial reinforcement extinction effect, attenuates prepulse inhibition of the acoustic startle reflex and induces transient hyperlocomotion, while sparing spontaneous object recognition memory in the rat. Neuroscience *95*, 675-689.

Zangrossi Junior, H., and Graeff, F.G. (1994). Behavioral effects of intra-amygdala injections of GABA and 5-HT acting drugs in the elevated plus-maze. Braz J Med Biol Res *27*, 2453-2456.

Zhu, X.O., and McNaughton, N. (1994). Effects of long-term administration of antidepressants on septal driving of hippocampal RSA. Int J Neurosci *79*, 91-98.